WILEY | Hindawi

Research Article

Optimal Placement and Sizing Problem for Power Loss Minimization and Voltage Profile Improvement of Distribution Networks under Seasonal Loads Using Harris Hawks Optimizer

Habib Ur Rahman Habib [iD],[1] **Asad Waqar** [iD],[2] **Sharoze Sohail** [iD],[3]
Abdul Khalique Junejo [iD],[4] **Mahmoud F. Elmorshedy** [iD],[5] **Sheheryar Khan** [iD],[6]
Yun-Su Kim [iD],[7] **and Moustafa Magdi Ismail** [iD][8]

[1]Department of Electrical Engineering, Faculty of Electrical and Electronics Engineering,
 University of Engineering and Technology Taxila, Taxila 47050, Pakistan
[2]Department of Electrical Engineering, Bahria University, Islamabad 44000, Pakistan
[3]Department of Electrical Engineering, Air University, Islamabad 44000, Pakistan
[4]Department of Electrical Engineering, Qaid-e-Awam University of Engineering, Science and Technology,
 Nawabshah 67450, Pakistan
[5]Electrical Power and Machines Engineering Department, Faculty of Engineering, Tanta University, Tanta 31512, Egypt
[6]School of Professional Education and Executive Development, College of Professional & Continuing Education,
 The Hong Kong Polytechnic University, Kowloon 100077, Hong Kong
[7]Graduate School of Energy Convergence, Gwangju Institute of Science and Technology (GIST), Gwangju 61005,
 Republic of Korea
[8]School of Electrical and Electronic Engineering, Minia University, El-Minya, Egypt

Correspondence should be addressed to Yun-Su Kim; yunsukim@gist.ac.kr

Improving efficiency with sustainable radial distribution networks (RDNs) is challenging for larger systems and small grid-connected RDNs. In this paper, the optimal placement of DGs with the Harris hawks optimizer (HHO) under seasonal load demands is proposed to simultaneously reduce total active and reactive power losses and minimize bus voltage drops with the consideration of operational constraints of RDNs. HHO is a newly inspired metaheuristic optimization algorithm primarily based on the Harris hawks' intelligent behaviors during the chasing of the prey. Furthermore, the authors have investigated four stages of DGs. The first stage involves the optimal allocation of one DG. The second stage includes an investigation with two DGs, the third stage considers three DGs, and the fourth stage investigates the integration of four DGs. The effectiveness of the applied HHO is validated on IEEE 33 and 69 bus RDNs, and results are analyzed by comparing with the standard optimization methods. The Big-O test is also executed for statistical analysis with standard algorithms. The simulation results reveal the better performance of the applied HHO under different circumstances than other algorithms. Furthermore, the total active and reactive power losses and bus voltage drops are improved by adding more DGs into IEEE 33 and 69 bus RDNs.

1. Introduction

1.1. Motivation. DG penetration in the RDNs has changed its structural behavior from passive to active under power flow in various directions. DGs are small power generation units integrated into RDNs to enhance reliable power delivery, reduce the total P and Q losses, and improve the bus voltage levels [1]. These DGs can be categorized into conventional power generation sources such as DEs and renewable energy resources (RERs) such as PV and wind power. Nevertheless, future expansion with high integration of RER-based DGs will have both positive and negative

outcomes. The adverse effects are power flow reversal, undesired bus voltages level, and power loss [2]. Therefore, these adverse outcomes can be tackled with the help of carefully optimizing the best possible locations and sizing of these DGs.

1.2. Literature Review. Different optimization techniques have been proposed in the literature studies to allocate DGs with their optimal sizes [3, 4]. These optimization issues have been tackled with single and multiple objectives. Minimizing the power loss has been taken as the prime objective in single-objective optimization problems. Meanwhile, both single and multi-objective issues have been optimized using metaheuristic optimization methods during the optimal allocation of DGs.

During single-objective optimization problems, GA has been used for optimal DG allocation with minimization of the total P and Q losses [5]. In [6, 7], PSO has been employed to minimize the active power losses with different load types. AI (artificial intelligence)-based optimization techniques have been introduced in [8, 9] for determining the optimal allocation of multiple DG units. The fuzzy-based technique has been used in [10] for the optimal allocation of DGs. Various nature-inspired optimization methods have been employed in the recent literature for the optimal placement of DGs. These methods include BFOA [11], SKHA (stud krill herd algorithm) [12], WOA [13], and CSCA [14].

Two schemes have been used in the literature studies to handle multi-objective problems. The first method includes the weighting sum of each objective function. Many researchers have used the same method for optimizing different objective functions such as power losses, VDI, and VSI. The optimization algorithms which have been used in this methodology include GA [15], PSO [15], GA-PSO [15], TLBO [16], QOTLBO [16], SIMBO-Q (swine influenza model-based optimization with quarantine) [17], QOSIMBO-Q [17], and ICA-GA [18]. This first method faces a few challenging problems while selecting the weighting factors. The second method incorporates multi-objective methodologies with trade-off concepts among different objectives using Pareto dominance (PD) criteria. In PD, all the feasible solution sets are categorized into two sets such as dominant and non-dominant. The decision-making expert can select the best possible solution from the non-dominant solution set [4]. Various algorithms have been used based on this second methodology. These algorithms include PAES, NSGA-II, SPEA (strength Pareto evolutionary algorithm), SPEA-II, and MOPSO [20]. MOPSO with fuzzy has been used in [19] to minimize power losses and VDI improvement. MOWOA has been applied in [20] to enhance VSI and reduce VDI and power losses. MOSBA has been employed in [21] for analyzing the DG influence under different load scenarios. TM and MOTA have been implemented for the optimal integration of DGs [22].

In the literature studies, researchers have also analyzed DG allocation using IEEE 33 [10] and 69 bus RDNs [23] to minimize power losses and VDI.

In [24], the authors have presented ALO (ant-lion optimizer) for optimal sizing and DG allocation with two cases for DGs such as one and two DGs. The authors in [25] applied one DG-based PSAT (power system analysis toolbox) method. In [26], the authors have employed ALO to allocate sites for PV-based one and two DGs. In [27], CSFS (chaotic stochastic fractal search) optimizer has been used to find many DGs with their sizing and site selection under multiple DGs scenarios. GWO (grey wolf optimizer) has been used in [28] for the DG allocation with one or two DGs for enhancing VSI and reducing power losses. In [29], an EMA has been proposed for optimal DG sizes and site selection of one or two DGs. The authors in [1] introduced the optimal DG allocation for accommodating the power flow, VSI, power factor, and lines loss. CDE (chaotic differential evolution) optimizer has been implemented in [30] for the optimal placement of DGs. Hybrid GA-GSA (genetic-gravitational search algorithm) has been employed [31] for DG allocation. In [32], a combined WIPSO-GSA (mixed weight improved particle swarm optimization-gravitational search) has also been used for the installation of two DGs along with capacitor banks.

An HSA has been introduced to scale three DGs [33]. The authors in [34] have implemented a BFA (bacterial foraging algorithm) to scale three DGs. In [35], a combined ACO-ABC method has been proposed for the optimal allocation of three DGs. In [36], the BA (bat algorithm) method has been employed to scale PV sizes. The HA (hybrid algorithm) method has been introduced in [7] to handle power loss and VSI for optimal allocation of three DGs. The HA method utilized an analytical variance of PSO. In [37], HGWO (hybrid grey wolf optimizer) has been employed on the Indian network for the optimal allocation of three DGs. In [12], the integration of three DGs in the Portuguese 94-bus grid has been implemented with SKHA. The authors in [29] have introduced an EMA for deploying three DGs in the chosen network. In [38], SPEA-II has been used for the optimal integration of three DGs into the testing network. In [39], WCA (water cycle algorithm) has been suggested for optimal sizing and site selection with three DGs parallel to capacitor banks. An SSA (salp swarm algorithm) has been chosen in [40] for the optimal allocation of three DGs with capacitor banks. The authors in [41] applied an ASFLA (adaptive shuffled frog leaping algorithm) for optimally allocating three DGs. A combined GSA-GAMS (gravitational search algorithm-general algebraic modeling system) method has been implemented in [31] for optimal DG allocation. In [42], the QOCSOS (quasi-oppositional chaotic symbiotic organisms search) algorithm has been applied to search optimal sites of three DGs. The authors in [14] have introduced the CSCA technique for the optimal placement of three DGs. A combined TLCHS optimizer has been validated in [43] for optimal scaling and siting of four DGs. In [44], GA has been implemented for optimal deployment of one, two, and three DG units using IEEE 33-bus RDN. The authors in [45] have proposed an AIS (artificial immune system) for optimal deployment of DG units in IEEE 33 and 15 node RDNs. In [46], the authors have employed EHO [47] for optimal sizing and placement of

DGs in IEEE 15, 33, and 69 bus systems. In [48], IHSA has been introduced for optimal sizing and site selection of three DGs in the IEEE 33-bus system.

HHO algorithm has been employed in recent literature studies. Optimal DN topology with network reconfiguration is proposed in [49] using the HHO algorithm to minimize power losses and bus voltage deviation. In [50], renewable DGs are integrated into the DNs for power loss reduction with improved bus voltage profiles by considering the seasonal uncertainties of load demands. The authors in [51] investigated the optimal sizing and deployment of WTs in DNs, considering the correlation between load demands and wind power generation.

1.3. Main Contributions and Paper Organization. This research study proposes the optimal sizing and allocation of DGs in radial distribution networks (RDNs). HHO [52] is applied based on the hunting method of Harris hawks. The main benefit of HHO is a simple implementation technique with few scenarios of exploration and exploitation. HHO algorithm has been introduced in literature studies for solving different optimization problems, namely, identifying parameters of FC [53] PV cell [54] modules. Nevertheless, HHO is presented in this research study for optimally allocating DGs with single-objective function-based optimization issues. In HHO, the exploration phase represents a vast expansion of a searching space, while the exploitation phase relates to finding the best local solution. That is why the HHO algorithm has enhanced diversity. However, the significant contributions of this research study are summed up as follows:

   (i) HHO algorithm is applied for optimally allocating DGs in the radial distribution networks (RDNs) for simultaneously reducing the total active and reactive power losses and bus voltage drops.

   (ii) Four seasons, namely, summer, autumn, winter, and spring, integrate one, two, three, and four DGs, missing in the literature studies. This study's main objectives include reducing total active and reactive power losses and minimizing the bus voltage drop.

   (iii) Detailed analysis under multiple deployment scenarios of four types of DGs integration with four seasonal load demands by employing HHO and two IEEE RDNs is also unattended in the past literature studies.

   (iv) The performance of the applied HHO algorithm is validated under various operating conditions.

   (v) The statistical analysis uses Big-O under different DG integration and weather conditions.

The remainder of the paper is organized as follows. In Section 2, the formulation of the problem with methodology is presented. It includes the formulation of objectives with system constraints. In Section 3, the mathematical modeling of the HHO optimization algorithm is explained under different searching scenarios. Section 4 presents the results and analysis with a detailed analysis of the IEEE 33 and 69

bus RDNs under various scenarios. The conclusion is drawn in Section 5.

2. Problem Formulation

In this section, the objectives for optimal DG placement are included. In this research, the analysis is performed for the rural town (Shah Allah Ditta) in Islamabad, Pakistan (33.7209642 °N 72.9143201 °E). This rural town is 700 years old and was recognized as an essential route from Kabul (Afghanistan) to the Gandharan city of Taxila (Hindustan) by Alexander the Great and Sher Shah Suri. Other emperors, including Mughal rulers, frequently moved through this route during their travel from Afghanistan to Hindustan.

2.1. Objective Functions. The main objective of DG allocation in the distributed power system is to minimize total active and reactive power losses and bus voltage drop. The mathematical modeling of all these objectives is discussed in this section as follows.

2.1.1. Minimizing Active Power Loss. Due to the radial distribution network, active power losses are more prominent. Therefore, these power losses (P_{loss}) should be reduced as follows:

$$f_{Obj1} = \min(P_{\text{loss}}). \tag{1}$$

The total P_{loss} can be calculated using the branch current losses relationship as follows [55]:

$$P_{\text{loss}} = \sum_{b=1}^{M_b} |I_b|^2 R_b, \tag{2}$$

where b denotes the branch number, M_b represents the total branches, I_b shows the current flowing, and R_b means branch resistance.

2.1.2. Minimizing Total Reactive Power Loss. Due to the radial distribution network, reactive power losses are more prominent. Therefore, these power losses (Q_{loss}) should be reduced as follows:

$$f_{Obj2} = \min(Q_{\text{loss}}). \tag{3}$$

The total P loss can be calculated using the branch current loss relationship as follows [55]:

$$Q_{\text{loss}} = \sum_{b=1}^{M_b} |I_b|^2 X_b, \tag{4}$$

where X_b means branch reactance.

2.1.3. Minimizing Voltage Deviation Index. The total deviated voltage V_D indicated the voltage level of the RDNs and how far V_D is from the targeted value V_t. Therefore, V_D of the RDN can be found by taking voltage magnitude v_j at bus j based on the targeted voltage as follows [56]:

$$V_D = \sum_{j=1}^{N_j} (V_t - V_j), \tag{5}$$

where V_t is considered as 1.0 per unit.

2.1.4. Maximizing Voltage Stability Index.

The voltage stability index (VSI) is the ability of the RDN to maintain the voltage value within the specified range. The main objective is to maximize VSI as follows [57]:

$$\text{VSI}_R = V_S^4 - 4(P_R R_{SR} + Q_R X_{SR})V_S^2 - 4(P_R X_{SR} - Q_R R_{SR}), \tag{6}$$

where SR denotes the sending and receiving end; P_R, Q_R represent real and imaginary power at the receiving end; and R_{SR}, X_{SR} show the resistance and reactance between sending and receiving ends.

2.2. System Constraints.

The main constraints of DG allocation in the distributed power system are defined as follows.

2.2.1. Equality Constraints.

The generation-demand balance with the consideration of total active and reactive power losses can be expressed as follows [58]:

$$\sum_{j=1}^{N_{dg}} P_{gj} = P_{\text{loss}} + P_{\text{load}}, \tag{7}$$

$$\sum_{j=1}^{N_{dg}} Q_{gj} = Q_{\text{loss}} + Q_{\text{load}}, \tag{8}$$

where N_{dg} indicates the total number of installed DGs, P_{gi} is the generated power of the jth DG, and P_{load} denotes the total demanded power of the loads.

2.2.2. Inequality Constraints.

The operating limits of the distributed power system (such as active/reactive power and voltage limits) can be considered as follows [59]:

$$P_{gj}^{\min} \leq P_{gj} \leq P_{gj}^{\max}, \tag{9}$$

$$Q_{gj}^{\min} \leq Q_{gj} \leq Q_{gj}^{\max}, \tag{10}$$

$$0.95 \leq V_j \leq 1.05. \tag{11}$$

3. Harris Hawks Optimizer (HHO)

HHO is a population-based method with two phases for implementation: exploration and exploitation. The mathematical derivation of both phases is explained as follows.

3.1. Exploration Stage.

The prime purpose of the Harris hawks is hunting the prey, which is primarily a rabbit. Therefore, the hawks search for the rabbit. This exploring process can be categorized into two scenarios. The first scenario supposes that the hawks' locations are near the family members and the prey. At the same time, the following scenario considers the hawks' locations at random trees. The mathematical formulation of these two scenarios can be written as follows [60]:

$$X(i+1) = \begin{cases} X_{rand}(i) - rand_1 |X_{rand}(i) - 2rand_2 X(i)|, & p \geq 0.5, \\ [X_{prey}(i) - X_m(i)] - rand_3 [S_L + rand_4 (S_U - S_L)], & p \geq 0.5, \end{cases} \tag{12}$$

where i indicates the current iteration, $X(i+1)$ is the hawks' position at iteration $i+1$, $X(i)$ represents the hawks' position at the current iteration i, $X_{prey}(i)$ represents the prey's position at the current iteration i, $X_{rand}(i)$ represents the random position selection at the current iteration i, Rand1, Rand2, Rand3, and Rand4 represent the random position selection within [0, 1], and S_L and S_U denote the searching space with the lower and upper limits, respectively. Both exploration scenarios can be activated using a random variable p between 0 and 1.

$X_m(i)$ represents the mean hawks' position at the current iteration i and can be expressed as follows [61]:

$$X_m(i) = \frac{1}{h} \sum_{y=1}^{h} X_y(i), \tag{13}$$

where $X_y(i)$ denotes the hawk's position y and h represents the total number of hawks.

3.2. Transformation from Exploration to Exploitation.

The running away of the energy of the rabbit E_R during the chasing process is considered for the transformation from exploration to exploitation in the HHO algorithm. It is defined as follows [61]:

$$E_R = 2E_o \left(1 - \frac{i}{I}\right), \tag{14}$$

where I denotes the maximum number of iterations and E_o denotes the randomly generated initial energy of the rabbit within $[-1, 1]$. If $E_R \geq 1$, it means the hawks still carry on prey's tendency to escape and explore. If $E_R \leq 1$, the hawks will begin the process of exploitation close to the prey position, and the target will shift to avoid running.

3.3. Exploitation Stage.

The exploitation stage is subjected to the chances of the prey escaping (e) and running away with the energy E_R. The target successfully runs away when $e < 0.5$ and is unsuccessful during $e > 0.5$. The hawks can have two

options based on running away energy: soft surround during $|E_R| \geq 0.5$ and hard surround during $|E_R| < 0.5$.

As a result, the exploitation method is categorized in four steps as follows.

3.3.1. Easy surround.
The easy surround indicates the prey's efforts to escape with the help of haphazard jumps; nevertheless, the hawks quickly surround it. The mathematical derivation of this easy surround is defined as follows [52]:

$$X(i+1) = \Delta X(i) - E \big| K X_{prey}(i) - X(i) \big|, \qquad (15)$$

$$K = 2(1 - rand_5), \qquad (16)$$

$$\Delta X(i) = X_{prey}(i) - X(i), \qquad (17)$$

where $\Delta X(i)$ represents the distance of prey from hawks' location, K represents the randomly taken jumps of the target, and $rand_5$ denotes the random number within $[0, 1]$.

3.3.2. Difficult Surround.
The difficult surround occurs when $e \geq 0.5$ and $E_R < 0.5$. In this step, the prey is very tired, and it is difficult for the hawks to surround the rabbit (target). The mathematical formulation is written as follows [62]:

$$X(i+1) = X_{prey}(i) - E|\Delta X(i)|. \qquad (18)$$

3.3.3. Easy Surround with Progressive Speedy Dives.
This surround is assumed to be an intelligent scheme that differentiates the HHO algorithm from the other swarm optimization techniques. When $e < 0.5$ and $|E_R| \geq 0.5$, the prey has the energy to run away, and the hawks can quickly surround the prey. A Lévy flight (LF) idea is used for the formulation of this surround step as follows [52]:

$$W = X_{prey}(i) - E \big| K X_{prey}(i) - X(i) \big|, \qquad (19)$$

where W represents the easy surround location. Based on LF, the hawks' speedy dives are formulated as follows [62]:

$$V = W + S_R * LF(D_P), \qquad (20)$$

where D_P represents the problem dimension and S_R denotes the vector with randomly generated values with the matrix size of $1 * D_P$. The LF is defined as follows [62]:

$$LF(D_P) = 0.01 \times \frac{\alpha \times \sigma}{|\beta|^{1/c}}, \qquad (21)$$

$$\sigma = \left(\frac{\Gamma(1+c) \times \sin(\pi c/2)}{\Gamma((1+c)/2) \times c \times 2^{((c-1)/2)}} \right)^{1/c}, \qquad (22)$$

where c represents a constant value taken as 1.5 and α and β denote randomly generated values $[0, 1]$. Therefore, the hawks' location at the next iteration is defined as follows [62]:

$$X(i+1) = \begin{cases} W, & F(W) < F[X(i)], \\ V, & F(Z) < F[X(i)]. \end{cases} \qquad (23)$$

3.3.4. Difficult surround with Progressive Speedy Dives.
The surround is considered when $e < 0.5$ and $|E_R| < 0.5$, the prey is very tired, and the hawks have difficulty surrounding the prey. A similar Lévy flight (LF) idea is used for the formulation in equations (18) to (21), while the estimation of W is as follows [62]:

$$W = X_{prey}(i) - E \big| K X_{prey}(i) - X_m(i) \big|. \qquad (24)$$

The implementation steps of the HHO algorithm for DGs allocation are defined as follows:

Step 1: collecting the system data for the input of the HHO algorithm, such as line/load data. The objective functions are also defined along with the constraints.

Step 2: initializing the set of hawks' searches with randomly generated values for upper and lower limits of DGs sizing with the location. It also includes the initialization of HHO parameters with maximum iterations i_{max}.

Step 3: simulating the model with power flow analysis to calculate the objective functions such as P_{loss} for every searching hawk.

Step 4: saving the best value of solution $X_{prey}(i)$.

Step 5: updating the HHO parameters such as E_R, E_o, and K.

Step 6: updating the sizing and location of the best possible solution sets based on the two stages such as exploration and exploitation.

Step 7: updating the limitations on sizing and location of DGs while updating position $X(i+1)$.

Step 8: observing if $i < i_{max}$. Go to step 3 again.

Step 9: saving the finalized best solution, i.e., DGs location and sizing.

Step 10: simulating the power analysis for obtaining the bus voltage profiles.

4. Results and Discussion

This section analyzes the simulation results of different scenarios using two RDNs, namely, IEEE 33 [63] and 69 bus RDNs [64]. The optimal sizing and placement of DGs are simulated using the HHO algorithm. The main objectives are to minimize the total active and reactive power losses and voltage drop and maximize VSI. The MATLAB simulation environment is used, and the simulations are run fifteen times for different scenarios to ensure result accuracy and algorithm robustness. Four strategies are analyzed for each RDN under four seasonal uncertainties of load demand. Case 1 includes one DG, case 2 considers deployment of two DGs, case 3 has three DGs, and case 4 incorporates four DGs. The result comparison with feasible solutions of four cases is analyzed with the standard

optimization techniques under four seasonal uncertainties of load demands. Table 1 shows the simulation parameters. Table 2 shows exponent values for different load types.

4.1. IEEE 33-Bus RDN.

Figure 1 [63] shows IEEE 33-bus RDN [63], which comprises thirty-seven lines connected with 33 buses. The total active load demand is 3720 kW, while the total reactive load demand is 2300 kVAR. The total P loss is 208.4592 kW, and the bus voltage magnitude is 0.929 (per unit) [69].

Table 3 compares the minimum and average bus voltage values of literature with the results of proposed HHO for 33-bus RDN for exponent values of $\alpha = 0.720$, $\beta = 2.960$. Table 4 compares the minimum and average bus voltage values of literature with the results of proposed HHO for 33-bus RDN for exponent values of $\alpha = 0.920$, $\beta = 4.040$. Table 5 compares the minimum and average bus voltage values of literature with the results of proposed HHO for 33-bus RDN for exponent values of $\alpha = 1.040$, $\beta = 4.190$. Table 6 compares the minimum and average bus voltage values of literature with the results of proposed HHO for 33-bus RDN for exponent values of $\alpha = 1.300$, $\beta = 4.380$.

Table 7 compares the literature simulation results with the proposed HHO based on four DGs (IEEE 33-bus RDN). It is observed that the maximum active power loss reduction of 66.8% is obtained compared to the other literature results except for one case with the ABC algorithm. The total Q loss reduction of 56.4% is obtained, higher than different algorithm results except for two cases with BFOA and ABC methods. Moreover, the bus voltage deviation is also improved with the applied HHO algorithm. The total active and reactive power loss reduction is 52.98 kW and 42.23 kVAR. At the same time, the bus voltage magnitude is upgraded to 0.9471 (per unit). The objective function for this case is 0.36579.

Table 8 compares the literature simulation results with the proposed HHO based on three DGs (IEEE 33-bus RDN). It is observed that the maximum active power loss reduction of 69.65% is obtained as compared to the other literature results. Moreover, the bus voltage deviation is also improved with the applied HHO algorithm. The total P loss reduction is 107.93 kW. At the same time, the bus voltage magnitude is upgraded to 0.9706 (per unit). The objective function for this case is 0.39752.

4.1.1. Case 1 (33-Bus RDN) for Winter.

Figure 2(a) illustrates the bus voltage magnitude of 33-bus RDN with and without considering the deployment of one DG for winter load. The bus voltage magnitude is upgraded from 0.89587 (per unit) to 0.90998 (per unit). The feasible bus selection is bus 3. The objective function for this case is obtained as 0.39695. Figure 2(b) shows the active power loss, reduced from 159.61 kW to 121.21 kW, while the decrease of total P loss is 24.06%. Figure 2(c) shows the entire Q loss profile. For this case, the whole Q loss is reduced from 96.89 kVAR to 76.82 kVAR, while the decrease of total Q loss is 20.72%.

Table 1: Simulation parameters.

Parameters	33-bus RDN	IEEE 69-bus RDN	Units
Population size	200	200	—
Maximum iterations	100	100	—
Size limit of DGs	10~6000	10~6000	kW
K_{PR} [38]	350	350	$/kW
G_T [65]	0.19	0.19	$/kWh
I_R [38]	12.5	12.5	%
I_F [38]	9	9	%
No. of Iterations	50	50	—

Table 2: Different values of exponent values and load categories.

Load		α	β
Constant [66]		0	0
Residential [67]	Spring	0.720	2.960
	Summer	0.920	4.040
	Autumn	1.040	4.190
	Winter	1.300	4.380
Commercial [68]	Spring	1.250	3.500
	Summer	0.990	3.950
	Autumn	1.500	3.150
	Winter	1.510	3.400

The optimal DG size is found as 2578.5 kW. Table 9 presents the result summary for case 1 of 33-bus RDN for all four seasons' data.

4.1.2. Case 1 (33-Bus RDN) for Spring.

Figure 3(a) illustrates the bus voltage magnitude of 33-bus RDN with and without considering the deployment of one DG for spring load. The bus voltage magnitude is upgraded from 0.81372 (per unit) to 0.84089 (per unit). The feasible bus selection is bus 3. The objective function for this case is obtained as 0.52997. Figure 3(b) shows the total P loss, which is reduced from 494.60 kW to 368.02 kW, while the decrease of total P loss is 25.59%. Figure 3(c) shows the entire Q loss profile. For this case, the whole Q loss is reduced from 302.26 kVAR to 234.53 kVAR, while the decrease of total Q loss is 22.40%. The optimal DG size is found as 4888.1 kW. Table 9 presents the result summary for case 1 of 33-bus RDN for all four seasons' data.

4.1.3. Case 1 (33-Bus RDN) for Summer.

Figure 4(a) illustrates the bus voltage magnitude of 33-bus RDN with and without considering the deployment of one DG for summer load. The bus voltage magnitude is upgraded from 0.7819 (per unit) to 0.81484 (per unit). The feasible bus selection is bus 3. The objective function for this case is obtained as 0.59875. Figure 4(b) shows the total P loss reduced from 668.91 kW to 495.38 kW, while the decrease of total P loss is 25.94%. Figure 4(c) shows the entire Q loss profile. For this case, the whole Q loss is reduced from 410.01 kVAR to 316.11 kVAR, while the decrease of total Q loss is 22.90%. The optimal DG size is found as 5805.5 kW. Table 9 presents the result summary for case 1 of 33-bus RDN for all four seasons' data.
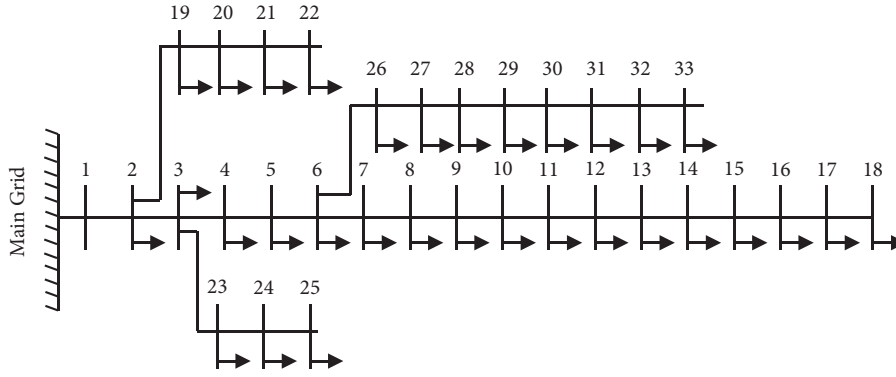
FIGURE 1: IEEE 33-bus RDN.

TABLE 3: Simulation results of system I ($\alpha = 0.720$, $\beta = 2.960$).

Algorithm	V_{ave} (per unit)	v_{min} (per unit)
FWA [70]	0.9694	0.9459
MBFOA [71]	0.9698	0.9430
ITS [72]	0.9677	0.9397
SLR [73]	0.9675	0.9397
PSO [68]	0.9557	0.9221
MPSO [68]	0.9675	0.9432
Proposed HHO	0.9786	0.9391

TABLE 4: Simulation results of system I ($\alpha = 0.920$, $\beta = 4.040$).

Algorithm	V_{ave} (per unit)	v_{min} (per unit)
FWA [70]	0.9700	0.9474
MBFOA [71]	0.9705	0.9446
ITS [72]	0.9684	0.9416
SLR [73]	0.9682	0.9416
PSO [68]	0.9552	0.9246
MPSO [68]	0.9682	0.9449
Proposed HHO	0.9758	0.9472

TABLE 5: Simulation results of system I ($\alpha = 1.040$, $\beta = 4.190$).

Algorithm	V_{ave} (per unit)	v_{min} (per unit)
FWA [70]	0.9702	0.9477
MBFOA [71]	0.9706	0.9450
ITS [72]	0.9686	0.9420
SLR [73]	0.9684	0.9420
PSO [68]	0.9556	0.9254
MPSO [68]	0.9684	0.9453
Proposed HHO	0.9843	0.9417

TABLE 6: Simulation results of system I ($\alpha = 1.300$, $\beta = 4.380$).

Algorithm	V_{ave} (per unit)	v_{min} (per unit)
FWA [70]	0.9705	0.9484
MBFOA [71]	0.9709	0.9457
ITS [72]	0.9689	0.9428
SLR [73]	0.9688	0.9428
PSO [68]	0.9564	0.9268
MPSO [68]	0.9688	0.9460
Proposed HHO	0.9871	0.9526

4.1.4. Case 1 (33-Bus RDN) for Autumn. Figure 5(a) illustrates the bus voltage magnitude of 33-bus RDN with and without considering the deployment of one DG for the autumn load. The bus voltage magnitude is upgraded from 0.87025 (per unit) to 0.8882 (per unit). The feasible bus selection is bus 3. The objective function for this case is obtained as 0.43087. Figure 5(b) shows the total P loss, which is reduced from 245.41 kW to 184.81 kW, while the decrease of total P loss is 24.69%. Figure 5(c) shows the entire Q loss profile. For this case, the whole Q loss is reduced from 149.26 kVAR to 117.38 kVAR, while the decrease of total Q loss is 21.36%. The optimal DG size is found as 3291.6 kW. Table 9 presents the result summary for case 1 of 33-bus RDN for all four seasons' data.

4.1.5. Case 2 (33-Bus RDN) for Winter. Figure 6(a) illustrates the bus voltage magnitude of 33-bus RDN with and without considering the deployment of two DGs for winter load. The bus voltage magnitude is upgraded from 0.89587 (per unit) to 0.9131 (per unit). The feasible buses are buses 3 and 6. The objective function for this case is obtained as 0.4016. Figure 6(b) shows the total P loss, which increased from 159.61 kW to 245.46 kW, while the percentage increase of total P loss is 53.78%. Figure 6(c) shows the entire Q loss profile. For this case, the whole Q loss increases from 96.89 kVAR to 142.43 kVAR, while the percentage increase of total Q loss is 46.9967%. Optimal DG sizes are found as 347.21 kW and 989.34 kW. Table 10 presents the result summary for case 2 of 33-bus RDN for all four seasons' data.

4.1.6. Case 2 (33-Bus RDN) for Spring. Figure 7(a) illustrates the bus voltage magnitude of 33-bus RDN with and without considering the deployment of two DGs for spring load. The bus voltage magnitude is upgraded from 0.81372 (per unit) to 0.84738 (per unit). The feasible buses are buses 3 and 6. The objective function for this case is obtained as 0.54649. Figure 7(b) shows the total P loss, which is increased from 494.60 kW to 736.49 kW, while the percentage increase of total P loss is 48.90%. Figure 7(c) shows the entire Q loss profile. For this case, the whole Q loss increases from 302.26 kVAR to 428.9 kVAR, while the percentage increase of total Q loss is 41.90%. Optimal DG sizes are found as

TABLE 7: Comparison of literature results with four DGs (33-bus RDN).

Algorithm Ref.	Year	$v_{\min}$ (per unit)	P loss (kW)	Q loss (kVAR)	P_{LOSS} reduction (%)	Q_{LOSS} reduction (%)	DG sizes (kW)	DG's location (bus no.)
Proposed HHO	2021	0.94714	52.9843	42.228	66.8047	56.4191	318.67, 42.94, 997.65, 322.88	3, 6, 8, 4
PPA [69]	2020	0.97900	58.36	—	72	—	1058.0, 2201.0, 171.70, 74.800	3, 6, 4, 5
GA [74]	2020	0.9810	64.190	19.9330	47.60	50.70	1500.0, 422.80, 1071.4, 5781.0	11, 29, 30, 8
PSO [74]	2020	0.9800	70.320	16.5420	48.20	50.40	1176.0, 981.60, 829.70, 959.00	8, 13, 32, 6
GA/PSO [74]	2020	0.9670	69.210	21.3200	49.20	43.70	925.00, 863.00, 1200.0, 1400.0	11, 16, 32, 5
HSA [65]	2020	0.9670	77.140	—	52.30	—	572.40, 107.00, 1046.2, 1034.0	17, 18, 33, 15
IWD [14]	2020	0.9696	68.720	—	57.70	—	600.30, 300.00, 1011.2, 1350.0	9, 16, 30, 13
BFOA [75]	2020	0.9640	—	—	51.50	57.30	633.00, 90.000, 947.00, 1000.0	17, 18, 33, 11
IWO [14]	2020	0.9716	68.710	—	57.70	54.30	624.00, 104.90, 1056.0, 879.40	14, 18, 32, 22
PSO & analytical [76]	2020	—	68.430	16.5400	64.10	52.30	790.00, 1070.0, 1010.0, 950.00	13, 24, 30, 20
SKHA [77]	2020	0.9687	73.450	—	64.70	52.10	801.80, 1091.0, 1053.6, 950.00	13, 24, 30, 43
ABC [65]	2020	0.9770	79.500	44.8540	67.30	58.40	514.00, 948.00, 635.16, 479.50	14, 28, 23, 3
SSA [40]	2019	0.9686	67.430	—	64.80	—	753.60, 1100.4, 1070.0, 570.00	13, 23, 29, 5
CDE [30]	2019	0.97020	67.12	—	67.8	—	926.69, 646.70, 967.30, 679.30	6, 14, 24, 31

TABLE 7: Continued.

Algorithm Ref.	Year	$v_{\min}$ (per unit)	P loss (kW)	Q loss (kVAR)	P_{LOSS} reduction (%)	Q_{LOSS} reduction (%)	DG sizes (kW)	DG's location (bus no.)
WCA [39]	2018	0.9730	74.530	—	64.00	—	854.6, 1101.7, 1180.0, 750.00	14, 24, 29, 11
BSOA [75]	2018	0.9554	65.350	—	56.10	53.40	32.000, 487.00, 550.00, 1000.0	13, 28, 31, 7
BA [78]	2018	0.9800	66.430	—	63.00	51.00	816.00, 952.50, 952.35, 598.00	15, 25, 30, 2
TLCHS [43]	2018	0.97700	67.28	—	67.72	—	941.20, 684.70, 966.40, 710.70	6, 14, 24, 31
ACO-ABC [68]	2017	0.9735	71.670	—	62.80	55.40	754.00, 1099.9, 1071.0, 589.40	14, 24, 30, 9
HGWO [79]	2013	—	77.430	—	64.40	53.30	802.00, 1090.0, 1054.0, 800.00	13, 24, 30, 21

715.63 and 1844.4 kW. Table 10 presents the result summary for case 2 of 33-bus RDN for all four seasons' data.

4.1.7. Case 2 (33-Bus RDN) for Summer. Figure 8(a) illustrates the bus voltage magnitude of 33-bus RDN with and without considering the deployment of two DGs for summer load. The bus voltage magnitude is upgraded from 0.7819 (per unit) to 0.8229 (per unit). The feasible buses are buses 3 and 6. The objective function for this case is obtained as 0.6219. Figure 8(b) shows the total P loss, which increased from 668.91 kW to 980.43 kW, while the percentage increase of total P loss is 46.57%. Figure 8(c) shows the entire Q loss profile. For this case, the whole Q loss increases from 410.01 kVAR to 571.85 kVAR, while the percentage increase of total Q loss is 39.47%. Optimal DG sizes are found as 873.16 and 2181.4 kW. Table 10 presents the result summary for case 2 of 33-bus RDN for all four seasons' data.

4.1.8. Case 2 (33-Bus RDN) for Autumn. Figure 9(a) illustrates the bus voltage magnitude of 33-bus RDN with and without considering the deployment of two DGs for the autumn load. The bus voltage magnitude is upgraded from 0.87025 (per unit) to 0.89229 (per unit). The feasible buses are buses 3 and 6. The objective function for this case is obtained as 0.43844. Figure 9(b) shows the total P loss, which increased from 245.41 kW to 374.05 kW, while the percentage increase of total P loss is 52.41%. Figure 9(c) shows the entire Q loss profile. For this case, the whole Q loss increases from 149.26 kVAR to 217.28 kVAR, while the percentage increase of total Q loss is 45.56%. Optimal DG

sizes are found as 457.26 and 1254.1 kW. Table 10 presents the result summary for case 2 of 33-bus RDN for all four seasons' data.

4.1.9. Case 3 (33-Bus RDN) for Winter. Figure 10(a) illustrates the bus voltage magnitude of 33-bus RDN with and without considering the deployment of three DGs for winter load. The bus voltage magnitude is upgraded from 0.89587 (per unit) to 0.95257 (per unit). The feasible buses are buses 3, 6, and 8. The objective function for this case is obtained as 0.36559. Figure 10(b) shows the total P loss, reduced from 159.61 kW to 52.52 kW, while the percentage decrease in P loss is 67.09%. Figure 10(c) illustrates the entire Q loss profile. For this case, the whole Q loss is reduced from 96.89 kVAR to 41.63 kVAR, while the percentage decrease of total Q loss is 57.03%. Optimal DG sizes are found as 728.58, 612.37, and 1092.6 kW. Table 11 presents the result summary for case 3 of 33-bus RDN for all four seasons' data.

4.1.10. Case 3 (33-Bus RDN) for Spring. Figure 11(a) illustrates the bus voltage magnitude of 33-bus RDN with and without considering the deployment of three DGs for spring load. The bus voltage magnitude is upgraded from 0.81372 (per unit) to 0.91907 (per unit). The feasible buses are buses 3, 6, and 8. The objective function for this case is obtained as 0.4185. Figure 11(b) shows the total P loss, reduced from 494.60 kW to 144.12 kW, while the percentage decrease of total P loss is 70.86%. Figure 11(c) illustrates the entire Q loss profile. For this case, the whole Q loss is reduced from 302.26 kVAR to 115.72 kVAR, while

TABLE 8: Comparison of literature results with three DGs (33-bus RDN).

Algorithm Ref.	Year	$v_{\min}$ (per unit)	FO	P loss (kW)	P_{LOSS} (%)	DG size (kW)	DG's location
ACO-ABC [35]	2015	0.9735	0.80075	77.540	62.800	754.700, 1099.90, 1071.40	14, 24, 30
BA [36]	2016	0.9800	0.80500	77.120	63.000	816.300, 952.350, 952.350	15, 25, 30
HA [7]	2016	—	0.32050	74.830	64.100	790.000, 1070.00, 1010.00	13, 24, 30
HGWO [37]	2017	—	0.32200	74.200	64.400	802.000, 1090.00, 1054.00	13, 24, 30
EMA [29]	2018	0.9684	0.80580	74.370	64.320	976.600, 1169.09, 943.540	30, 24, 12
SPEA2 [38]	2018	0.9616	0.83630	60.240	71.100	691.000, 733.400, 742.900	18, 29, 8
SSA [40]	2019	0.9686	0.80830	73.370	64.800	753.600, 1100.40, 1070.60	13, 23, 29
GSA-GAMS [31]	2019	0.9686	0.81250	71.620	65.640	801.220, 1091.30, 1053.59	13, 24, 30
GA [44]	2019	0.9860	0.82800	68.780	67.000	761.000, 1170.00, 1082.00	14, 24, 30
QOCSOS [42]	2020	—	0.32750	71.910	65.500	801.700, 1091.30, 1053.60	13, 24, 30
CSCA [14]	2020	0.9690	0.80700	73.990	64.500	871.000, 1091.47, 954.080	13, 24, 30
IHSA [48]	2020	—	0.32600	72.540	65.200	800.800, 1087.60, 1050.70	13, 24, 30
PPA [69]	2020	0.9700	0.84450	58.410	71.900	1141.80, 161.71, 2214.30	13, 23, 28
Proposed HHO	2021	0.9706	0.39752	107.925	69.647	1304.8, 751.02, 1735.5	3, 6, 8

the percentage decrease of total Q loss is 61.71%. Optimal DG sizes are found as 1161, 1177.6, and 1966.1 kW. Table 11 presents the result summary for case 3 of 33-bus RDN for all four seasons' data.

4.1.11. Case 3 (33-Bus RDN) for Summer. Figure 12(a) illustrates the bus voltage magnitude of 33-bus RDN with and without considering the deployment of three DGs for summer load. The bus voltage magnitude is upgraded from 0.7819 (per unit) to 0.90725 (per unit). The feasible buses are buses 3, 6, and 8. The objective function for this case is obtained as 0.44344. Figure 12(b) shows the total P loss

reduced from 668.91 kW to 187.69 kW, while the percentage decrease of total P loss is 71.94%. Figure 12(c) depicts the entire Q loss profile. For this case, the whole Q loss is reduced from 410.01 kVAR to 150.77 kVAR, while the total Q loss percentage decrease is 63.22%. Optimal DG sizes are found as 1419.6, 1288.6, and 2287.9 kW. Table 11 presents the result summary for case 3 of 33-bus RDN for all four seasons' data.

4.1.12. Case 3 (33-Bus RDN) for Autumn. Figure 13(a) illustrates the bus voltage magnitude of 33-bus RDN with and without considering the deployment of three DGs for the

(a)

(b)

(c)
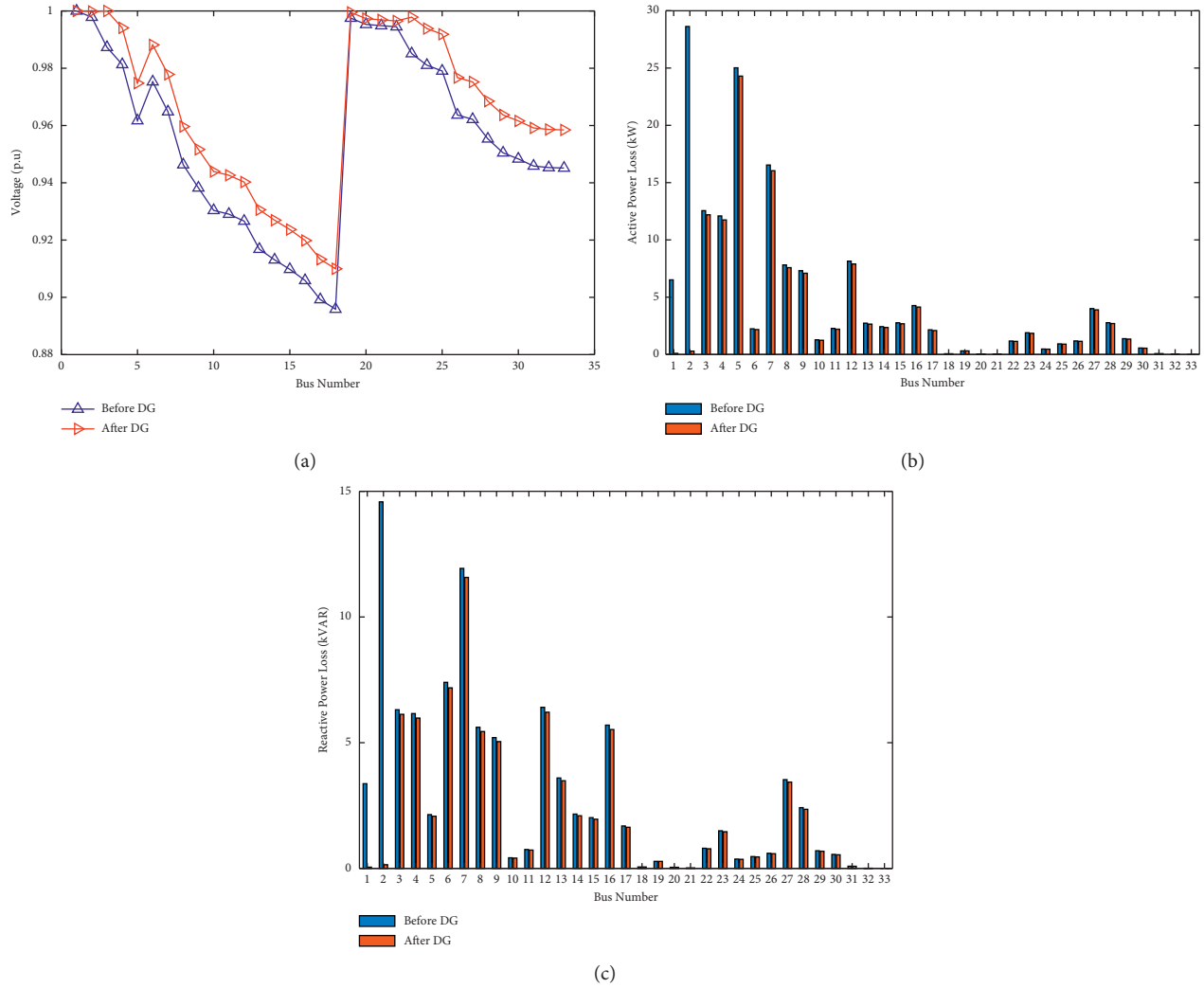
FIGURE 2: Case 1 (33-bus RDN) for winter. (a) Bus voltage profile. (b) Total *P* loss. (c) Total *Q* loss.

TABLE 9: Results of case 1 (33-bus RDN with HHO).

Season	v_{min} (per unit)	FO	P loss (kW)	Q loss (kVAR)	P_{LOSS} reduction (%)	Q_{LOSS} reduction (%)	DG's size (kW)	DG's location (bus no.)
Winter	0.90998	0.39695	121.2107	76.817	24.0599	20.7221	2578.5	3
Without DGs	0.89587	—	159.6136	96.8958	—	—	—	—
Spring	0.84089	0.52997	368.0215	234.5364	25.5925	22.4061	4888.1	3
Without DGs	0.81372	—	494.6027	302.2616	—	—	—	—
Summer	0.81484	0.59875	495.3813	316.1161	25.9429	22.9014	5805.5	3
Without DGs	0.7819	—	668.9179	410.0154	—	—	—	—
Autumn	0.8882	0.43087	184.8168	117.3823	24.6921	21.3622	3291.6	3
Without DGs	0.87025	—	245.4149	149.2695	—	—	—	—

autumn load. The bus voltage magnitude is upgraded from 0.87025 (per unit) to 0.9417 (per unit). The feasible buses are buses 3, 6, and 8. The objective function for this case is obtained as 0.37977. Figure 13(b) shows the total *P* loss, which is reduced from 245.41 kW to 77.19 kW, while the percentage decrease of total *P* loss is 68.54%. Figure 13(c) shows the entire *Q* loss profile. For this case, the whole *Q* loss is reduced from 149.26 kVAR to 61.62 kVAR, while the percentage decrease of total *Q* loss is 58.71%. Optimal DG

sizes are found as 804.21, 826.6, and 1369.4 kW. Table 11 presents the result summary for case 3 of 33-bus RDN for all four seasons' data.

4.1.13. Case 4 (33-Bus RDN) for Winter. Figure 14(a) illustrates the bus voltage magnitude of 33-bus RDN with and without considering the deployment of four DGs for winter load. The bus voltage magnitude is upgraded from 0.89587

(a)

(b)

(c)
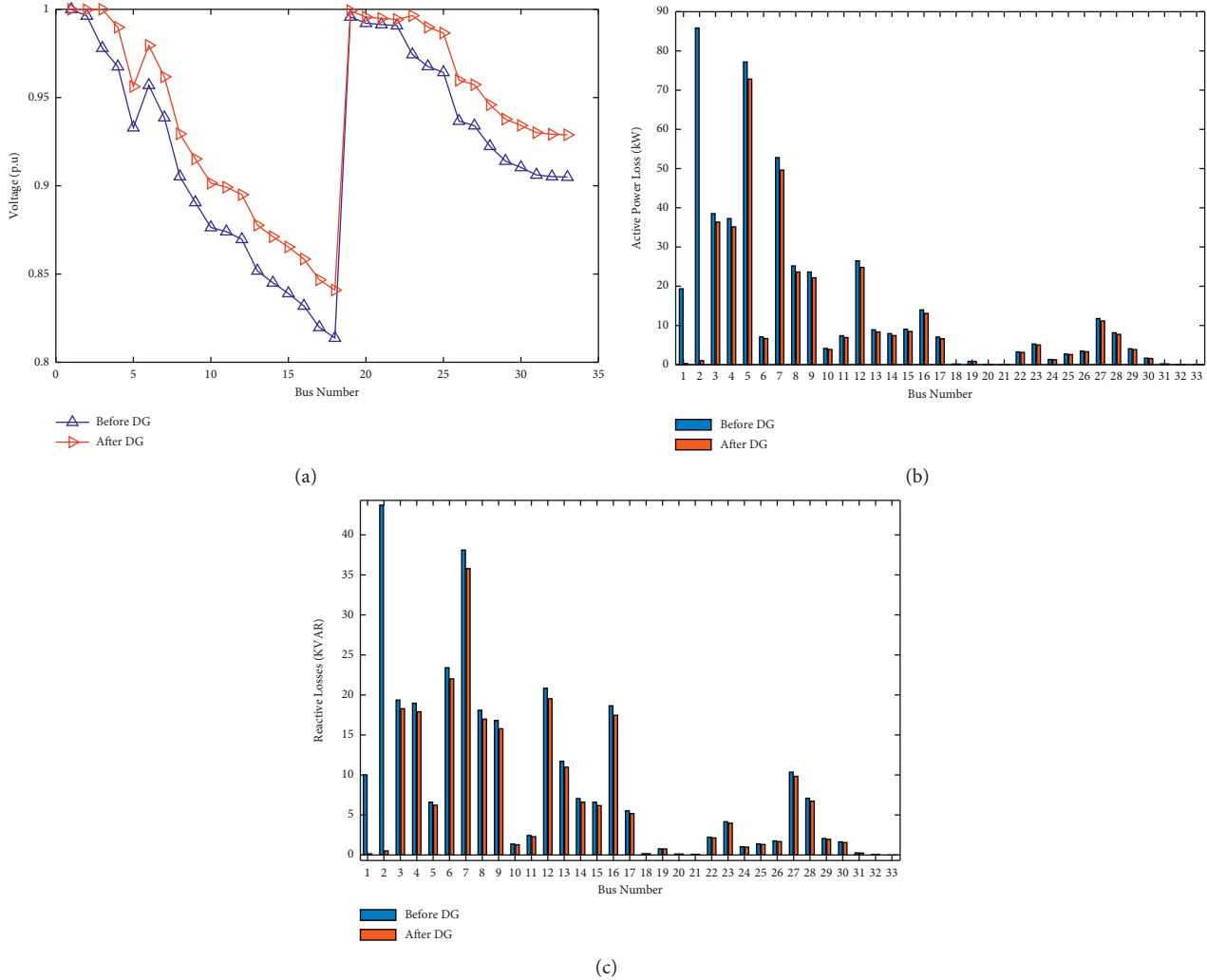
FIGURE 3: Case 1 (33-bus RDN) for spring. (a) Bus voltage profile. (b) Total P loss. (c) Total Q loss.

(per unit) to 0.95257 (per unit). The feasible buses are buses 3, 6, 8, and 4. The objective function for this case is obtained as 0.37277. Figure 14(b) shows the total P loss, reduced from 159.61 kW to 53.74 kW, while the percentage decrease of total P loss is 66.32%. Figure 14(c) depicts the entire Q loss profile. For this case, the whole Q loss is reduced from 96.89 kVAR to 42.04 kVAR, while the total Q loss percentage decrease is 56.60%. Optimal DG sizes are 579.36, 587.25, 1102.9, and 174.16 kW. Table 12 presents the result summary for case 4 of 33-bus RDN for all four seasons' data.

4.1.14. Case 4 (33-Bus RDN) for Spring. Figure 15(a) illustrates the bus voltage magnitude of 33-bus RDN with and without considering the deployment of four DGs for spring load. The bus voltage magnitude is upgraded from 0.81372 (per unit) to 0.91907 (per unit). The feasible buses are buses 3, 6, 8, and 4. The objective function for this case is obtained as 0.44263. Figure 15(b) shows the total P loss, reduced from 494.60 kW to 151.61 kW, while the percentage decrease in P loss is 69.34%. Figure 15(c) illustrates the entire Q loss profile. For this case, the whole Q loss is

reduced from 302.26 kVAR to 117.46 kVAR, while the total Q loss percentage decrease is 61.1376%. Optimal DG sizes are 987.93, 1116.1, 1997.2, and 290.95 kW. Table 12 presents the result summary for case 4 of 33-bus RDN for all four seasons' data.

4.1.15. Case 4 (33-Bus RDN) for Summer. Figure 16(a) illustrates the bus voltage magnitude of 33-bus RDN with and without considering the deployment of four DGs for summer load. The bus voltage magnitude is upgraded from 0.7819 (per unit) to 0.90725 (per unit). The feasible buses are buses 3, 6, 8, and 4. The objective function for this case is obtained as 0.47614. Figure 16(b) shows the total P loss, reduced from 668.91 kW to 199.11 kW, while the percentage decrease of total P loss is 70.23%. Figure 16(c) illustrates the entire Q loss profile. For this case, the complete Q loss is reduced from 410.01 kVAR to 153.37 kVAR, while the total Q loss percentage decrease is 62.59%. Optimal DG sizes are 1246, 1376.5, 2300.6, and 188.48 kW. Table 12 presents the result summary for case 4 of 33-bus RDN for all four seasons' data.

(a)

(b)

(c)
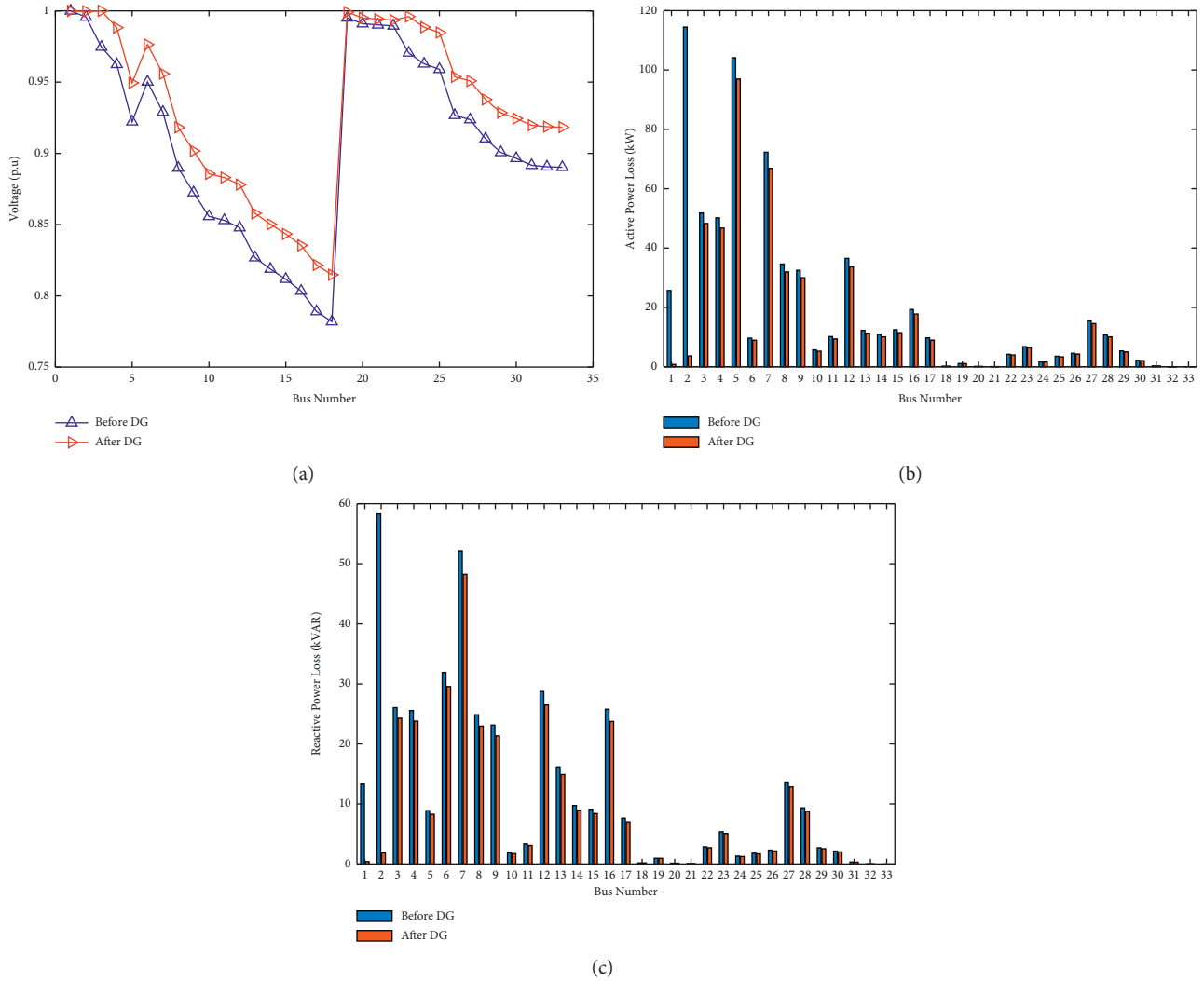
FIGURE 4: Case 1 (33-bus RDN) for summer. (a) Bus voltage profile. (b) Total P loss. (c) Total Q loss.

4.1.16. Case 4 (33-Bus RDN) for Autumn. Figure 17(a) illustrates the bus voltage magnitude of 33-bus RDN with and without considering the deployment of four DGs for the autumn load. The bus voltage magnitude is upgraded from 0.87025 (per unit) to 0.9417 (per unit). The feasible buses are buses 3, 6, 8, and 4. The objective function for this case is obtained as 0.3913. Figure 17(b) shows the total P loss, which is reduced from 245.41 kW to 79.70 kW, while the percentage decrease of total P loss is 67.52%. Figure 17(c) shows the entire Q loss profile. For this case, the whole Q loss is reduced from 149.26 kVAR to 62.25 kVAR, while the total Q loss percentage decrease is 58.29%. Optimal DG sizes are 749.27, 753.49, 1389.8, and 184.74 kW. Table 12 presents the result summary for case 4 of 33-bus RDN for all four seasons' data.

4.2. IEEE 69-Bus RDN. Figure 18 shows IEEE 69-bus RDN [80]. The total active load demand capacity of this IEEE 69-bus RDN is 3802 kW, while this system's total reactive load demand is 2696 kVAR. The total P loss is 225.007 kW, and the bus voltage is 0.9091 (per unit) [69].

Table 13 compares the literature simulation results with the proposed HHO based on four DGs (IEEE 33-bus RDN). It is observed that the maximum total P loss reduction of 72.75% is obtained as compared to the other literature results. The total Q loss reduction of 77.86% is obtained, which is higher than different algorithms results. Moreover, the bus voltage deviation is also improved with the applied HHO algorithm. The total active and Q loss reduction is 28.48 kW and 22.62 kVAR. In comparison, the bus voltage magnitude is upgraded to 0.97827 (per unit). The objective function for this case is 0.35001.

Table 14 compares the literature simulation results with the proposed HHO based on three DGs (IEEE 33-bus RDN). It is observed that the maximum total P loss reduction of 68.55% is obtained compared to the other literature results. The total Q loss reduction of 69.86% is obtained, which is higher than different algorithms results. Moreover, the bus voltage deviation is also improved with the applied HHO algorithm. The total active and Q loss reduction is 32.87 kW and 30.79 kVAR. At the same time, the bus voltage magnitude is upgraded to 0.9710 (per unit). The objective function for this case is 0.35373.

(a)

(b)

(c)
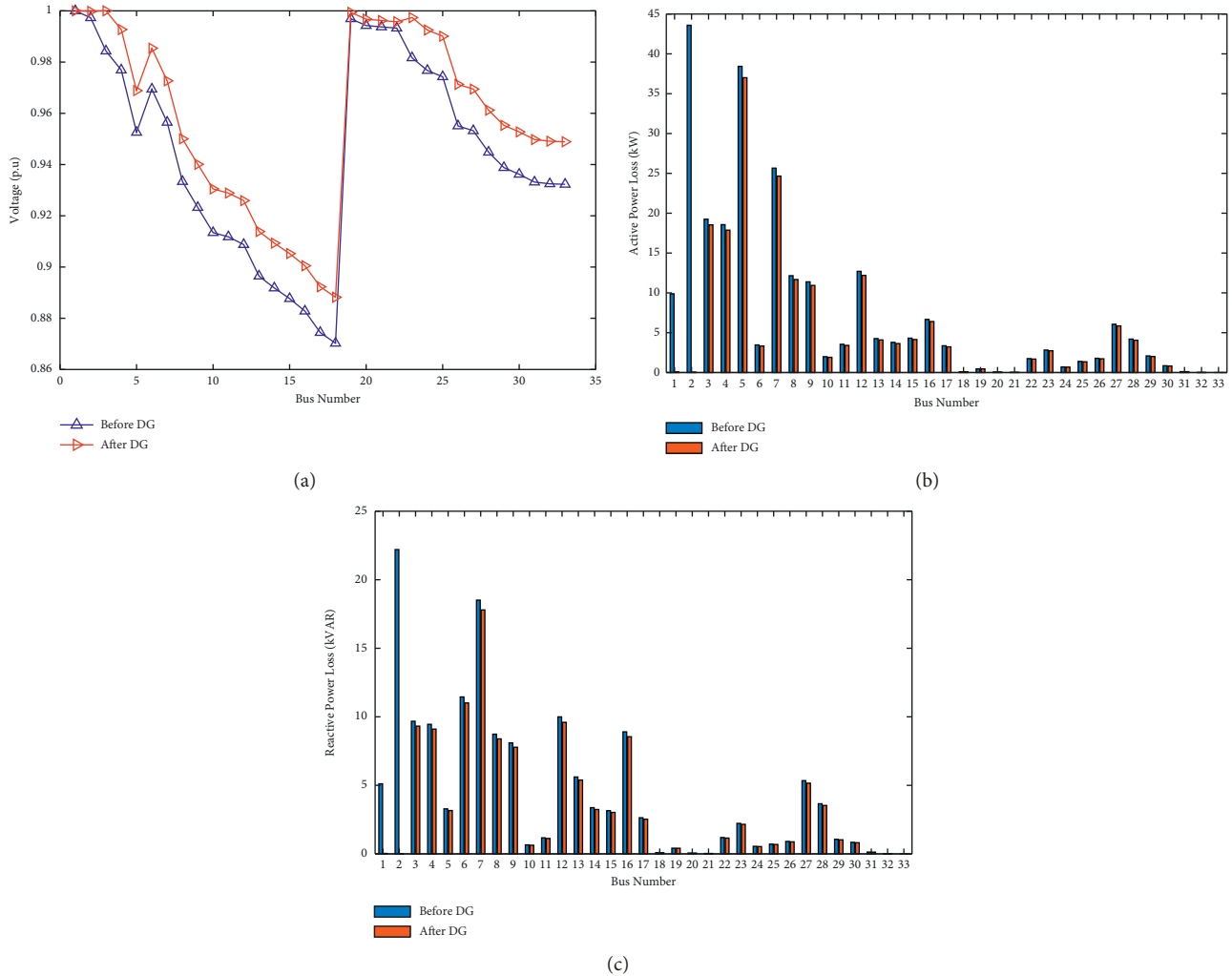
FIGURE 5: Case 1 (33-bus RDN) for autumn. (a) Bus voltage profile. (b) Total P loss. (c) Total Q loss.

Table 15 compares the literature simulation results with the proposed HHO based on two DGs (IEEE 33-bus RDN). It is observed that the maximum total P loss reduction of 67.16% is obtained as compared to the other literature results. Moreover, the bus voltage deviation is also improved with the applied HHO algorithm. The total P loss reduction is 34.32 kW, while the bus voltage magnitude is upgraded to 0.9710 (per unit). The objective function for this case is 0.35361.

Table 16 compares the literature simulation results with the proposed HHO based on one DG (IEEE 33-bus RDN). It is observed that the maximum total P loss reduction of 65.56% is obtained compared to the other literature results. Moreover, the bus voltage deviation is also improved with the applied HHO algorithm. The total P loss reduction is 36.01 kW. In comparison, the bus voltage magnitude is upgraded to 0.9710 (per unit). The objective function for this case is 0.35442.

4.2.1. Case 1 (69-Bus RDN) for Winter. Figure 19(a) illustrates the bus voltage of 69-bus RDN considering the deployment of one DG for winter load. The bus voltage

magnitude is upgraded from 0.93825 (per unit) to 0.97991 (per unit). The feasible bus selection is bus 57. The objective function for this case is obtained as 0.36388. Figure 19(b) shows the total P loss reduced from 104.53 kW to 35.74 kW while the percentage decrease of total P loss is 65.80%. Figure 19(c) depicts the entire Q loss profile. For this case, the whole Q loss is reduced from 47.61 kVAR to 15.93 kVAR, while the total Q loss percentage decrease is 66.53%. The optimal DG size is found as 1346.9 kW. Table 17 presents the result summary for case 1 of IEEE 69-bus RDN for all four seasons' data.

4.2.2. Case 1 (69-Bus RDN) for Spring. Figure 20(a) illustrates the bus voltage of 69-bus RDN considering the deployment of one DG for spring load. The bus voltage magnitude is upgraded from 0.89392 (per unit) to 0.96656 (per unit). The feasible bus selection is bus 57. The objective function for this case is obtained as 0.41038. Figure 20(b) shows the total P loss reduced from 306.20 kW to 97.97 kW while the percentage decrease of total P loss is 68.00%. Figure 20(c) illustrates the entire Q loss profile. For this case,

(a)

(b)

(c)
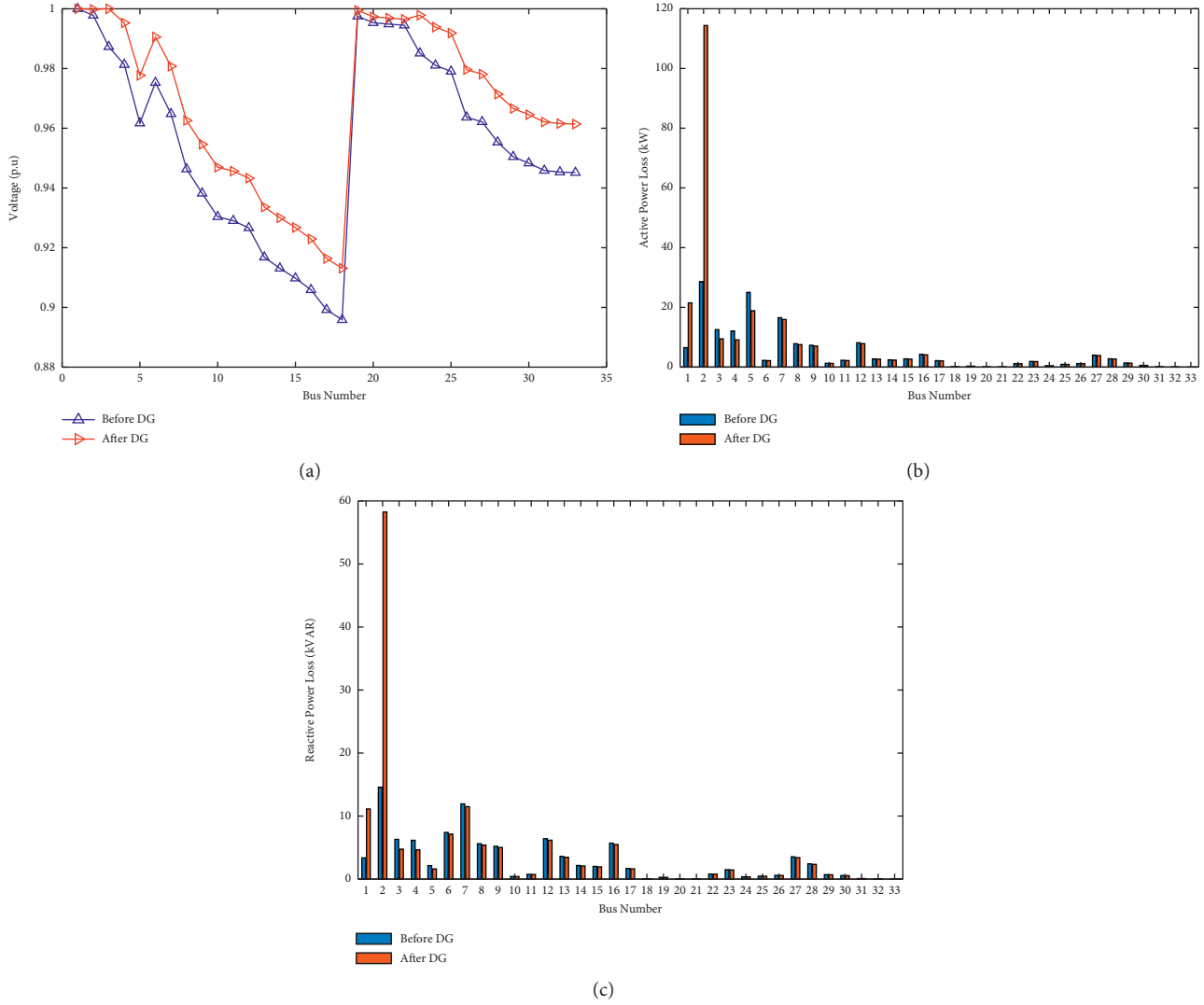
FIGURE 6: Case 2 (33-bus RDN) for winter. (a) Bus voltage profile. (b) Total P loss. (c) Total Q loss.

TABLE 10: Results of case 2 (33-bus RDN with HHO).

Season	v_{min} (per unit)	FO	P loss (kW)	Q loss (kVAR)	P_{LOSS} reduction (%)	Q_{LOSS} reduction (%)	DG's size (kW)	DG's location (bus no.)
Winter	0.9131	0.4016	245.4671	142.4336	−53.7883	−46.9967	347.21, 989.34	3, 6
Without DGs	0.89587	—	159.6136	96.8958	—	—	—	—
Spring	0.84738	0.54649	736.4943	428.922	−48.9062	−41.9042	715.63, 1844.4	3, 6
Without DGs	0.81372	—	494.6027	302.2616	—	—	—	—
Summer	0.8229	0.6219	980.4337	571.8549	−46.5701	−39.4716	873.16, 2181.4	3, 6
Without DGs	0.7819	—	668.9179	410.0154	—	—	—	—
Autumn	0.89229	0.43844	374.0595	217.289	−52.4192	−45.5682	457.26, 1254.1	3, 6
Without DGs	0.87025	—	245.4149	149.2695	—	—	—	—

the complete Q loss is reduced from 138.81 kVAR to 43.65 kVAR, while the total Q loss percentage decrease is 68.55%. The optimal DG size is found as 2357.2 kW. Table 17 presents the result summary for case 1 of IEEE 69-bus RDN for all four seasons' data.

4.2.3. Case 1 (69-Bus RDN) for Summer. Figure 21(a) illustrates the bus voltage of 69-bus RDN considering the deployment of one DG for summer load. The bus voltage magnitude is upgraded from 0.87809 (per unit) to 0.96204 (per unit). The feasible bus selection is bus 57. The objective

(a)

(b)

(c)
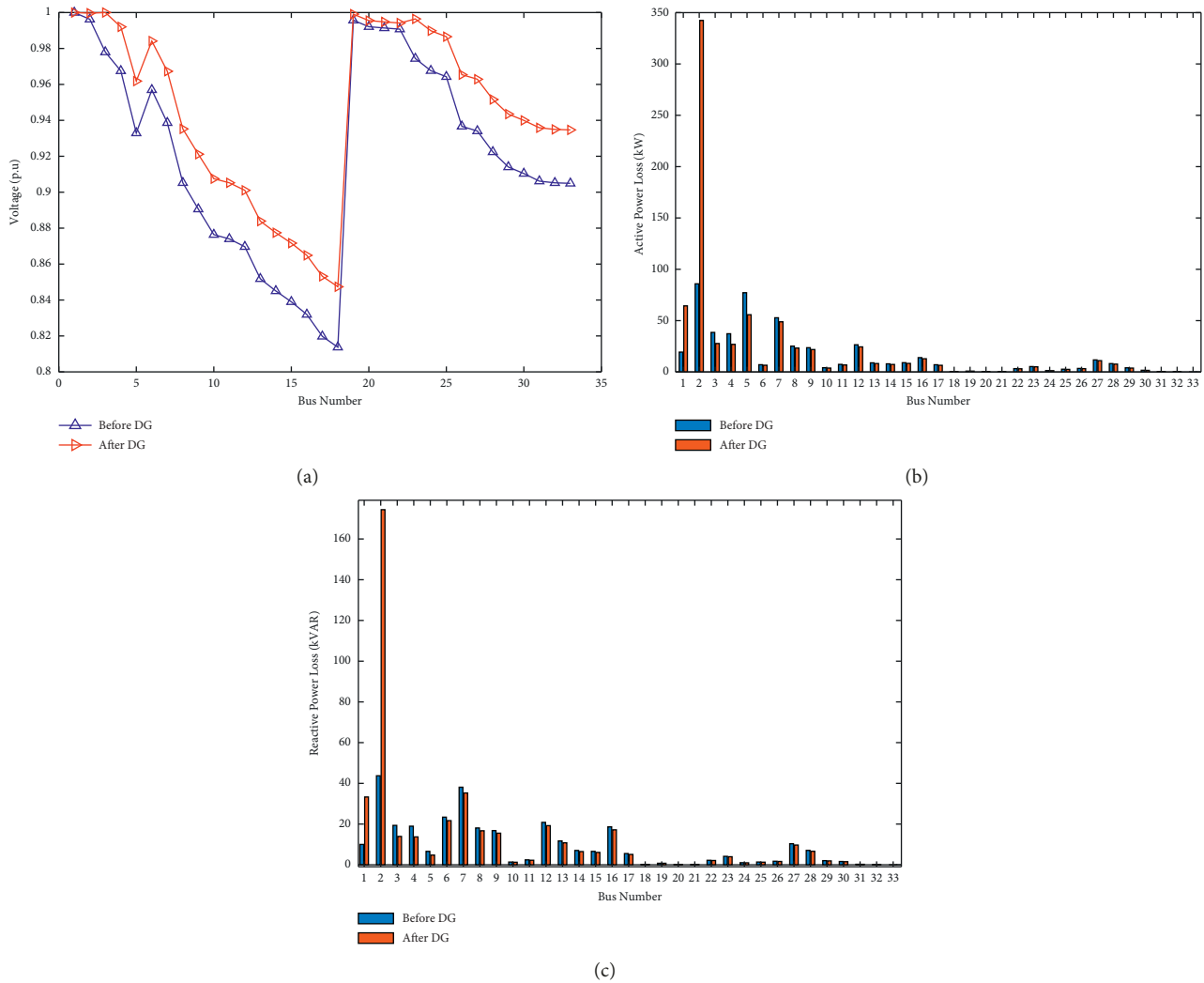
FIGURE 7: Case 2 (33-bus RDN) for spring. (a) Bus voltage profile. (b) Total P loss. (c) Total Q loss.

function for this case is obtained as 0.43178. Figure 21(b) shows the total P loss reduced from 403.28 kW to 126.69 kW while the percentage decrease of total P loss is 68.58%. Figure 21(c) illustrates the entire Q loss profile. For this case, the whole Q loss is reduced from 182.51 kVAR to 56.41 kVAR, while the total Q loss percentage decrease is 69.08%. The optimal DG size is found as 2710.8 kW. Table 17 presents the result summary for case 1 of IEEE 69-bus RDN for all four seasons' data.

4.2.4. Case 1 (69-Bus RDN) for Autumn. Figure 22(a) illustrates the bus voltage of 69-bus RDN considering the deployment of one DG for the autumn load. The bus voltage magnitude is upgraded from 0.92395 (per unit) to 0.9755 (per unit). The feasible bus selection is bus 57. The objective function for this case is obtained as 0.37651. Figure 22(b) shows the total P loss reduced from 158.1946 kW to 52.7248 kW, while percentage decrease of total P loss is 66.67%. Figure 22(c) depicts the entire Q loss profile. For this case, the total Q loss is reduced from 71.94 kVAR to 23.50 kVAR, while the total Q loss percentage decrease is 67.32%. The optimal DG size is

found as 1675.6 kW. Table 17 presents the result summary for case 1 of IEEE 69-bus RDN for all four seasons' data.

4.2.5. Case 2 (69-Bus RDN) for Winter. Figure 23(a) illustrates the bus voltage of 69-bus RDN considering the deployment of two DGs for winter load. The bus voltage magnitude is upgraded from 0.93825 (per unit) to 0.97991 (per unit). The feasible buses are 57 and 7. The objective function for this case is obtained as 0.37332. Figure 23(b) shows the total P loss, which increased from 104.5347 kW to 346.82 kW, while the percentage increase of total P loss is 231.77%. Figure 23(c) depicts the entire Q loss profile. The total Q loss for this case is increased from 47.61 kVAR to 155.20 kVAR, while the percentage increase of total Q loss is 225.97%. Optimal DG sizes are found as 868.32 and 419.28 kW. Table 18 presents case 2 of IEEE 69-bus RDN for all four seasons' data.

4.2.6. Case 2 (69-Bus RDN) for Spring. Figure 24(a) illustrates the bus voltage of 69-bus RDN considering the deployment of two DGs for spring load. The bus voltage magnitude is

(a)

(b)

(c)
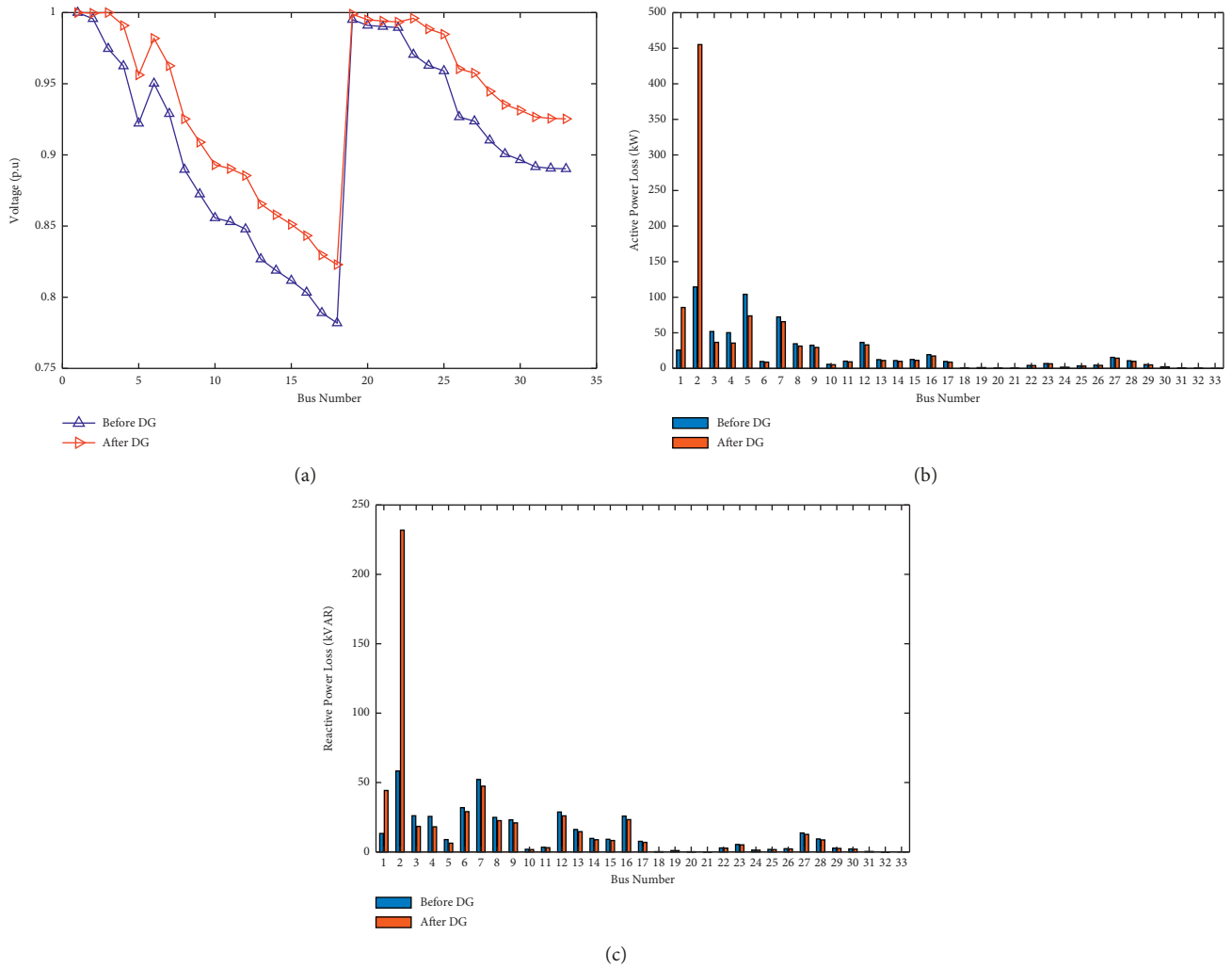
FIGURE 8: Case 2 (33-bus RDN) for summer. (a) Bus voltage profile. (b) Total P loss. (c) Total Q loss.

upgraded from 0.89392 (per unit) to 0.96656 (per unit). The feasible buses are 57 and 7. The objective function for this case is obtained as 0.4422. Figure 24(b) shows the total P loss, which is increased from 306.2051 kW to 1122.09 kW, while the percentage increase of total P loss is 266.45%. Figure 24(c) shows the entire Q loss profile. The total Q loss for this case is increased from 138.81 kVAR to 504.27 kVAR, while the percentage increase of total Q loss is 263.28%. Optimal DG sizes are found as 1484.7 and 788.66 kW. Table 18 presents case 2 of IEEE 69-bus RDN for all four seasons' data.

4.2.7. Case 2 (69-Bus RDN) for Summer. Figure 25(a) illustrates the bus voltage of 69-bus RDN considering the deployment of two DGs for summer load. The bus voltage magnitude is upgraded from 0.87809 (per unit) to 0.96204 (per unit). The feasible buses are 57 and 7. The objective function for this case is obtained as 0.4752. Figure 25(b) shows the total P loss, which is increased from 403.28 kW to 1542.18 kW, while the percentage increase of total P loss is 282.40%. Figure 25(c) shows the entire Q loss profile. The total Q loss for this case is increased from 182.51 kVAR to 694.29 kVAR, while the

percentage increase of total Q loss is 280.40%. Optimal DG sizes are found as 1699.7 and 923.42 kW. Table 18 presents case 2 of IEEE 69-bus RDN for all four seasons' data.

4.2.8. Case 2 (69-Bus RDN) for Autumn. Figure 26(a) illustrates the bus voltage of 69-bus RDN considering the deployment of two DGs for the autumn load. The bus voltage magnitude is upgraded from 0.92395 (per unit) to 0.9755 (per unit). The feasible buses are 57 and 7. The objective function for this case is obtained as 0.39162. Figure 26(b) shows the total P loss, which increased from 158.19 kW to 540.53 kW, while the percentage increase of total P loss is 241.68%. Figure 26(c) depicts the entire Q loss profile. The total Q loss for this case is increased from 71.94 kVAR to 242.19 kVAR, while the percentage increase of total Q loss is 236.64%. Optimal DG sizes are found as 1068.5 and 540.77 kW. Table 18 presents case 2 of IEEE 69-bus RDN for all four seasons' data.

4.2.9. Case 3 (69-Bus RDN) for Winter. Figure 27(a) illustrates the bus voltage of 69-bus RDN considering the deployment of three DGs for winter load. The bus voltage

(a)

(b)

(c)
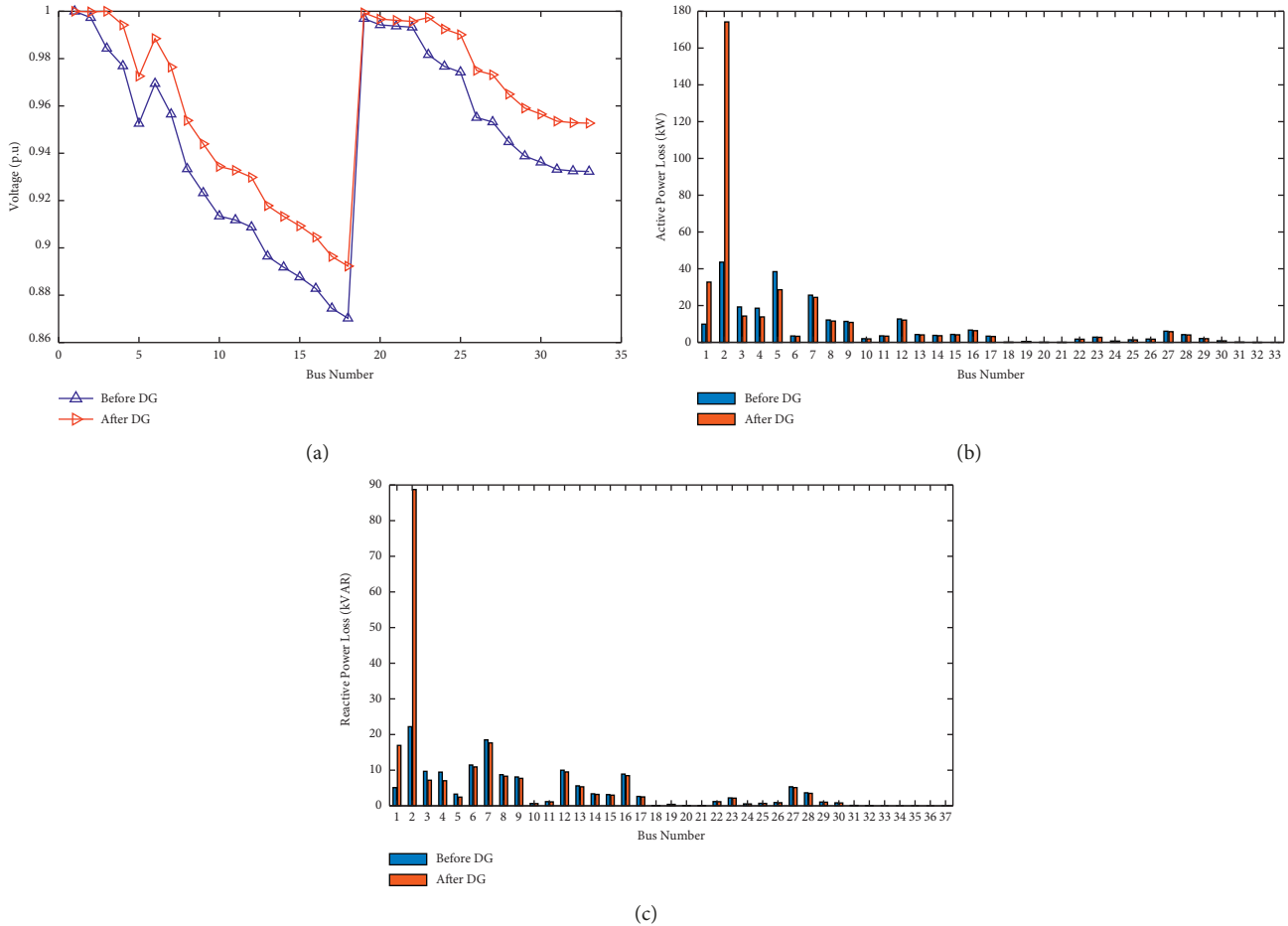
FIGURE 9: Case 2 (33-bus RDN) for autumn. (a) Bus voltage profile. (b) Total P loss. (c) Total Q loss.

magnitude is upgraded from 0.9091 (per unit) to 0.97991 (per unit). The feasible buses are 57, 7, and 6. The objective function for this case is obtained as 0.36328. Figure 27(b) shows the total P loss, reduced from 225.00 kW to 33.27 kW, while the percentage decrease of total P loss is 33.27%. Figure 27(c) illustrates the entire Q loss profile. For this case, the total Q loss is reduced from 33.27 kVAR to 14.74 kVAR, while the total Q loss percentage decrease is 14.74%. Optimal DG sizes are found as 1212.5, 552.87, and 19.166 kW. Table 19 presents case 3 of IEEE 69-bus RDN for all four seasons' data.

4.2.10. Case 3 (69-Bus RDN) for Spring. Figure 28(a) illustrates the bus voltage of 69-bus RDN considering the deployment of three DGs for spring load. The bus voltage magnitude is upgraded from 0.89392 (per unit) to 0.96656 (per unit). The feasible buses are 57, 7, and 6. The objective function for this case is obtained as 0.3799. Figure 28(b) shows the total P loss reduced from 306.20 kW to 92.49 kW while the percentage decrease of total P loss is 69.79%. Figure 28(c) illustrates the entire Q loss profile. For this case, the total Q loss is reduced from 138.81 kVAR to 40.90 kVAR, while the percentage decrease in Q loss is 70.53%. Optimal

DG sizes are found as 2108.7, 706.76, and 247.28 kW. Table 19 presents case 3 of IEEE 69-bus RDN for all four seasons' data.

4.2.11. Case 3 (69-Bus RDN) for Summer. Figure 29(a) illustrates the bus voltage of 69-bus RDN considering the deployment of three DGs for summer load. The bus voltage magnitude is upgraded from 0.87809 (per unit) to 0.96204 (per unit). The feasible buses are 57, 7, and 6. The objective function for this case is obtained as 0.39179. Figure 29(b) shows the total P loss, reduced from 403.28 kW to 117.10 kW, while the percentage decrease of total P loss is 70.96%. Figure 29(c) illustrates the entire Q loss profile. For this case, the total Q loss is reduced from 70.96 kVAR to 51.63 kVAR, while the percentage decrease is 71.70%. Optimal DG sizes are found as 2361.5, 1059.3, and 128.55 kW. Table 19 presents case 3 of IEEE 69-bus RDN for all four seasons' data.

4.2.12. Case 3 (69-Bus RDN) for Autumn. Figure 30(a) illustrates the bus voltage of 69-bus RDN considering the deployment of three DGs for the autumn load. The bus voltage magnitude is upgraded from 0.92395 (per unit) to

(a)

(b)

(c)
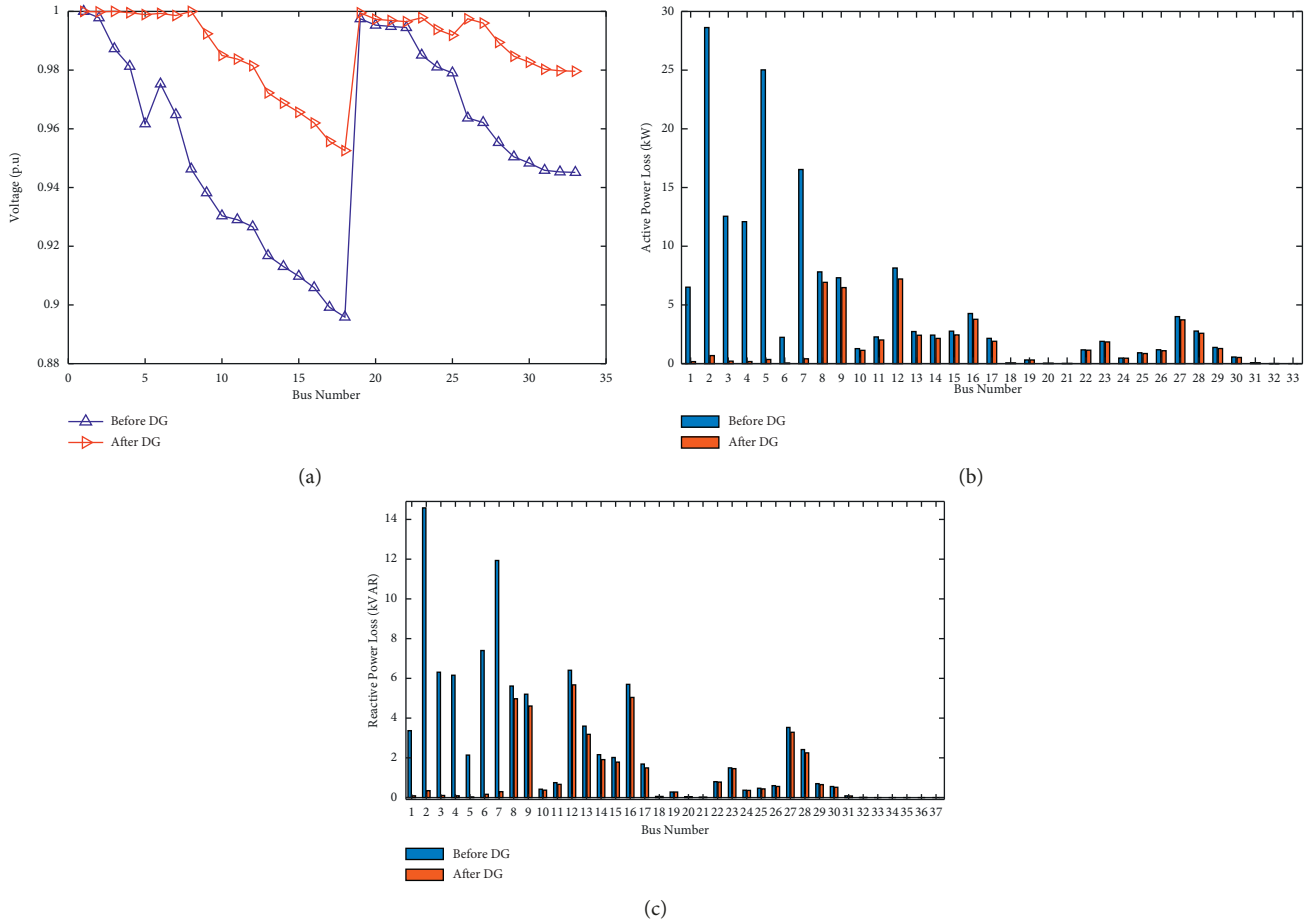
FIGURE 10: Case 3 (33-bus RDN) for winter. (a) Bus voltage profile. (b) Total P loss. (c) Total Q loss.

TABLE 11: Results of case 3 (33-bus RDN with HHO).

Season	v_{min} (per unit)	FO	P loss (kW)	Q loss (kVAR)	P_{LOSS} reduction (%)	Q_{LOSS} reduction (%)	DG's size (kW)	DG's location (bus no.)
Winter	0.95257	0.36559	52.528	41.6315	67.0905	57.0347	728.58, 612.37, 1092.6	3, 6, 8
Without DGs	0.89587	—	159.6136	96.8958			—	—
Spring	0.91907	0.4185	144.1232	115.7245	70.8608	61.7138	1161, 1177.6, 1966.1	3, 6, 8
Without DGs	0.81372	—	494.6027	302.2616	—	—	—	—
Summer	0.90725	0.44344	187.6912	150.7715	71.9411	63.2278	1419.6, 1288.6, 2287.9	3, 6, 8
Without DGs	0.7819	—	668.9179	410.0154	—	—	—	—
Autumn	0.9417	0.37977	77.1988	61.6239	68.5435	58.7164	804.21, 826.6, 1369.4	3, 6, 8
Without DGs	0.87025	—	245.4149	149.2695			—	—

0.9755 (per unit). The feasible buses are 57, 7, and 6. The objective function for this case is obtained as 0.36075. Figure 30(b) shows the total P loss reduced from 158.19 kW to 49.35 kW while the percentage decrease of total P loss is 68.80%. Figure 30(c) illustrates the entire Q loss profile. For this case, the total Q loss is reduced from 71.94 kVAR to 21.85 kVAR, while the total Q loss percentage decrease is 69.62%. Optimal DG sizes are found as 1483.8, 674.15, and

(a)

(b)

(c)
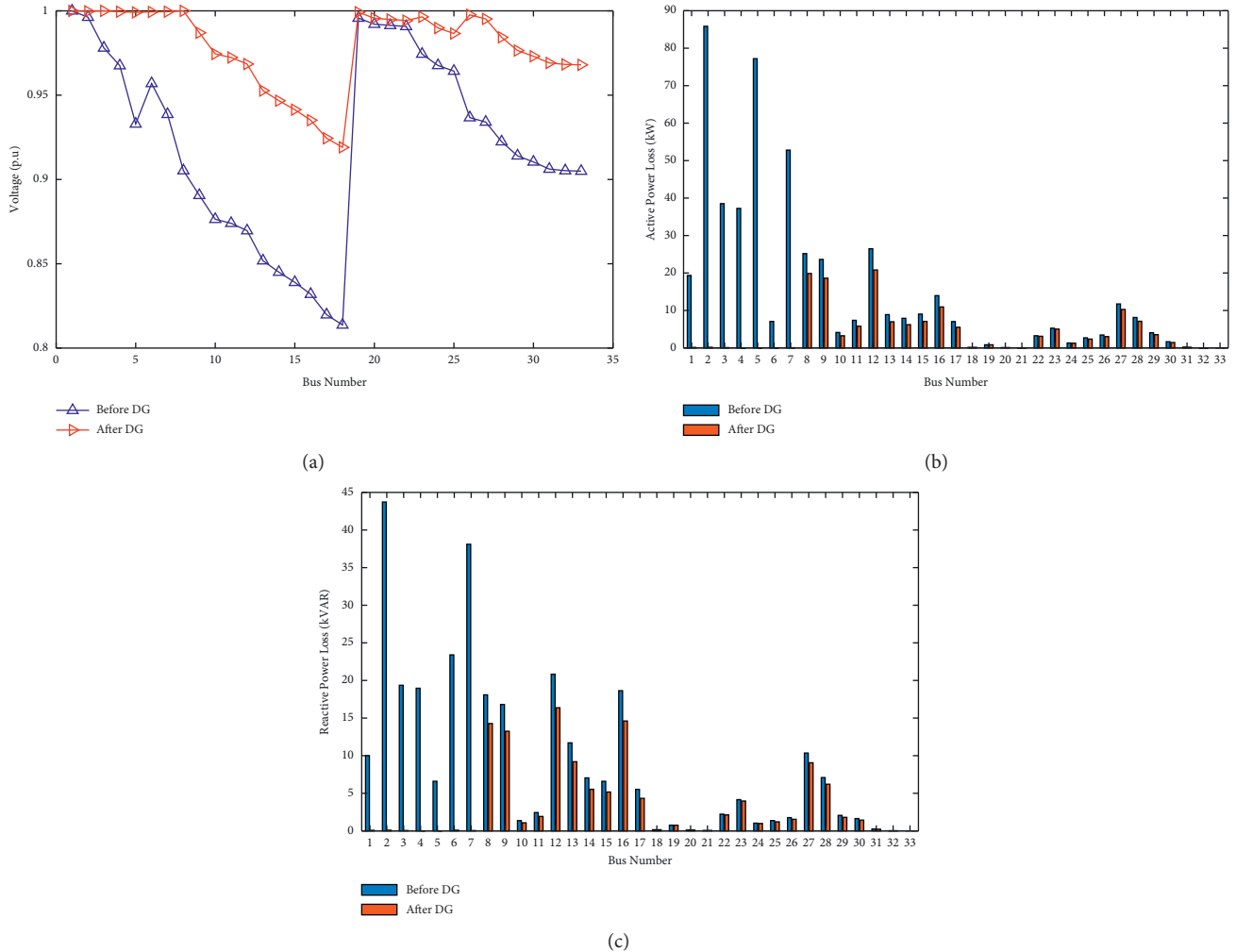
FIGURE 11: Case 3 (33-bus RDN) for spring. (a) Bus voltage profile. (b) Total P loss. (c) Total Q loss.

23.574 kW. Table 19 presents case 3 of IEEE 69-bus RDN for all four seasons' data.

4.2.13. Case 4 (69-Bus RDN) for Winter. Figure 31(a) illustrates the bus voltage of 69-bus RDN considering the deployment of four DGs for winter load. The bus voltage magnitude is upgraded from 0.93825 (per unit) to 0.9849 (per unit). The feasible buses are 57, 7, 6, and 58. The value of the objective function for this case is 0.36025. Figure 31(b) shows the total P loss reduced from 104.53 kW to 22.76 kW while the percentage decrease of total P loss is 78.22%. Figure 31(c) depicts the entire Q loss profile. For this case, the total Q loss is reduced from 47.61 kVAR to 11.21 kVAR, while the total Q loss percentage decrease is 76.45%. Optimal DG sizes are 40.66, 553.91, 19.998, and 1156.8 kW. Table 20 presents the result summary for case 4 of IEEE 69-bus RDN for all four seasons' data.

4.2.14. Case 4 (69-Bus RDN) for Spring. Figure 32(a) illustrates the bus voltage of 69-bus RDN considering the deployment of four DGs for spring load. The bus voltage

magnitude is upgraded from 0.89392 (per unit) to 0.97496 (per unit). The feasible buses are 57, 7, 6, and 58. The value of the objective function for this case is 0.39921. Figure 32(b) shows the total P loss, reduced from 306.20 kW to 61.15 kW, while the percentage decrease of total P loss is 80.02%. Figure 32(c) illustrates the entire Q loss profile. For this case, the total Q loss is reduced from 138.81 kVAR to 30.04 kVAR, while the percentage decrease in Q loss is 78.35%. Optimal DG sizes are 108.65, 1032.2, 31.762, and 1957.5 kW. Table 20 presents the result summary for case 4 of IEEE 69-bus RDN for all four seasons' data.

4.2.15. Case 4 (69-Bus RDN) for Summer. Figure 33(a) illustrates the bus voltage of 69-bus RDN considering the deployment of four DGs for summer load. The bus voltage magnitude is upgraded from 0.87809 (per unit) to 0.97161 (per unit). The feasible buses are 57, 7, 6, and 58. The value of the objective function for this case is 0.417. Figure 33(b) shows the total P loss, which is reduced from 403.28 kW to 78.85 kW, while the percentage decrease of total P loss is 80.44%. Figure 33(c) shows the

(a)

(b)

(c)
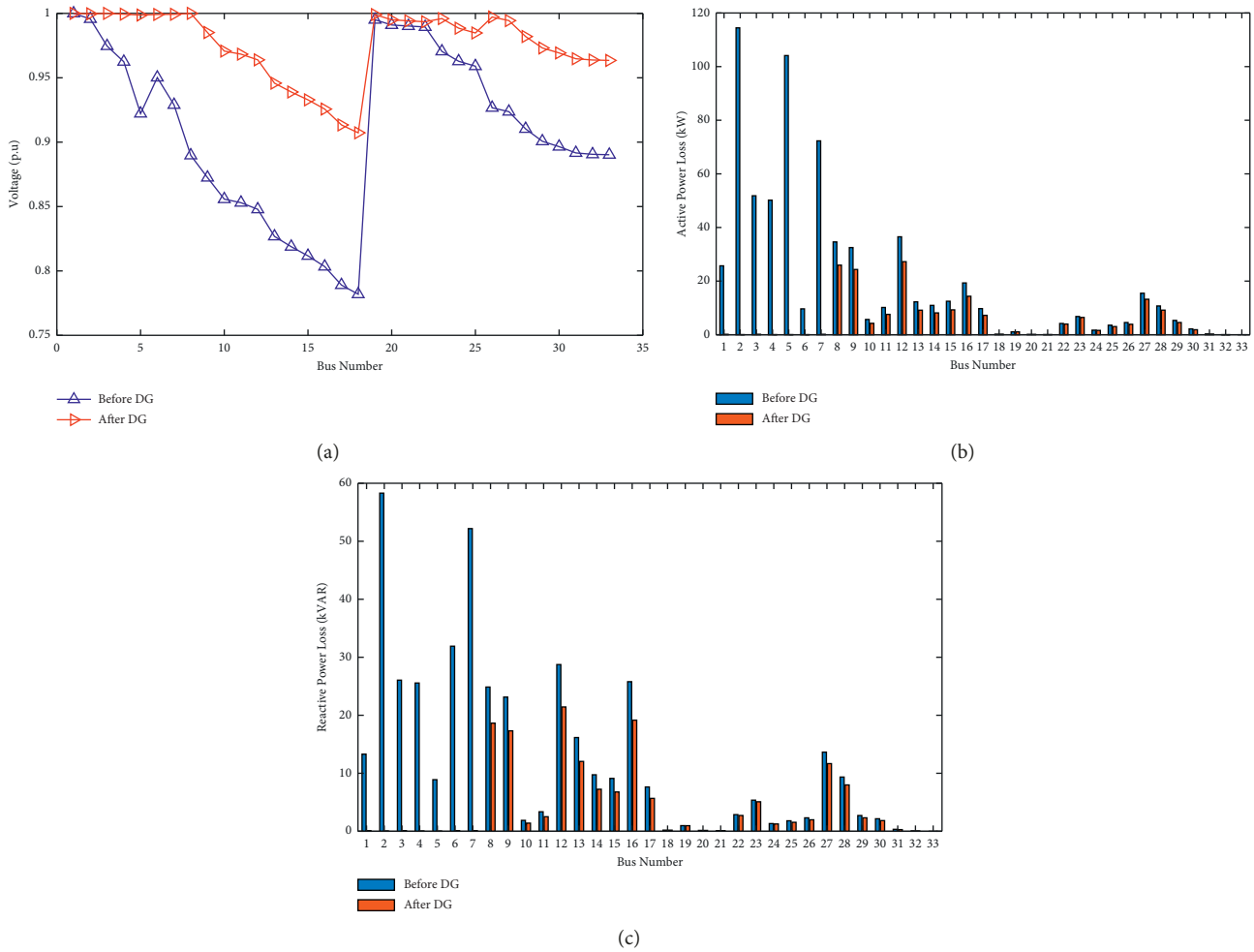
FIGURE 12: Case 3 (33-bus RDN) for summer. (a) Bus voltage profile. (b) Total P loss. (c) Total Q loss.

total Q loss profile. For this case, the total Q loss is reduced from 182.51 kVAR to 38.68 kVAR, while the percentage decrease in Q loss is 78.80%. Optimal DG sizes are 123.63, 1198.9, 41.268, and 2240.5 kW. Table 20 presents the result summary for case 4 of IEEE 69-bus RDN for all four seasons' data.

4.2.16. Case 4 (69-Bus RDN) for Autumn. Figure 34(a) illustrates the bus voltage of 69-bus RDN considering the deployment of four DGs for the autumn load. The bus voltage magnitude is upgraded from 0.92395 (per unit) to 0.98161 (per unit). The feasible buses are 57, 7, 6, and 58. The value of the objective function for this case is 0.37089. Figure 34(b) shows the total P loss, reduced from 158.19 kW to 33.24 kW, while the percentage decrease of total P loss is 33.24%. Figure 34(c) shows the total Q loss profile. For this case, the total Q loss is reduced from 71.94 kVAR to 16.36 kVAR, while the percentage decrease in Q loss is 77.24%. Optimal DG sizes are 54.404, 700.2, 39.572, and 1427.1 kW. Table 20 presents the result summary for case 4 of IEEE 69-bus RDN for all four seasons' data.

4.3. Comparison of Cases. Figures 35(a) and 35(b) show the bus voltage and total P loss profiles of 33-bus RDN with the deployment of one, two, three, and four DGs for all four cases, respectively.

For winter load, the bus voltage drop is minimized in case 3 of 33-bus RDN, which is 0.95257 (per unit), which shows more improved value than other cases. The total P loss reduction for case 3 of 33-bus RDN is 52.52 kW, while the percentage decrease of total P loss, in this case, is 67.09% which shows that deployment of three DGs in a 33-bus system is more feasible in terms of minimized total P loss with improved bus voltage. The total Q loss for case 3 of 33-bus RDN is 41.63 kVAR, while the percentage decrease of total Q loss is 57.03% which shows that deployment of three DGs in a 33-bus system is still more feasible in terms of minimized total Q loss with improved bus voltage. However, case 2 of 33-bus RDN is not feasible due to increasing total P and Q losses. The increase of total P and Q losses of case 2 is 245.46 kW and 142.43 kVAR, respectively. The percentage increase of total P and Q losses of case 2 is 53.78% and 46.99%, respectively, showing that deploying two DGs in 33-bus RDS is not feasible to minimize total P and Q losses with improved bus voltage. Table 21 presents the result summary

(a)

(b)

(c)
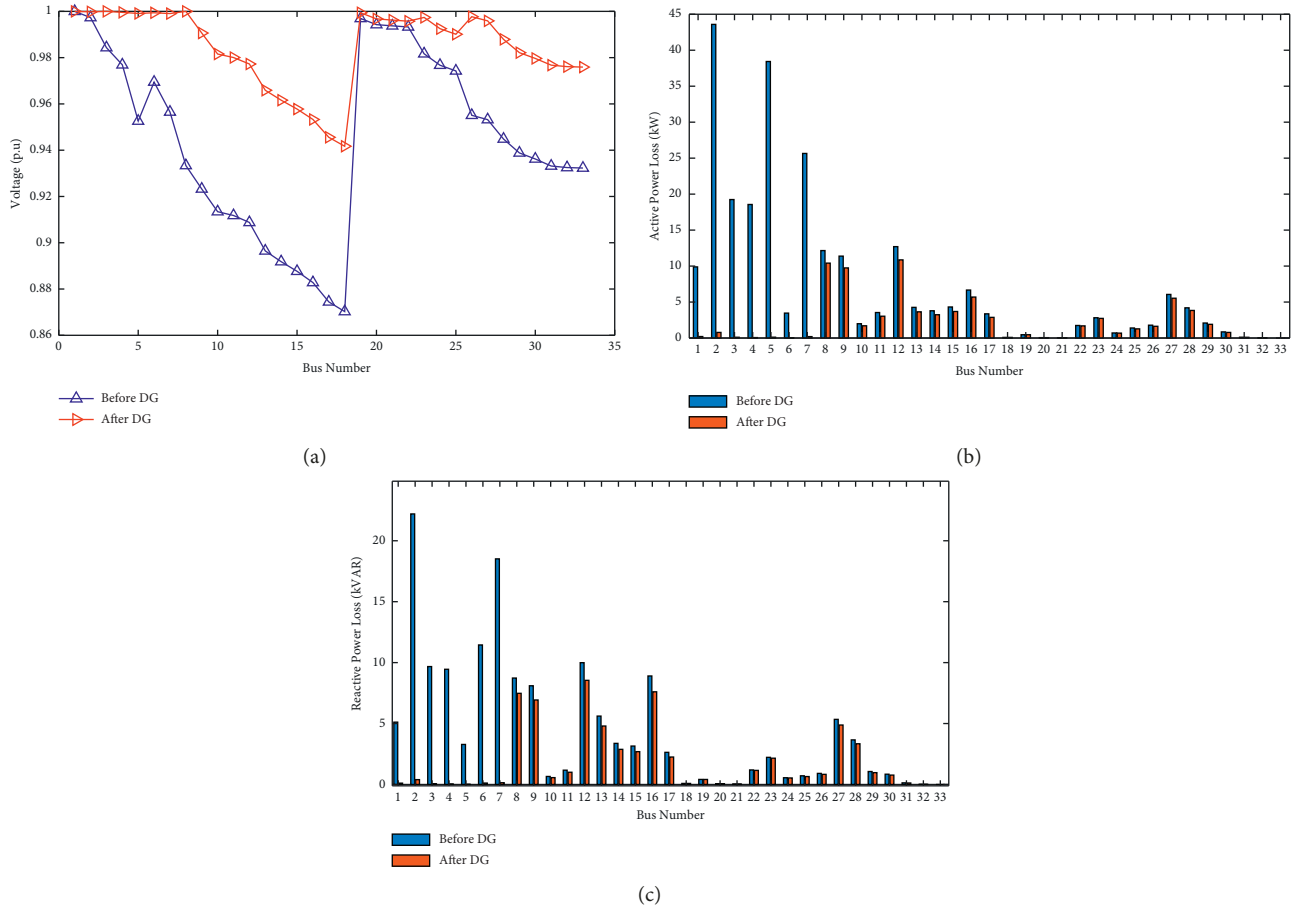
FIGURE 13: Case 3 (33-bus RDN) for autumn. (a) Bus voltage profile. (b) Total P loss. (c) Total Q loss.

for all four cases of 33-bus RDN with seasonal load data of winter.

For spring load, the bus voltage drop is minimized in case 3 of 33-bus RDN, 0.91907 (per unit), which shows more improved value than other cases. The total P loss reduction for case 3 of 33-bus RDN is 144.12 kW, while the percentage decrease of total P loss, in this case, is 144.12% which shows that deployment of three DGs in a 33-bus system is more feasible in terms of minimized total P loss with improved bus voltage. The total Q loss for case 3 of 33-bus RDN is 144.12 kVAR, while the percentage decrease of total Q loss is 144.12% which shows that deploying three DGs in a 33-bus system is still more feasible, minimizing total Q loss with improved bus voltage. However, case 2 of 33-bus RDN is not feasible due to increasing total P and Q losses. The increase of total P and Q losses of case 2 is 736.49 kW and 428.92 kVAR, respectively. The percentage increase of total P and Q losses of case 2 is 48.90% and 41.90%, respectively, which shows that deploying two DGs in 33-bus RDS is not feasible in minimizing total P and Q losses with improved bus voltage. Table 22 presents the result summary for all four cases of 33-bus RDN with seasonal load data of spring.

For summer load, the bus voltage drop is minimized in case 3 of 33-bus RDN, which is 0.90725 (per unit), which shows more improved value than other cases. The total P loss reduction for case 3 of 33-bus RDN is 187.69 kW, while the

percentage decrease of total P loss, in this case, is 187.69% which shows that deployment of three DGs in a 33-bus system is more feasible in terms of minimized total P loss with improved bus voltage. The total Q loss for case 3 of 33-bus RDN is 187.69 kVAR, while the percentage decrease of total Q loss is 63.22% which shows that deployment of three DGs in a 33-bus system is still more feasible in terms of minimized total Q loss with improved bus voltage. However, case 2 of 33-bus RDN is not feasible due to increasing total P and Q losses. The increase of total P and Q losses of case 2 is 63.22 kW and 571.85 kVAR, respectively. The percentage increase of total P and Q losses of case 2 is 46.57% and 39.47%, respectively, which shows that deploying two DGs in 33-bus RDS is not feasible in minimizing total P and Q losses with improved bus voltage. Table 23 presents the result summary for all four cases of 33-bus RDN with seasonal load data of summer.

For autumn load, the bus voltage drop is minimized in case 3 of 33-bus RDN, which is 0.9417 (per unit), which shows more improved value than other cases. The total P loss reduction for case 3 of 33-bus RDN is 77.19 kW, while the percentage decrease of total P loss, in this case, is 68.54% which shows that deployment of three DGs in a 33-bus system is more feasible in terms of minimized total P loss with improved bus voltage. The total Q loss for case 3 of 33-bus RDN is 61.62 kVAR, while the percentage decrease of

(a)

(b)

(c)
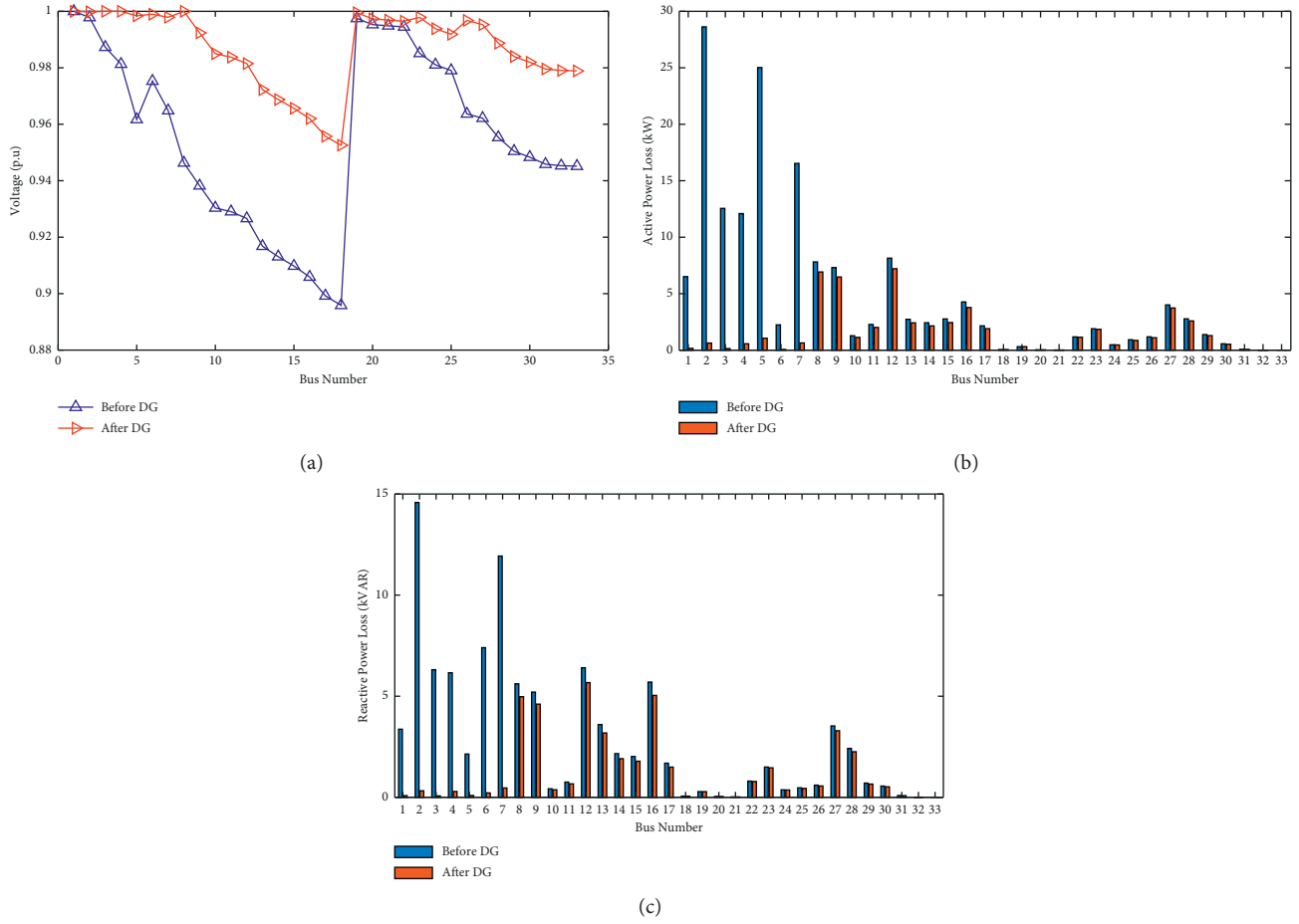
FIGURE 14: Case 4 (33-bus RDN) for winter. (a) Bus voltage profile. (b) Total P loss. (c) Total Q loss.

TABLE 12: Results of case 4 (33-bus RDN with HHO).

Season	v_{min} (per unit)	FO	P loss (kW)	Q loss (kVAR)	P_{LOSS} reduction (%)	Q_{LOSS} reduction (%)	DG's size (kW)	DG's location (bus no.)
Winter	0.95257	0.37277	53.7481	42.0459	66.3261	56.607	579.36, 587.25, 1102.9, 174.16	3, 6, 8, 4
Without DGs	0.89587	—	159.6136	96.8958	—	—	—	—
Spring	0.91907	0.44263	151.6158	117.4661	69.3459	61.1376	987.93, 1116.1, 1997.2, 290.95	3, 6, 8, 4
Without DGs	0.81372	—	494.6027	302.2616	—	—	—	—
Summer	0.90725	0.47614	199.115	153.3774	70.2333	62.5923	1246, 1376.5, 2300.6, 188.48	3, 6, 8, 4
Without DGs	0.7819	—	668.9179	410.0154	—		—	—
Autumn	0.9417	0.3913	79.7039	62.2535	67.5228	58.2945	749.27, 753.49, 1389.8, 184.74	3, 6, 8, 4
Without DGs	0.87025	—	245.4149	149.2695	—		—	—

(a)

(b)

(c)
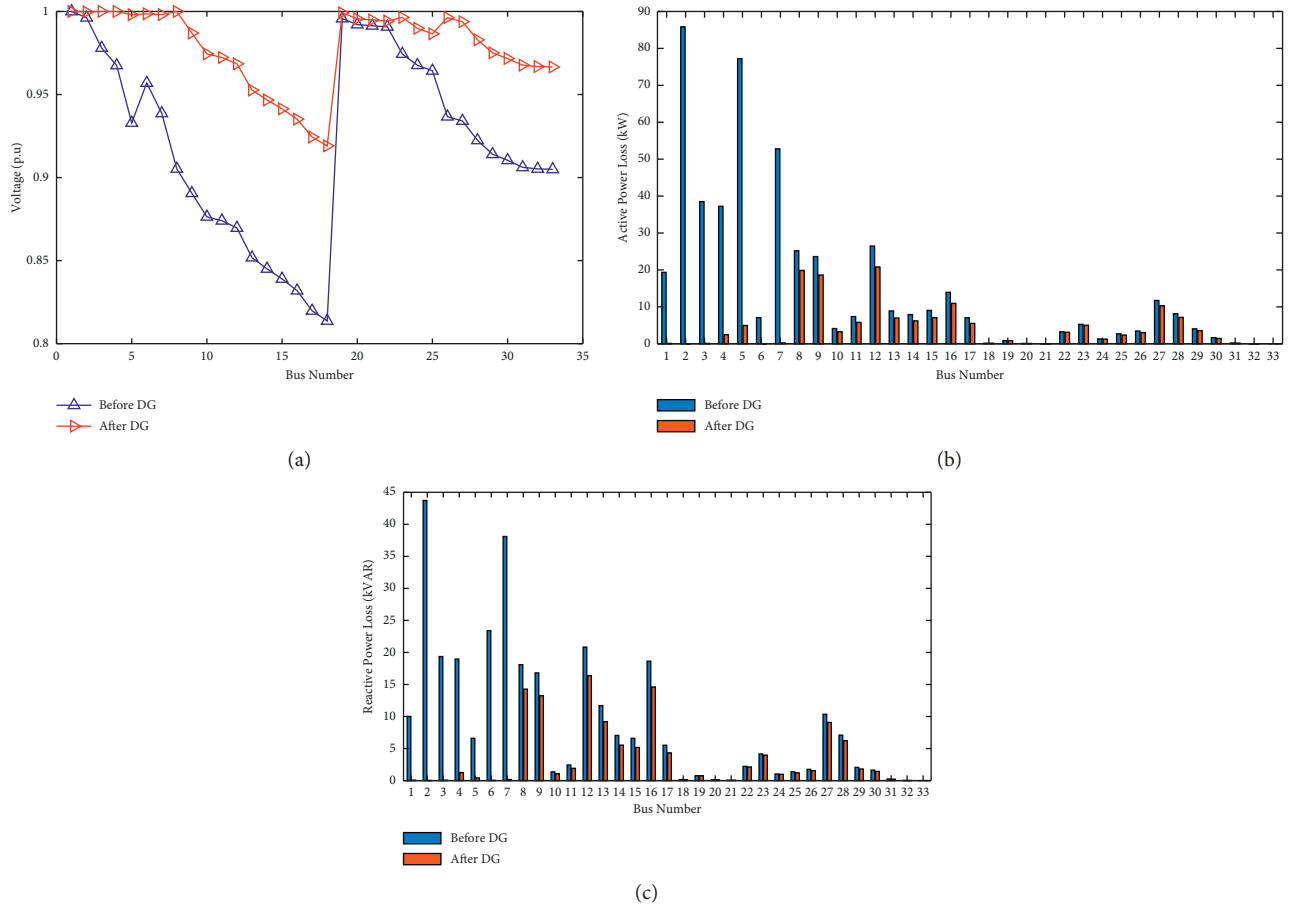
FIGURE 15: Case 4 (33-bus RDN) for spring. (a) Bus voltage profile. (b) Total P loss. (c) Total Q loss.

total Q loss is 58.71% which shows that deployment of three DGs in a 33-bus system is still more feasible in terms of minimized total Q loss with improved bus voltage. However, case 2 of 33-bus RDN is not feasible due to increasing total P and Q losses. The increase of total P and Q losses of case 2 is 374.05 kW and 217.28 kVAR, respectively. The percentage increase of total P and Q losses of case 2 is 52.41% and 45.56%, respectively, which shows that deploying two DGs in 33-bus RDS is not feasible in minimizing total P and Q losses with improved bus voltage. Table 24 presents the result summary for all four cases of 33-bus RDN with seasonal load data of autumn.

Figures 36(a) and 36(b) show the bus voltage and total P loss profiles of 33-bus RDN with the deployment of one, two, three, and four DGs for all four cases, respectively.

For winter load, the bus voltage drop is minimized in case 4 of IEEE 69-bus RDN, which is 0.9849 (per unit), which shows more improved value than other cases. The total P loss reduction for case 4 of IEEE 69-bus RDN is 22.76 kW, while the percentage decrease of total P loss, in this case, is 78.22% which shows that deployment of three DGs in a 69-bus system is more feasible in terms of minimized total P loss with improved bus voltage. The total Q loss for case 4 of IEEE 69-bus RDN is 11.21 kVAR, while the percentage decrease of total Q loss is 76.45% which shows that deployment of three DGs in a 69-bus system is

still more feasible in terms of minimized total Q loss with improved bus voltage. However, case 2 of IEEE 69-bus RDN is not feasible due to increasing total P and Q losses. The increase of total P and Q losses of case 2 is 346.82 kW and 155.20 kVAR, respectively. The percentage increase of total P and Q losses of case 2 is 231.77% and 225.97%, respectively, showing that deploying two DGs in 69-bus RDS is not feasible to minimize total P and Q losses with improved bus voltage. Table 25 presents the result summary for all four cases of IEEE 69-bus RDN with seasonal load data of winter.

For spring load, the bus voltage drop is minimized in case 4 of IEEE 69-bus RDN, 0.97496 (per unit), which shows more improved value than other cases. The total P loss reduction for case 4 of IEEE 69-bus RDN is 61.15 kW, while the percentage decrease of total P loss, in this case, is 80.02% which shows that deployment of three DGs in a 69-bus system is more feasible in terms of minimized total P loss with improved bus voltage. The total Q loss for case 4 of IEEE 69-bus RDN is 30.04 kVAR, while the percentage decrease of total Q loss is 78.35% which shows that deployment of three DGs in a 69-bus system is still more feasible in terms of minimized total Q loss with improved bus voltage. However, case 2 of IEEE 69-bus RDN is not feasible due to increasing total P and Q losses. The increase of total P and Q losses of case 2 is 1122.09 kW and 504.27 kVAR, respectively. The
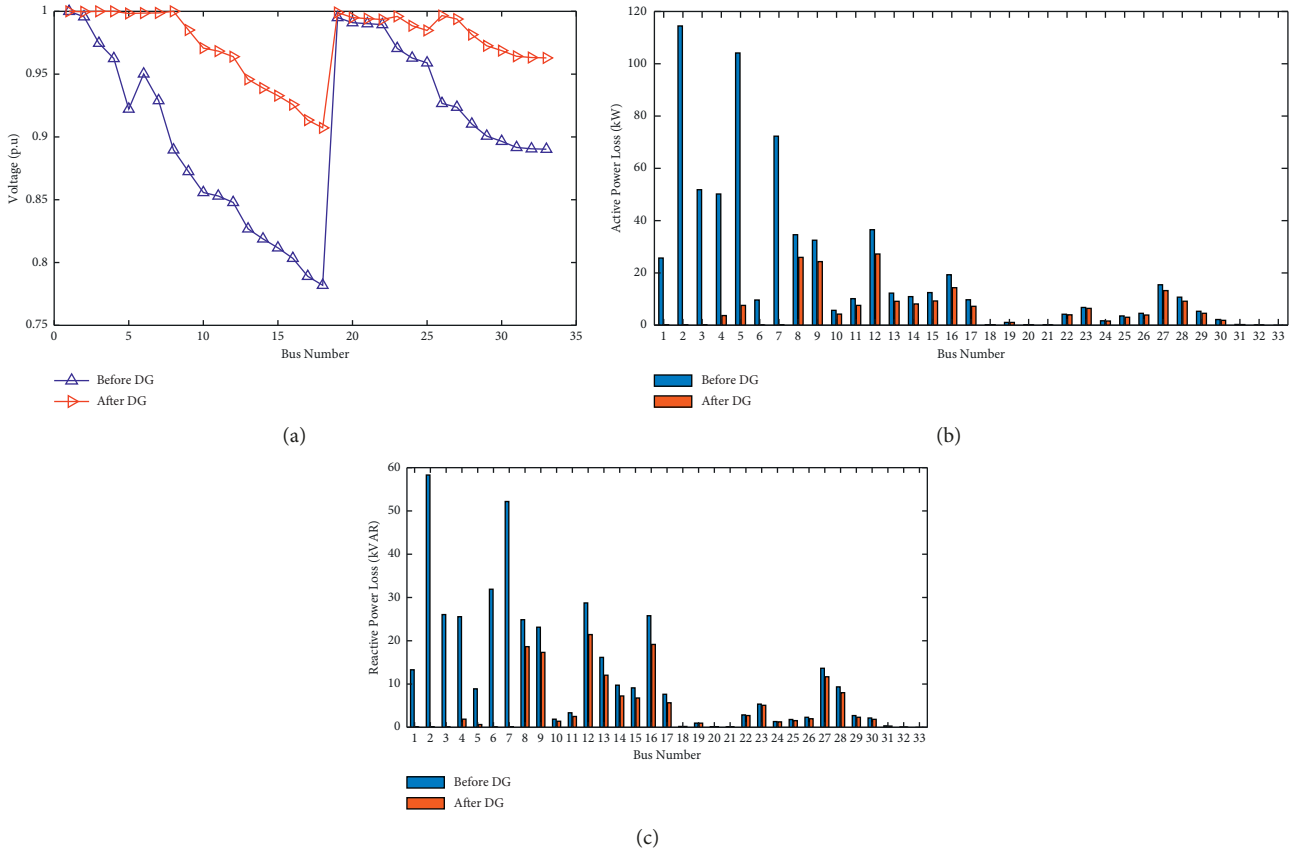
Figure 16: Case 4 (33-bus RDN) for summer. (a) Bus voltage profile. (b) Total P loss. (c) Total Q loss.

percentage increase of total P and Q losses of case 2 is 266.45% and 263.28%, respectively, showing that deploying two DGs in 69-bus RDS is not feasible in minimizing total P and Q losses with improved bus voltage. Table 26 presents the result summary for all four cases of IEEE 69-bus RDN with seasonal load data of spring.

For summer load, the bus voltage drop is minimized in case 4 of IEEE 69-bus RDN, which is 0.97161 (per unit), which shows more improved value than other cases. The total P loss reduction for case 4 of IEEE 69-bus RDN is 78.85 kW, while the percentage decrease of total P loss, in this case, is 80.44% which shows that deployment of three DGs in a 69-bus system is more feasible in terms of minimized total P loss with improved bus voltage. The total Q loss for case 4 of IEEE 69-bus RDN is 38.68 kVAR, while the percentage decrease of total Q loss is 78.80% which shows that deployment of three DGs in a 69-bus system is still more feasible in terms of minimized total Q loss with improved bus voltage. However, case 2 of IEEE 69-bus RDN is not feasible due to increasing total P and Q losses. The increase of total P and Q losses of case 2 is 1542.18 kW and 694.29 kVAR, respectively. The percentage increase of total P and Q losses of case 2 is 282.40% and 280.40%, respectively, showing that deploying two DGs in 69-bus RDS is not feasible to minimize total P and Q losses with improved bus voltage. Table 27 presents the result summary for all four cases of IEEE 69-bus RDN with seasonal load data of summer.

For autumn load, the bus voltage drop is minimized in case 4 of IEEE 69-bus RDN, which is 0.98161 (per unit), which shows more improved value than other cases. The total P loss reduction for case 4 of IEEE 69-bus RDN is 33.24 kW, while the percentage decrease of total P loss, in this case, is 78.98% which shows that deployment of three DGs in a 69-bus system is more feasible in terms of minimized total P loss with improved bus voltage. The total Q loss for case 4 of IEEE 69-bus RDN is 16.36 kVAR, while the percentage decrease of total Q loss is 77.24% which shows that deployment of three DGs in a 69-bus system is still more feasible in terms of minimized total Q loss with improved bus voltage. However, case 2 of IEEE 69-bus RDN is not feasible due to increasing total P and Q losses. The increase of total P and Q losses of case 2 is 540.53 kW and 242.19 kVAR, respectively. The percentage increase of total P and Q losses of case 2 is 241.68% and 236.64%, respectively, showing that deploying two DGs in 69-bus RDS is not feasible in minimizing total P and Q losses with improved bus voltage. Table 28 presents the result summary for all four cases of IEEE 69-bus RDN with seasonal load data of autumn.

Moreover, Figures 37 and 38 illustrate the graphical comparison of literature results with four and three DGs for IEEE 33-bus RDN, respectively. Figures 39 and 40 illustrate the graphical comparison of literature results with four and three DGs for IEEE 69-bus RDN, respectively. For four DGs in 33-bus RDN, the voltage profile improvement of the proposed HHO is less than that of other literature-based algorithms such as GA, BA, PSO, PPA, ABC and TLCHS.

(a)

(b)

(c)
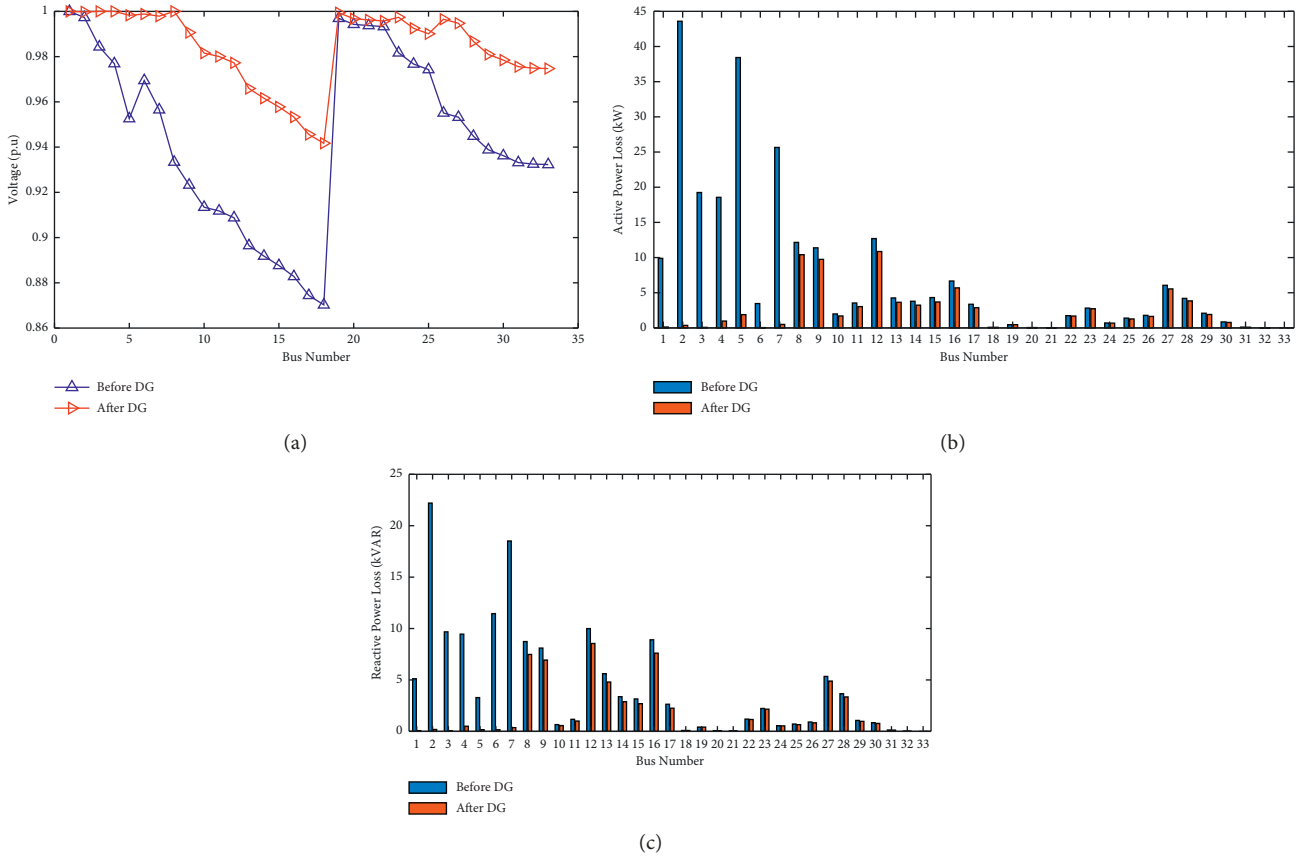
FIGURE 17: Case 4 (33-bus RDN) for autumn. (a) Bus voltage profile. (b) Total P loss. (c) Total Q loss.
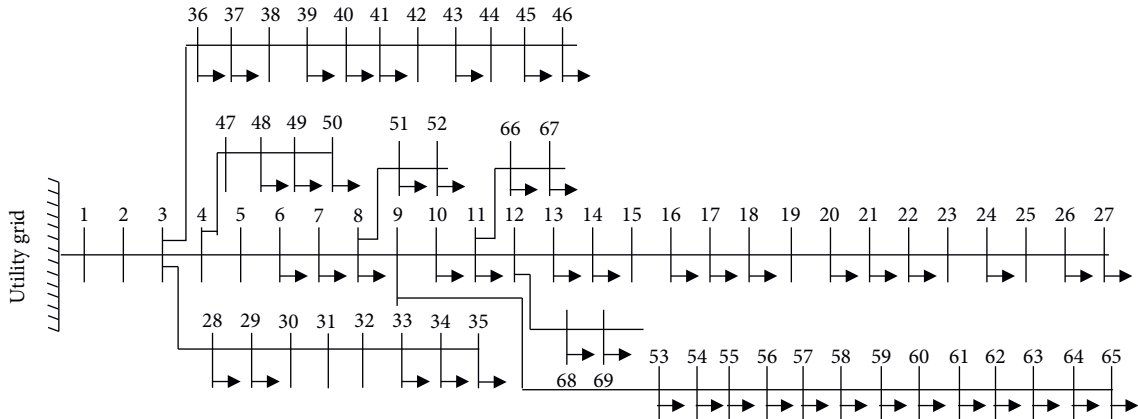

FIGURE 18: IEEE 69-bus RDN.

Active power loss reduction is better with the proposed HHO. For three DGs in 33-bus RDN, the voltage profile improvement of the proposed HHO is better than that of other literature-based algorithms such as GA, BA, GSA-GAMS, SSA, EMA, SPEA2, CSCA, PPA, and ACO-ABC. Active power loss reduction is higher with the proposed HHO. For four DGs in 69-bus RDN, the voltage profile improvement of the proposed HHO is better than that of other literature-based algorithms such as GA, SSA, PPA, WCA, HAS, HGWO, and ABC. Active power loss reduction

is higher with the proposed HHO, PPA, and ABC. For three DGs in 69-bus RDN, the voltage profile improvement of the proposed HHO is better than that of other literature-based algorithms. Active power loss reduction is higher with the proposed HHO, PPA, and ABC.

4.4. Statistical Analysis. This section investigates the statistical analysis for the objective functions taken using the HHO algorithm. The statistical analysis is carried out on the

TABLE 13: Results of literature with four DGs (69-bus RDN).

Algorithm Ref.	Year	v_{min} (per unit)	P loss (kW)	P_{LOSS} reduction (%)	Q loss (kVAR)	Q_{LOSS} reduction (%)	DG sizes (kW)	DG's location (bus no.)
Proposed HHO	2021	0.97827	28.4818	72.7537	22.62	77.86	329.88, 229.42, 112.03, 924.13	57, 7, 6, 58
PPA [69]	2020	0.97829	17.23	92.3415	—	—	1014, 47.22, 145, 1586.3	7, 57, 58, 61
GA [74]	2020	0.970	18.43	60.40	14.32	59.30	929.00, 1075.0, 984.80, 1321.3	21, 62, 64, 45
PSO [74]	2020	—	20.31	63.02	15.45	54.30	1199.0, 795.60, 992.50, 889.20	61, 63, 17, 32
GA/PSO [74]	2020	—	19.56	63.90	14.32	60.20	910.50, 1192.0, 884.90, 978.60	21, 61, 63, 57
HSA [65]	2020	0.967	34.21	61.40	—	58.30	1302.0, 369.00, 101.80, 978.50	63, 64, 65, 56
BFOA [75]	2020	—	—	66.56	—	61.50	295.40, 447.00, 1345.1, 1000.0	27, 65, 61, 32
ABC [65]	2020	0.960	32.04	85.80	19.98	76.40	1000.0, 200.00, 338.20, 1100.0	61, 51, 62, 32
SSA [40]	2019	0.970	23.40	69.10	—	62.40	380.00, 527.00, 1718.0, 467.00	17, 10, 60, 32
WCA [39]	2018	0.970	22.43	68.20	—	61.20	775.00, 1105.0, 438.00, 890.00	61, 62, 23, 21
HGWO [79]	2013	0.960	20.41	69.14	—	64.30	527.00, 380.00, 1718.0, 398.50	11, 17, 61, 45

objective function in which voltage and PQ loss reduction (LR) is part of the objective function. The formula for real and reactive power loss is taken from [55]. The technique to calculate the losses is applied from existing literature [55, 81, 82]. The algorithm is simulated fifteen times during the load flow analysis for both IEEE RDNs, and results from the Big-O analysis are shown in Table 29 [54]. It is observed that the changes in the objective functions for the maximum and minimum values taken from the HHO have no significant variations. It validates the efficient and robust behavior of the applied HHO method. However, case 2 of IEEE

33-bus RDN shows a significant difference among best, worst, and mean values of total P loss. It shows that case 2 of 33-bus RDN cannot be taken under consideration during the planning stages. Moreover, case 4 of IEEE 69-bus RDN shows a significant difference among best, worst, and mean values of minimum bus voltages. It also shows that case 4 of IEEE 69-bus RDN cannot be considered during the planning stages.

Table 30 illustrates the analysis of variance (ANOVA). ANOVA tests help determine the variance of the objective function under various algorithms [83]. For IEEE 33-bus

TABLE 14: Results of literature with three DGs (69-bus RDN).

Algorithm Ref.	Year	$v_{\min}$ (per unit)	P loss (kW)	P_{LOSS} reduction (%)	Q loss (kVAR)	Q_{LOSS} reduction (%)	DG sizes (kW)	DG's location (bus no.)
Proposed HHO	2021	0.97100	32.8719	68.554	30.7883	69.86	1764.3, 617.55, 399.66	57, 7, 6
PPA [69]	2020	0.982	40.50	82	—	—	27.919, 1108.3, 1558.3	51, 61, 62
GA [74]	2020	0.9700	19.875	60.40	7.112	52.2	929.70, 1075.0, 984.80	21, 62, 64
PSO [74]	2020	—	19.430	63.02	12.320	51.2	1199.0, 795.60, 992.50	61, 63, 17
GA/PSO [74]	2020	—	28.720	63.90	13.570	53.0	910.50, 1192.0, 884.90	21, 61, 63
HSA [65]	2020	0.9670	35.430	61.40	—	51.0	1302.4, 369.00, 101.80	63, 64, 65
BFOA [75]	2020	0.9608	—	66.56	—	56.5	295.40, 447.60, 1345.0	27, 65, 61
ABC [65]	2020	0.9600	32.056	86.80	19.980	77.3	1000.0, 200.00, 338.20	61, 51, 62
QOCSOS [42]	2020	—	69.43	69.14	—	—	526.8, 380.4, 1719.0	11, 18, 61
CSCA [14]	2020	0.98	70.20	68.8	—	—	365.9, 1675.85, 65.52	17, 61, 67
SSA [40]	2019	0.9789	69.52	69.1	—	—	380, 527, 1718	17, 10, 60
FWA [41]	2019	0.974	77.87	65.39	—	—	480.5, 1198.6, 225.8	65, 61, 27
SFLA [41]	2019	0.9752	77.784	65.43	—	—	1088.7, 167.3, 980.9	57, 63, 26
SSA [40]	2019	0.9789	27.540	69.10	—	59.2	380.00, 527.00, 1718.0	17, 10, 60
WCA [39]	2018	0.987	71.55	68.2	—	—	775, 1105, 438	61, 62, 23
WCA [39]	2018	0.9670	21.450	68.20	—	51.1	775.00, 1105.0, 438.00	61, 62, 23
HGWO [37]	2017	0.98	69.43	69.14	—	—	527, 380, 1718	11, 17, 61
BFOA [34]	2014	0.9808	75.24	66.56	—	—	295.4, 447.6, 1345.1	27, 65, 61

TABLE 14: Continued.

Algorithm Ref.	Year	v_{min} (per unit)	P loss (kW)	P_{LOSS} reduction (%)	Q loss (kVAR)	Q_{LOSS} reduction (%)	DG sizes (kW)	DG's location (bus no.)
HSA [33]	2013	0.967	86.85	61.4	—	—	1302.4, 369, 101.8	63, 64, 65
HGWO [79]	2013	0.9600	24.230	69.14	—	59.1	527.00, 380.00, 1718.0	11, 17, 61

TABLE 15: Comparison of literature results with two DGs (case 2 (69-bus RDN)).

Algorithm Ref.	Year	v_{min} (per unit)	P loss (kW)	P_{LOSS} (%)	DG's size (kW)	DG's location	FO
ALO [24]	2017	0.98010	70.77	68.5470	538.70, 1700.0	17, 61	0.83200
ALO [26]	2018	0.97890	71.68	68.1400	531.48, 1781.5	17, 61	0.83000
EMA [29]	2018	0.97940	71.86	68.0600	1886.9, 649.30	61, 69	0.83000
CSFS-III [27]	2018	—	71.68	68.1400	531.00, 1781.0	17, 61	0.34000
PPA [69]	2020	0.97105	69.11	69.2400	1040.0, 1856.0	7, 57	0.83500
Proposed HHO	2021	0.97100	34.3245	67.1644	1232.0, 414.99	57, 7	0.35361

TABLE 16: Comparison of literature results with one DG (case 1 (69-bus RDN)).

| Algorithm Ref.	Year	v_{min} (per unit)	P loss (kW)	P_{LOSS} (%)	DG's size (kW)	DG's location	FO
ALO [24]	2017	0.96790	81.8010	63.6450	1800.0	61	0.80200
ALO [26]	2018	0.96820	83.2500	63.0000	1872.7	61	0.79900
EMA [29]	2018	0.96890	82.8700	63.1700	1910.3	57	0.80000
GA [1]	2019	0.96820	63.0000	72.0000	1850.0	60	0.84400
CSFS-III [27]	2018	—	83.2300	63.0100	1873.0	61	0.31500
CDE [30]	2019	0.96830	83.2500	63.0000	1872.4	61	0.79900
PPA [69]	2020	0.97105	74.2500	67.0000	2088.0	57	0.82900
Proposed HHO	2021	0.97100	36.0069	65.5551	1330.2	57	0.35442

(a)

(b)
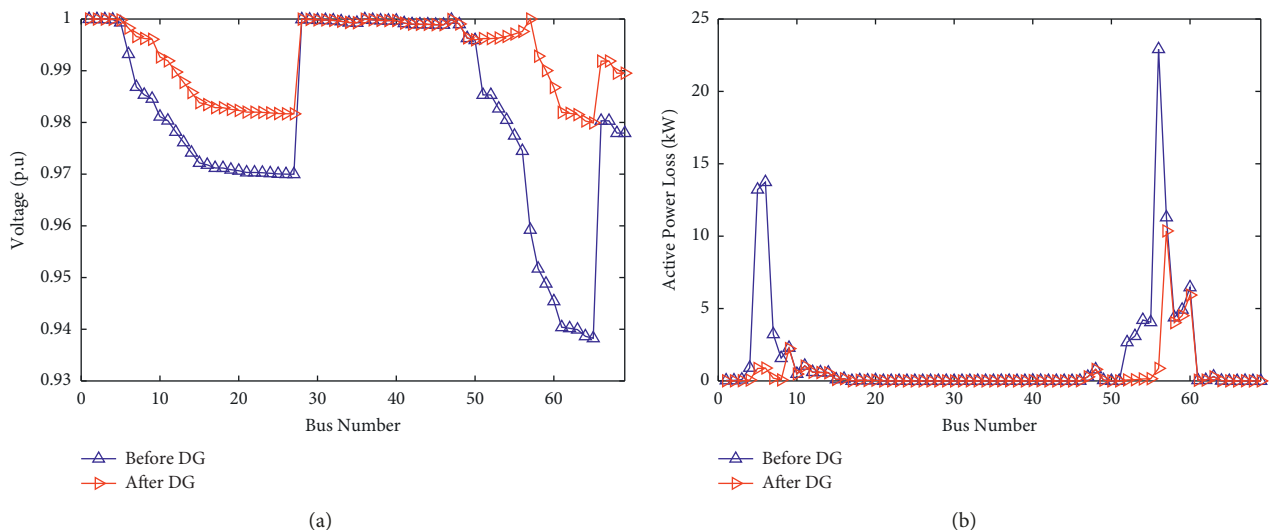
FIGURE 19: Continued.
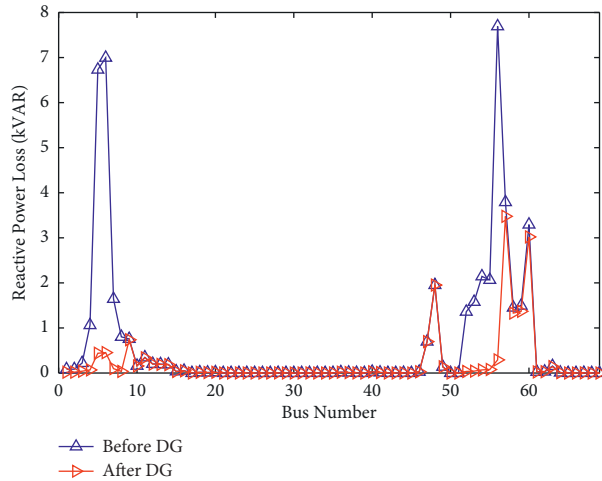
(c)

FIGURE 19: Case 1 (69-bus RDN) for winter. (a) Bus voltage profile. (b) Total *P* loss. (c) Total *Q* loss.

TABLE 17: Results with one DG (case 1 (69-bus RDN)) with proposed HHO.

Season	v_{min} (per unit)	FO	P loss (kW)	Q loss (kVAR)	P_{LOSS} reduction (%)	Q_{LOSS} reduction (%)	DG's size (kW)	DG's location (bus no.)
Winter	0.97991	0.36388	35.7486	15.9355	65.8022	66.5308	1346.9	57
Without DGs	0.93825		104.5347	47.6124	—	—	—	—
Spring	0.96656	0.41038	97.9764	43.6535	68.003	68.5519	2357.2	57
Without DGs	0.89392		306.2051	138.8112	—	—	—	—
Summer	0.96204	0.43178	126.6908	56.4194	68.5854	69.0875	2710.8	57
Without DGs	0.87809		403.2863	182.5134	—	—	—	—
Autumn	0.9755	0.37651	52.7248	23.5051	66.6709	67.3284	1675.6	57
Without DGs	0.92395		158.1946	71.9434	—	—	—	—
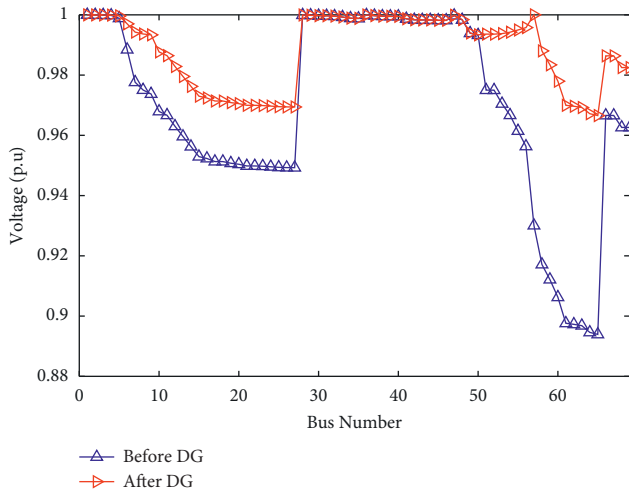
(a)
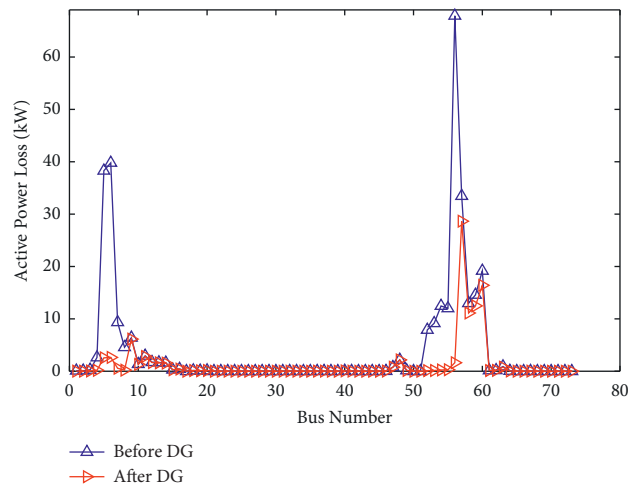
(b)

FIGURE 20: Continued.
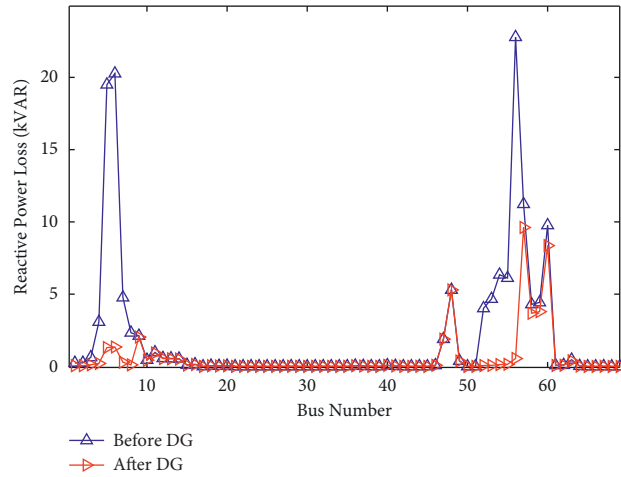
(c)

FIGURE 20: Case 1 (69-bus RDN) for spring. (a) Bus voltage profile. (b) Total P loss. (c) Total Q loss.
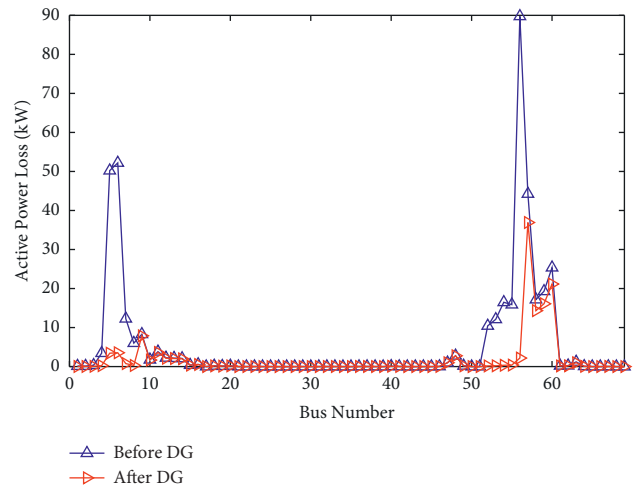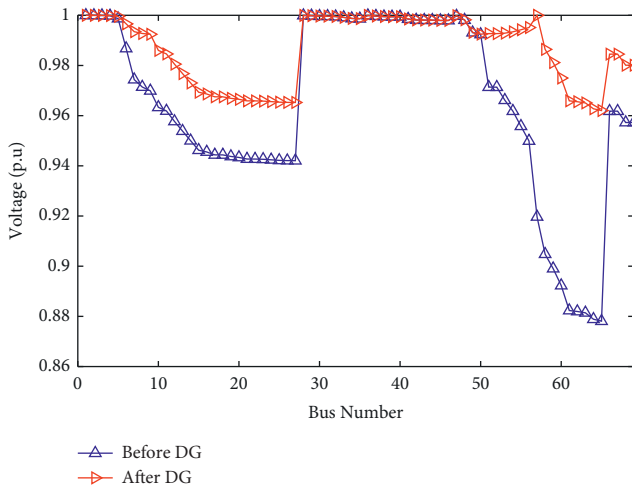

(a)

(b)
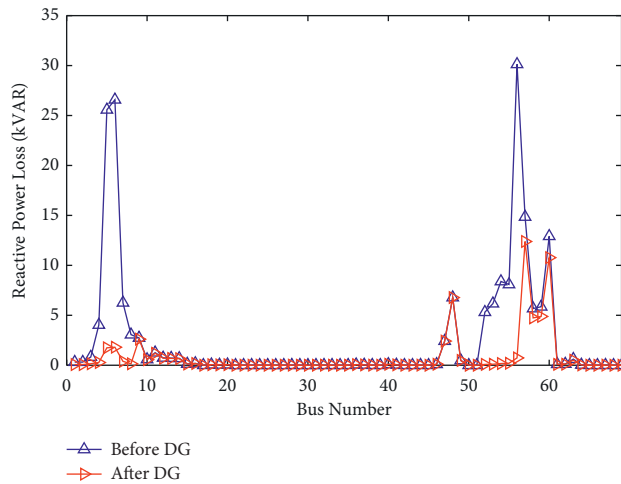
(c)

FIGURE 21: Case 1 (69-bus RDN) for summer. (a) Bus voltage profile. (b) Total P loss. (c) Total Q loss.
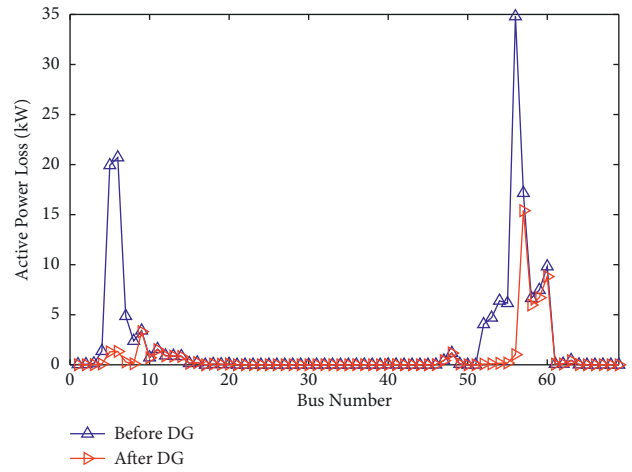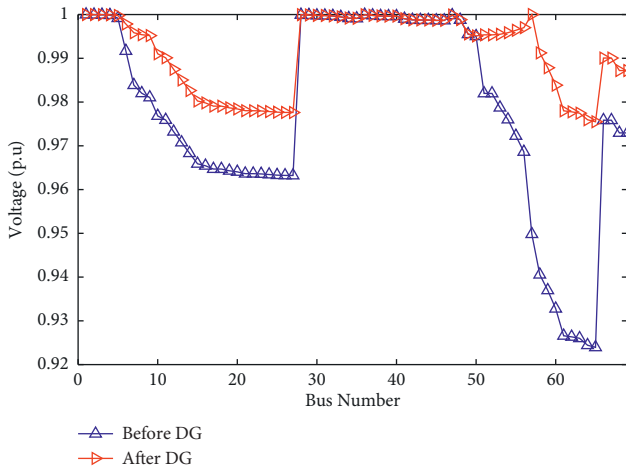
(a)

(b)
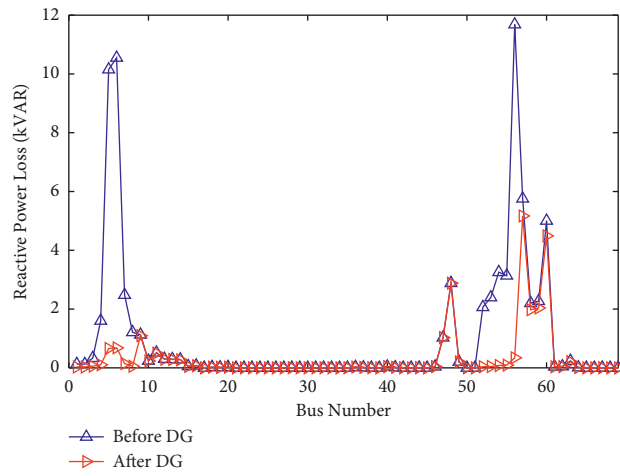
(c)

FIGURE 22: Case 1 (69-bus RDN) for autumn. (a) Bus voltage profile. (b) Total P loss. (c) Total Q loss.
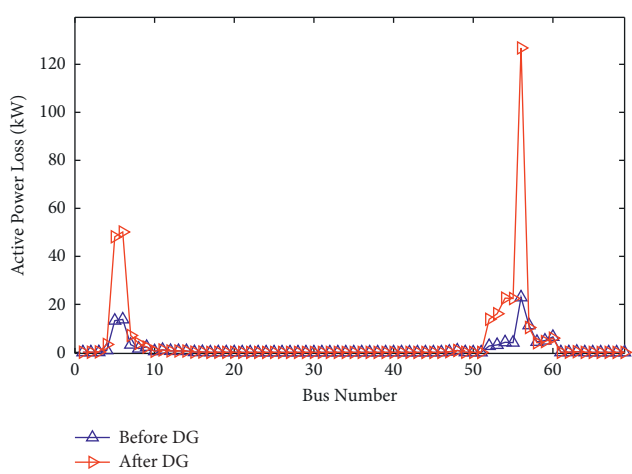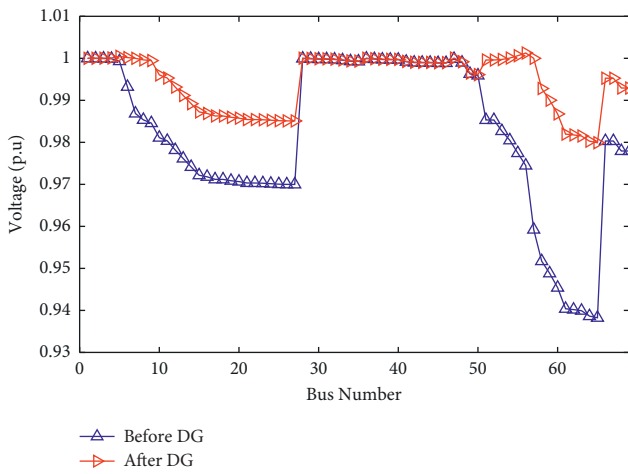
(a)

(b)

FIGURE 23: Continued.

(c)
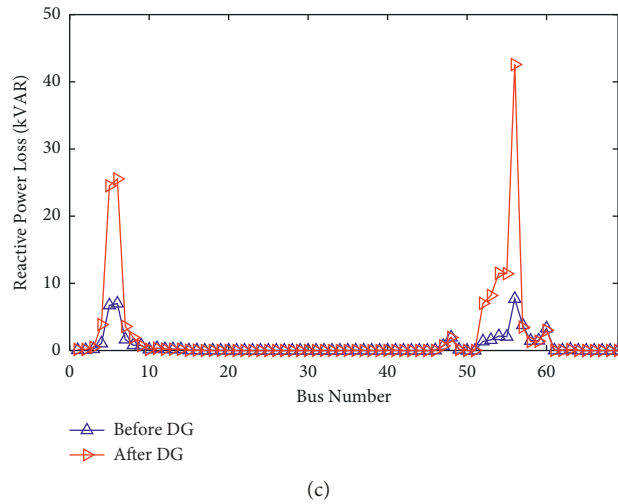
FIGURE 23: Case 2 (69-bus RDN) for winter. (a) Bus voltage profile. (b) Total P loss. (c) Total Q loss.

TABLE 18: Results with two DGs (case 2 (69-bus RDN)) with proposed HHO.

Season	v_{min} (per unit)	FO	P loss (kW)	Q loss (kVAR)	P_{LOSS} reduction (%)	Q_{LOSS} reduction (%)	DG's size (kW)	DG's location (bus no.)
Winter	0.97991	0.37332	346.8215	155.2039	−231.7765	−225.9733	868.32, 419.28	57, 7
Without DGs	0.93825		104.5347	47.6124	—		—	—
Spring	0.96656	0.4422	1122.0975	504.2769	−266.4529	−263.2826	1484.7, 788.66	57, 7
Without DGs	0.89392		306.2051	138.8112	—		—	—
Summer	0.96204	0.4752	1542.1811	694.2981	−282.4035	−280.4094	1699.7, 923.42	57, 7
Without DGs	0.87809		403.2863	182.5134	—		—	—
Autumn	0.9755	0.39162	540.5331	242.1968	−241.6888	−236.6492	1068.5, 540.77	57, 7
Without DGs	0.92395	—	158.1946	71.9434	—	—	—	—
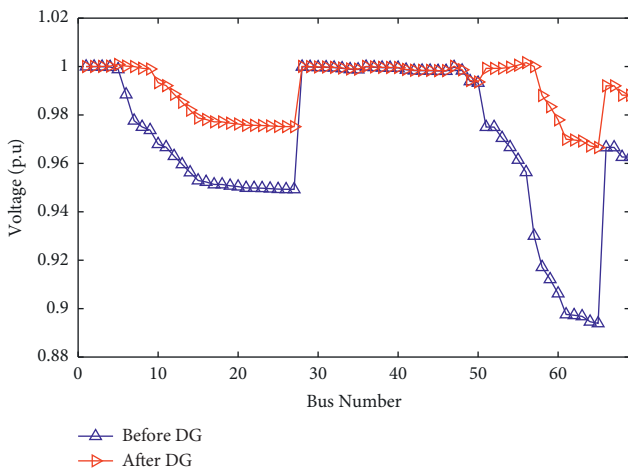
(a)
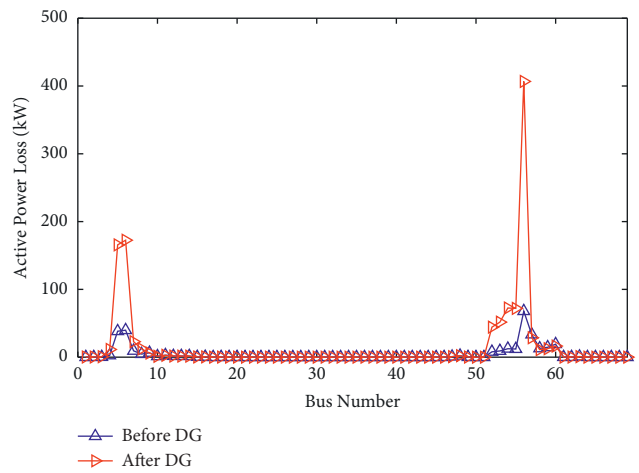
(b)

FIGURE 24: Continued.
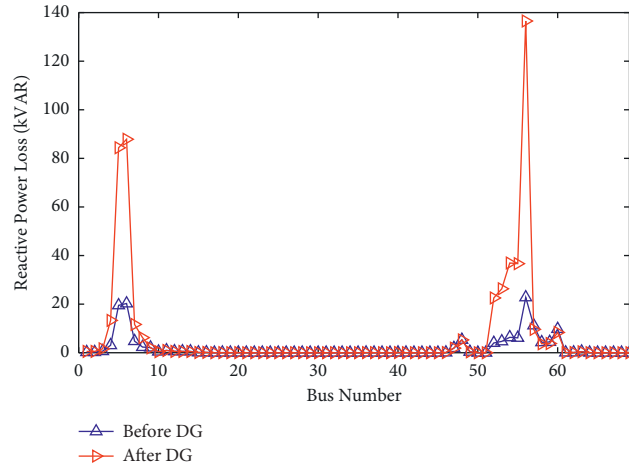
(c)

FIGURE 24: Case 2 (69-bus RDN) for spring. (a) Bus voltage profile. (b) Total P loss. (c) Total Q loss.
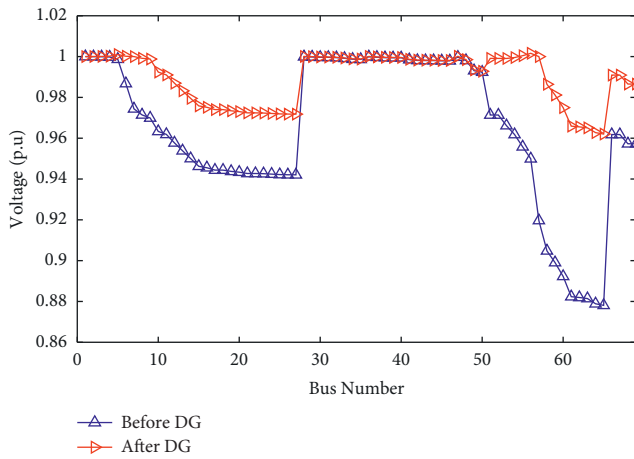

(a)
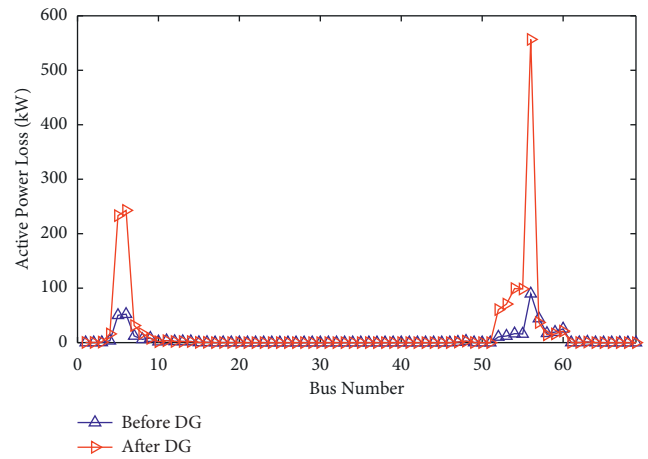
(b)
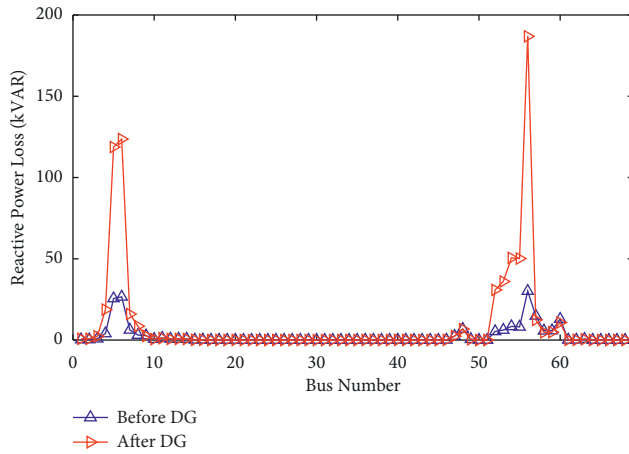
(c)

FIGURE 25: Case 2 (69-bus RDN) for summer. (a) Bus voltage profile. (b) Total P loss. (c) Total Q loss.

(a)

(b)

(c)
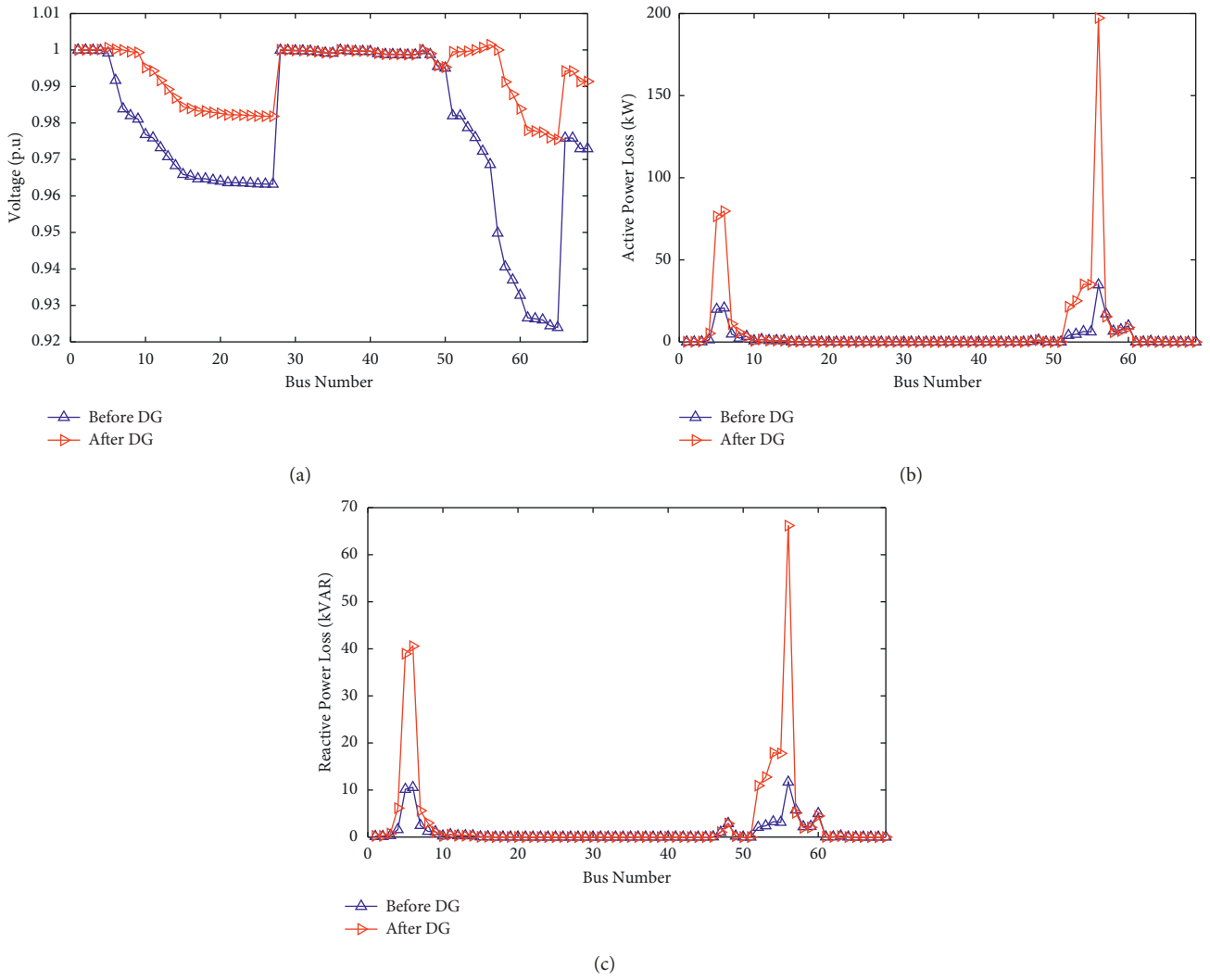
FIGURE 26: Case 2 (69-bus RDN) for autumn. (a) Bus voltage profile. (b) Total P loss. (c) Total Q loss.

(a)

(b)
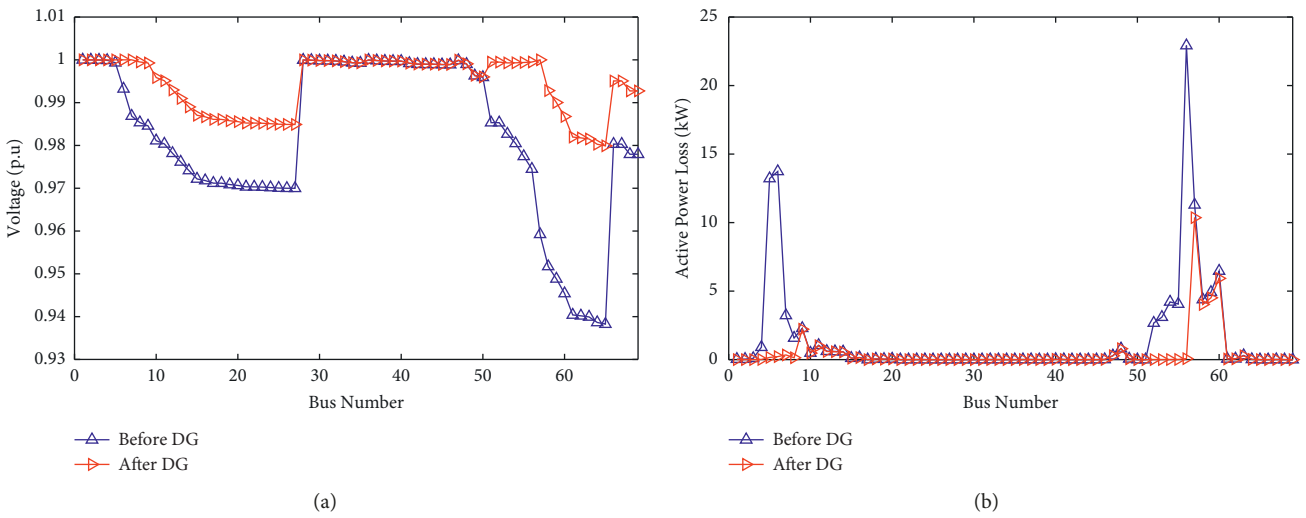
FIGURE 27: Continued.
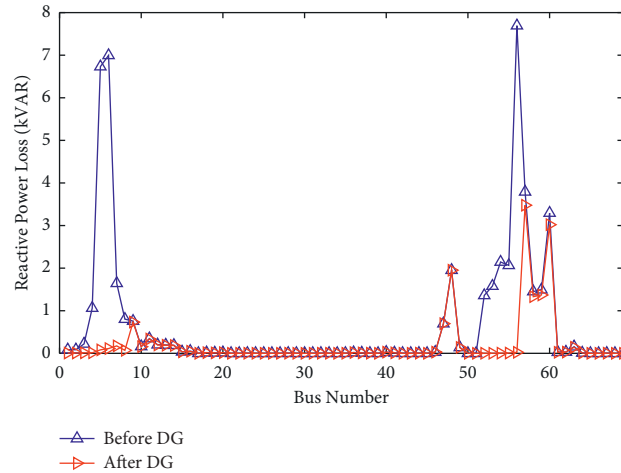
(c)

FIGURE 27: Case 3 (69-bus RDN) for winter. (a) Bus voltage profile. (b) Total P loss. (c) Total Q loss.

TABLE 19: Results with three DGs (case 3 (69-bus RDN)) with proposed HHO.

Season	v_{min} (per unit)	FO	P loss (kW)	Q loss (kVAR)	P_{LOSS} reduction (%)	Q_{LOSS} reduction (%)	DG's size (kW)	DG's location (bus no.)
Winter	0.97991	0.36328	33.2763	14.7497	68.1672	69.0214	1212.5, 552.87, 19.166	57, 7, 6
Without DGs	0.9091		225.007	47.6124	—		—	—
Spring	0.96656	0.3799	92.4901	40.9044	69.7947	70.5324	2108.7, 706.76, 247.28	57, 7, 6
Without DGs	0.89392		306.2051	138.8112	—		—	—
Summer	0.96204	0.39179	117.1096	51.6342	70.9612	71.7094	2361.5, 1059.3, 128.55	57, 7, 6
Without DGs	0.87809		403.2863	182.5134	—		—	—
Autumn	0.9755	0.36075	49.3542	21.8535	68.8016	69.624	1483.8, 674.15, 23.574	57, 7, 6
Without DGs	0.92395		158.1946	71.9434	—		—	—
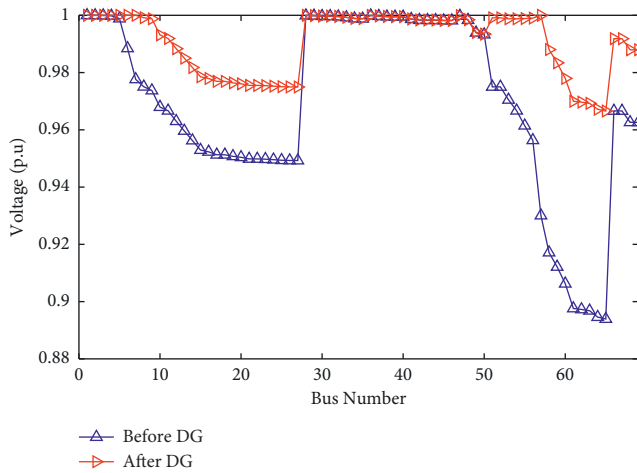
(a)
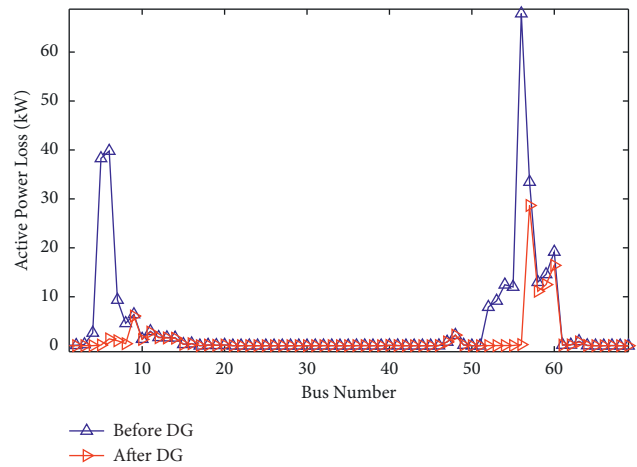
(b)

FIGURE 28: Continued.
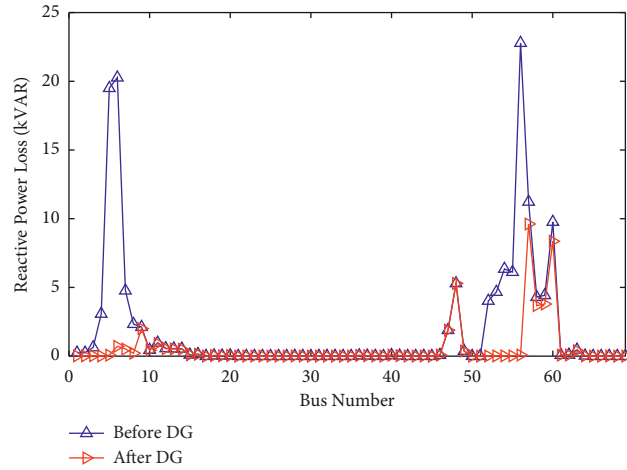
(c)

FIGURE 28: Case 3 (69-bus RDN) for spring. (a) Bus voltage profile. (b) Total *P* loss. (c) Total *Q* loss.
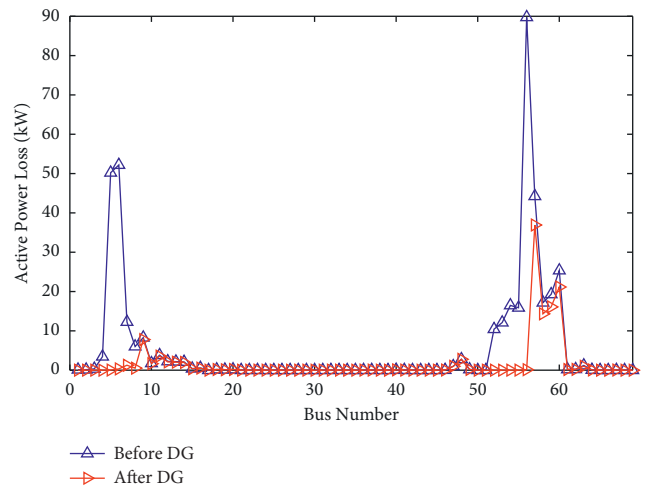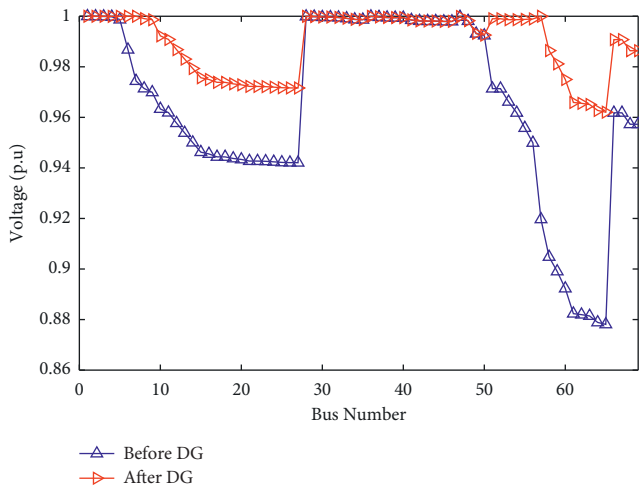
(a)

(b)
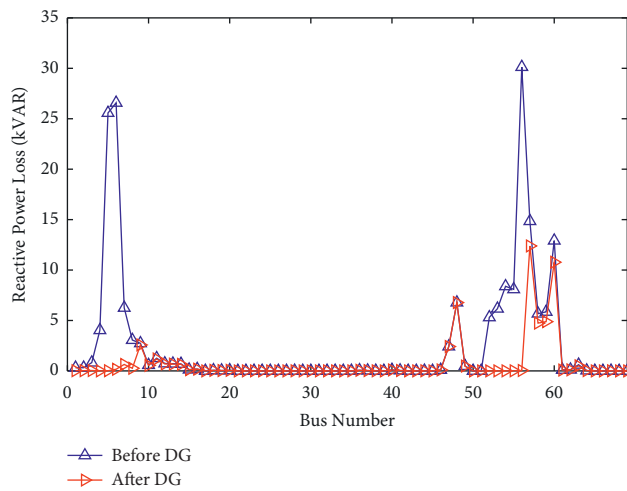
(c)

FIGURE 29: Case 3 (69-bus RDN) for summer. (a) Bus voltage profile. (b) Total *P* loss. (c) Total *Q* loss.

(a)

(b)

(c)
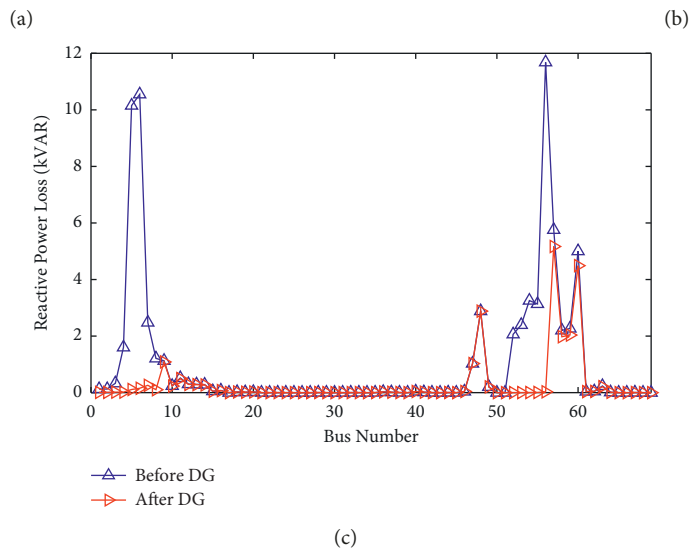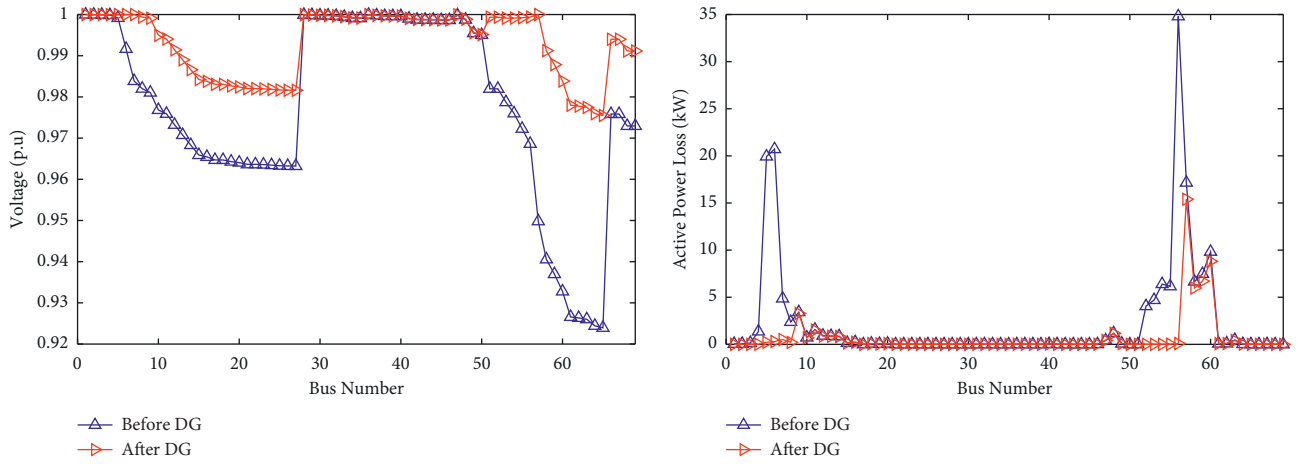
Figure 30: Case 3 (69-bus RDN) for autumn. (a) Bus voltage profile. (b) Total P loss. (c) Total Q loss.


(a)

(b)
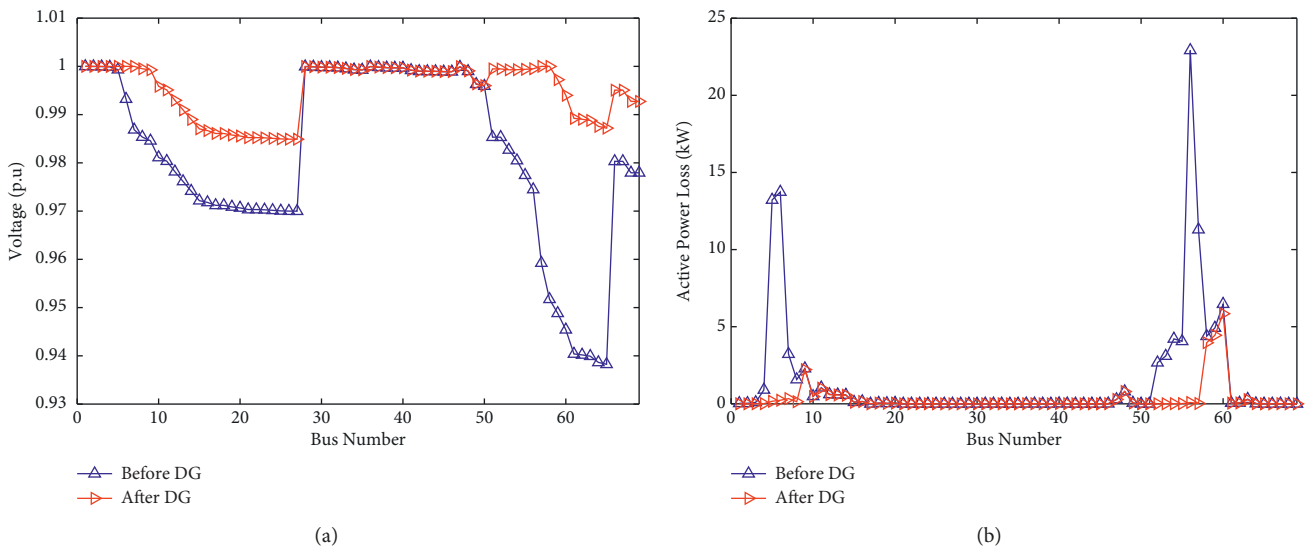
Figure 31: Continued.
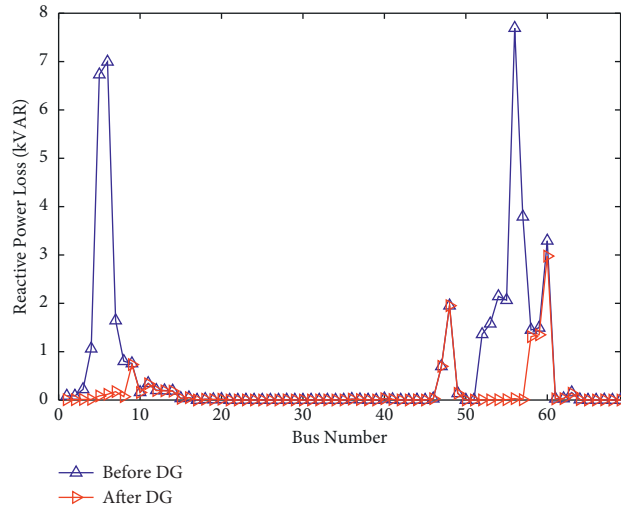
(c)

FIGURE 31: Case 4 (69-bus RDN) for winter. (a) Bus voltage profile. (b) Total P loss. (c) Total Q loss.

TABLE 20: Results with four DGs (case 4 (69-bus RDN)) with proposed HHO.

| Season	v_{min} (per unit)	FO	P loss (kW)	Q loss (kVAR)	P_{LOSS} reduction (%)	Q_{LOSS} reduction (%)	DG's size (kW)	DG's location (bus no).
Winter	0.9849	0.36025	22.7626	11.2125	78.2248	76.4505	40.66, 553.91, 19.998, 1156.8	57, 7, 6, 58
Without DGs	0.93825		104.5347	47.6124	—		—	—
Spring	0.97496	0.39921	61.1562	30.0424	80.0277	78.3574	108.65, 1032.2, 31.762, 1957.5	57, 7, 6, 58
Without DGs	0.89392		306.2051	138.8112	—		—	—
Summer	0.97161	0.417	78.8558	38.6836	80.4467	78.805	123.63, 1198.9, 41.268, 2240.5	57, 7, 6, 58
Without DGs	0.87809		403.2863	182.5134	—		—	—
Autumn	0.98161	0.37089	33.2468	16.3679	78.9836	77.2489	54.404, 700.2, 39.572, 1427.1	57, 7, 6, 58
Without DGs	0.92395		158.1946	71.9434	—		—	—
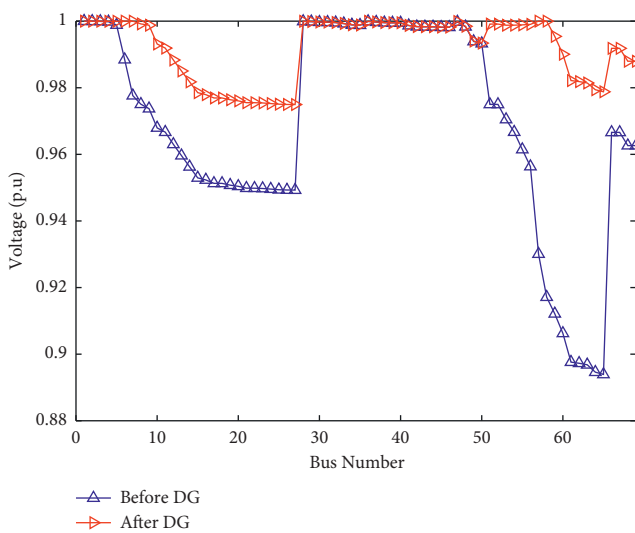
(a)
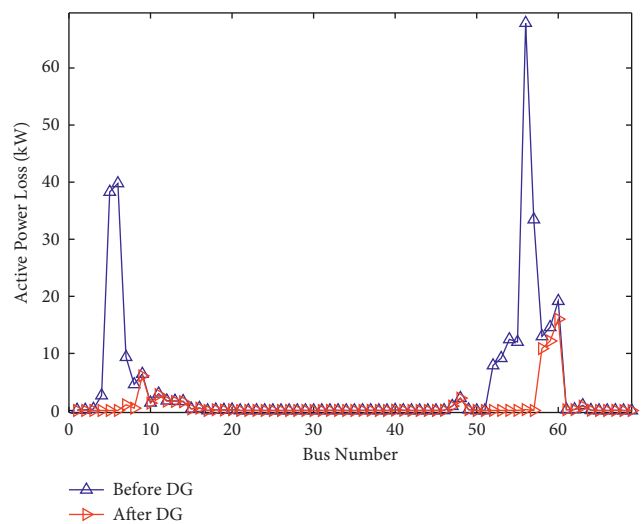
(b)

FIGURE 32: Continued.
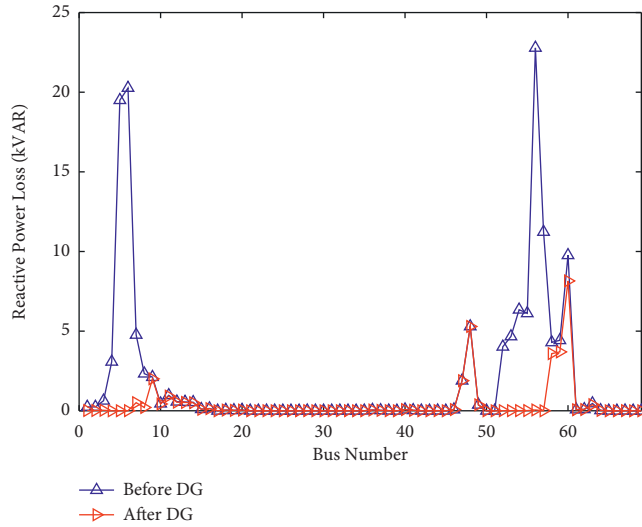
(c)

FIGURE 32: Case 4 (69-bus RDN) for spring. (a) Bus voltage profile. (b) Total P loss. (c) Total Q loss.
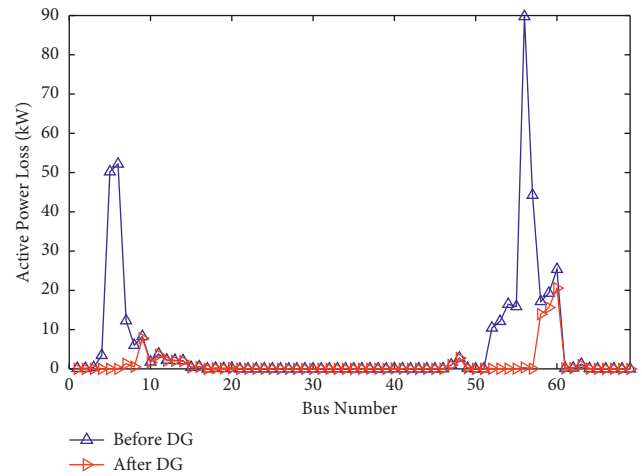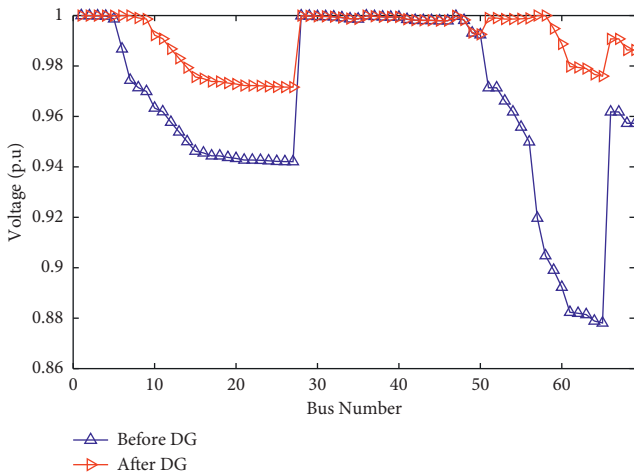

(a)

(b)
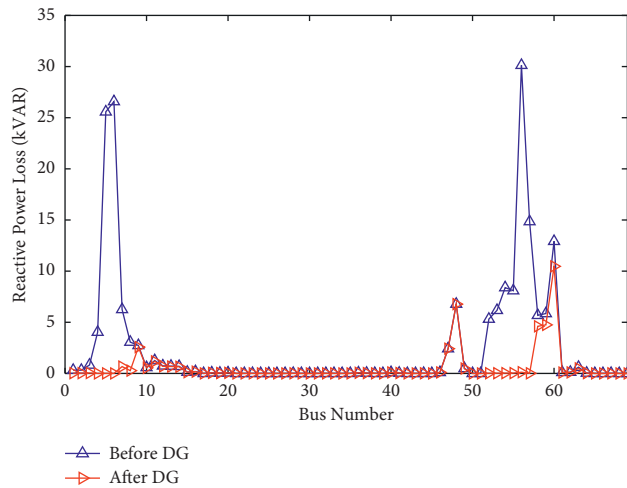
(c)

FIGURE 33: Case 4 (69-bus RDN) for summer. (a) Bus voltage profile. (b) Total P loss. (c) Total Q loss.

(a)

(b)

(c)
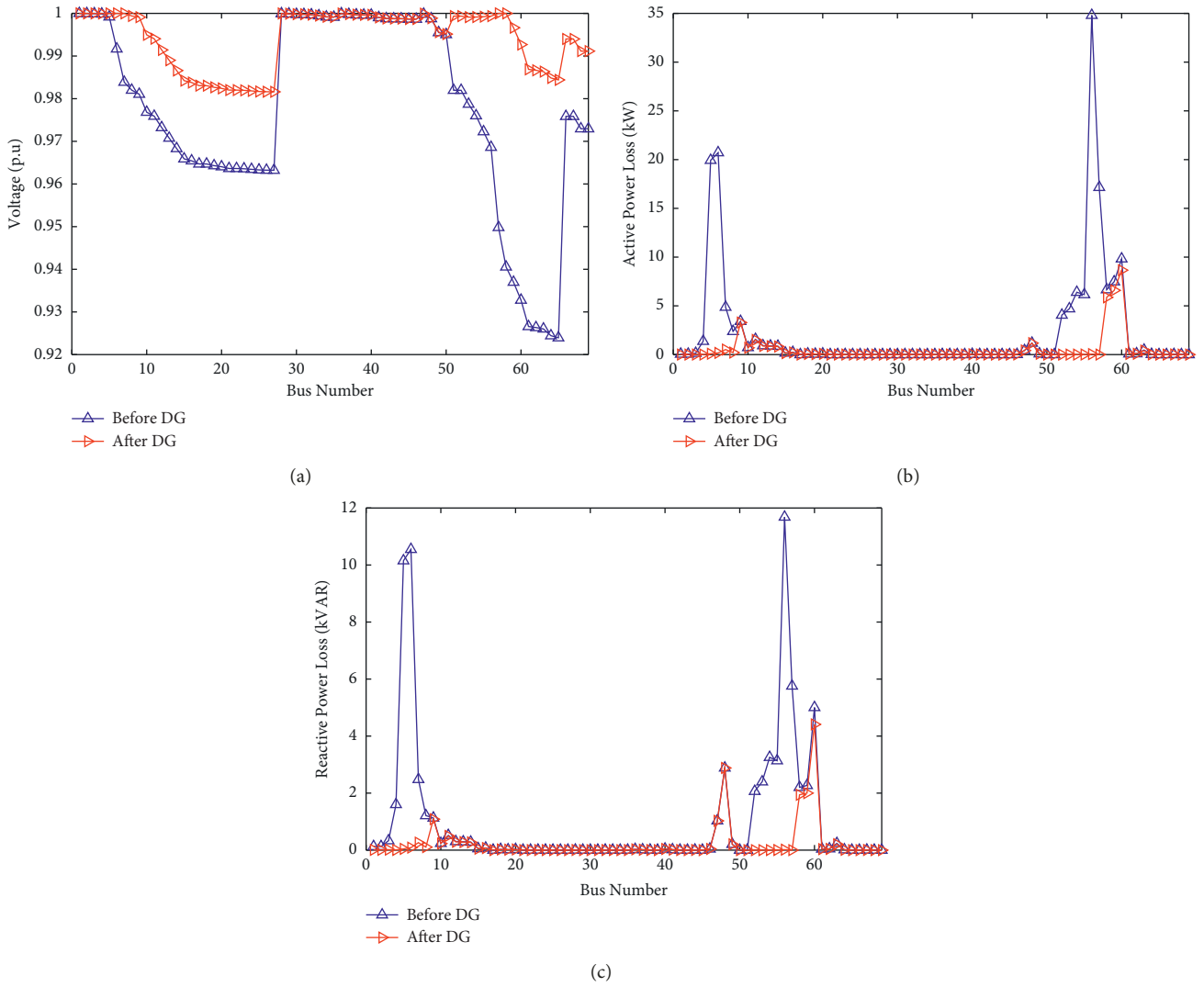
Figure 34: Case 4 (69-bus RDN) for autumn. (a) Bus voltage profile. (b) Total P loss. (c) Total Q loss.

(a)

(b)
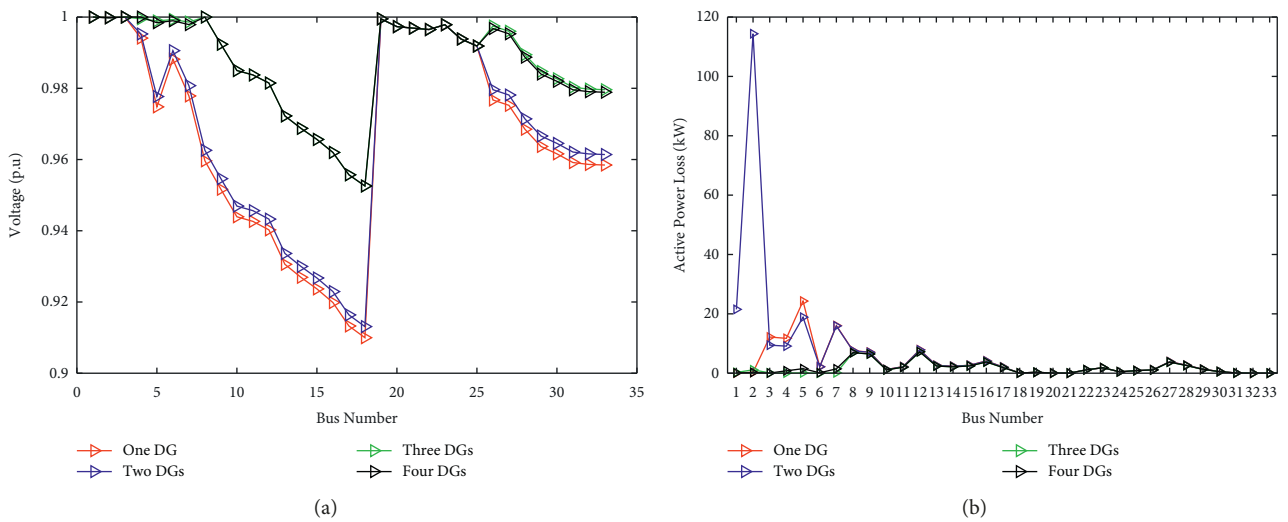
Figure 35: Comparison of (a) bus voltage profiles and (b) total P loss profiles in IEEE 33-bus RDN.

TABLE 21: Result comparison of 33-bus RDN for winter.

Case	v_{min} (per unit)	FO	P loss (kW)	Q loss (kVAR)	P_{LOSS} reduction (%)	Q_{LOSS} reduction (%)
Case 1	0.90998	0.39695	121.2107	76.817	24.0599	20.7221
Case 2	0.9131	0.4016	245.4671	142.4336	−53.7883	−46.9967
Case 3	0.95257	0.36559	52.528	41.6315	67.0905	57.0347
Case 4	0.95257	0.37277	53.7481	42.0459	66.3261	56.607

TABLE 22: Result comparison of 33-bus RDN for spring.

Case	v_{min} (per unit)	FO	P loss (kW)	Q loss (kVAR)	P_{LOSS} reduction (%)	Q_{LOSS} reduction (%)
Case 1	0.84089	0.52997	368.0215	234.5364	25.5925	22.4061
Case 2	0.84738	0.54649	736.4943	428.922	−48.9062	−41.9042
Case 3	0.91907	0.4185	144.1232	115.7245	70.8608	61.7138
Case 4	0.91907	0.44263	151.6158	117.4661	69.3459	61.1376

TABLE 23: Result comparison of 33-bus RDN for summer.

Case	v_{min} (per unit)	FO	P loss (kW)	Q loss (kVAR)	P_{LOSS} reduction (%)	Q_{LOSS} reduction (%)
Case 1	0.81484	0.59875	495.3813	316.1161	25.9429	22.9014
Case 2	0.8229	0.6219	980.4337	571.8549	−46.5701	−39.4716
Case 3	0.90725	0.44344	187.6912	150.7715	71.9411	63.2278
Case 4	0.90725	0.47614	199.115	153.3774	70.2333	62.5923

TABLE 24: Result comparison of 33-bus RDN for autumn.

| Case	v_{min} (per unit)	FO	P loss (kW)	Q loss (kVAR)	P_{LOSS} reduction (%)	Q_{LOSS} reduction (%)
Case 1	0.8882	0.43087	184.8168	117.3823	24.6921	21.3622
Case 2	0.89229	0.43844	374.0595	217.289	−52.4192	−45.5682
Case 3	0.9417	0.37977	77.1988	61.6239	68.5435	58.7164
Case 4	0.9417	0.3913	79.7039	62.2535	67.5228	58.2945

(a)

(b)
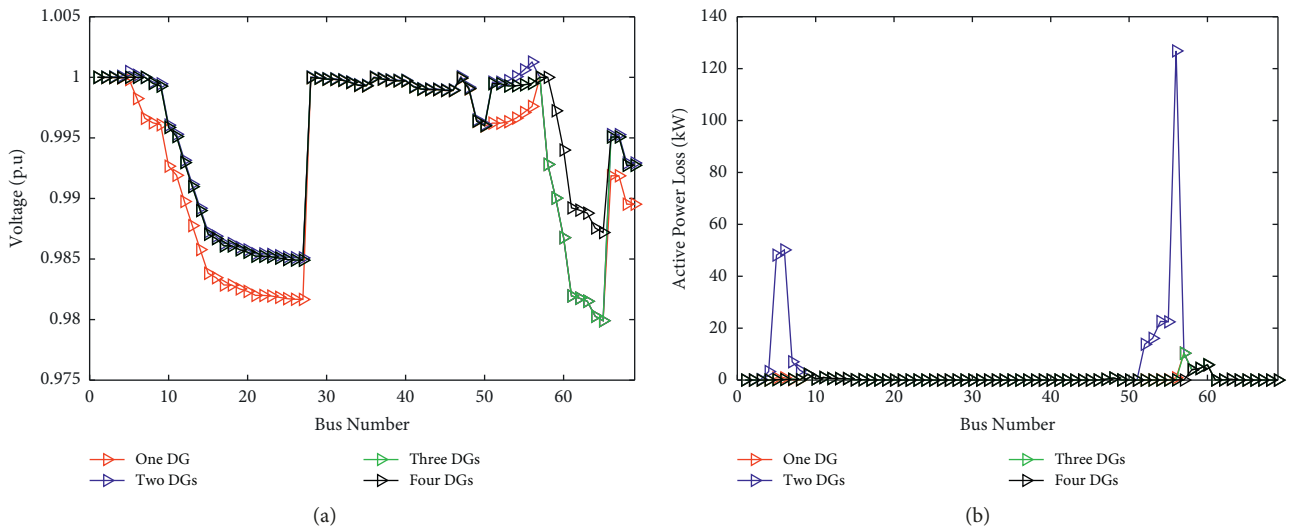
FIGURE 36: Comparison of (a) bus voltage profiles and (b) total P loss profiles in IEEE 69-bus RDN.

TABLE 25: Result comparison of IEEE 69-bus RDN for winter.

Case	v_{min} (per unit)	FO	P loss (kW)	Q loss (kVAR)	P_{LOSS} reduction (%)	Q_{LOSS} reduction (%)
Case 1	0.97991	0.36388	35.7486	15.9355	65.8022	66.5308
Case 2	0.97991	0.37332	346.8215	155.2039	−231.7765	−225.9733
Case 3	0.97991	0.36328	33.2763	14.7497	68.1672	69.0214
Case 4	0.9849	0.36025	22.7626	11.2125	78.2248	76.4505

TABLE 26: Result comparison of IEEE 69-bus RDN for spring.

Case	v_{min} (per unit)	FO	P loss (kW)	Q loss (kVAR)	P_{LOSS} reduction (%)	Q_{LOSS} reduction (%)
Case 1	0.96656	0.41038	97.9764	43.6535	68.003	68.5519
Case 2	0.96656	0.4422	1122.0975	504.2769	−266.4529	−263.2826
Case 3	0.96656	0.3799	92.4901	40.9044	69.7947	70.5324
Case 4	0.97496	0.39921	61.1562	30.0424	80.0277	78.3574

TABLE 27: Result comparison of IEEE 69-bus RDN for summer.

Case	v_{min} (per unit)	FO	P loss (kW)	Q loss (kVAR)	P_{LOSS} reduction (%)	Q_{LOSS} reduction (%)
Case 1	0.96204	0.43178	126.6908	56.4194	68.5854	69.0875
Case 2	0.96204	0.4752	1542.1811	694.2981	−282.4035	−280.4094
Case 3	0.96204	0.39179	117.1096	51.6342	70.9612	71.7094
Case 4	0.97161	0.417	78.8558	38.6836	80.4467	78.805

TABLE 28: Result comparison of IEEE 69-bus RDN for autumn.

Case	v_{min} (per unit)	FO	P loss (kW)	Q loss (kVAR)	P_{LOSS} reduction (%)	Q_{LOSS} reduction (%)
Case 1	0.9755	0.37651	52.7248	23.5051	66.6709	67.3284
Case 2	0.9755	0.39162	540.5331	242.1968	−241.6888	−236.6492
Case 3	0.9755	0.36075	49.3542	21.8535	68.8016	69.624
Case 4	0.98161	0.37089	33.2468	16.3679	78.9836	77.2489
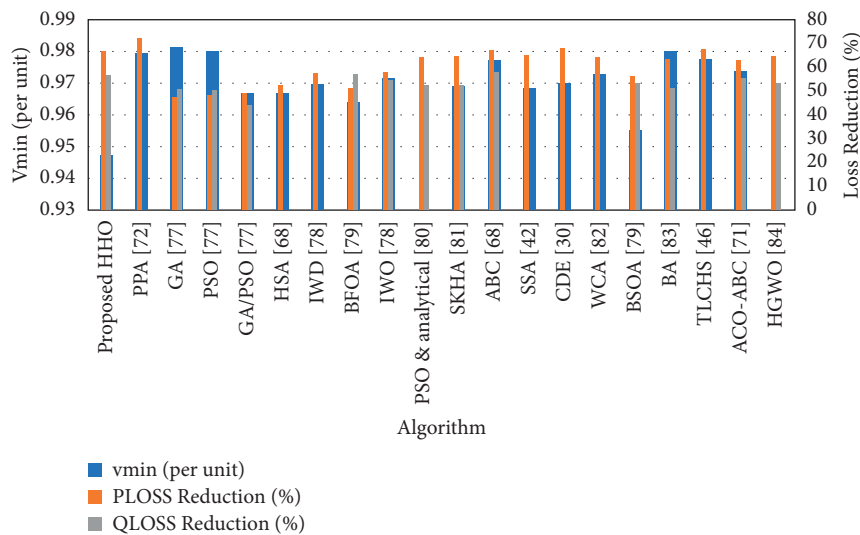
FIGURE 37: Graphical comparison of literature results with four DGs (33-bus RDN).
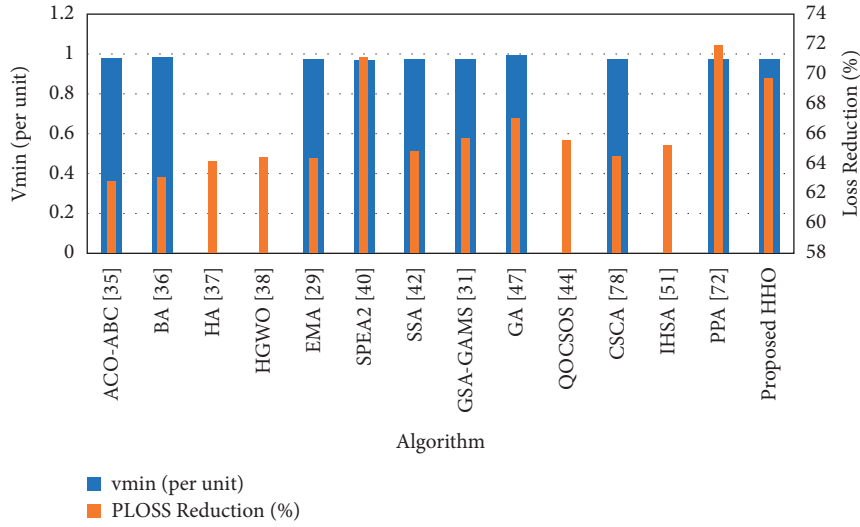
FIGURE 38: Graphical comparison of literature results with three DGs (33-bus RDN).
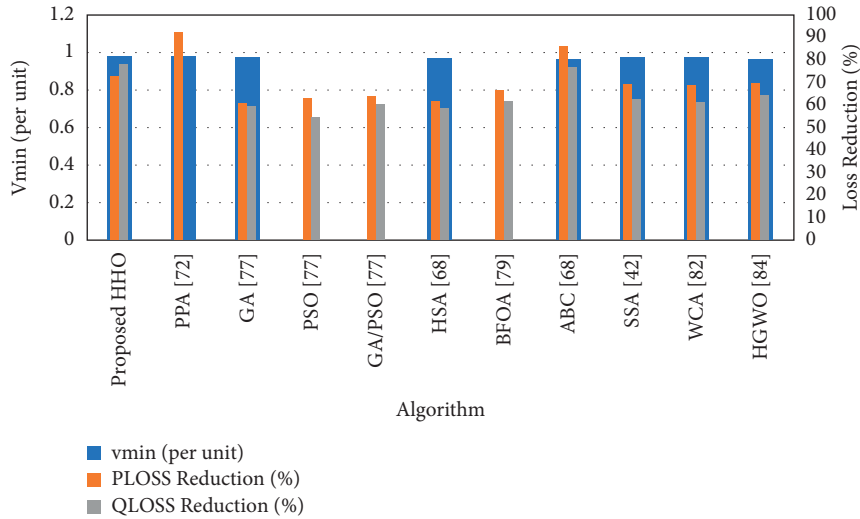

FIGURE 39: Graphical comparison of literature results with four DGs (69-bus RDN).
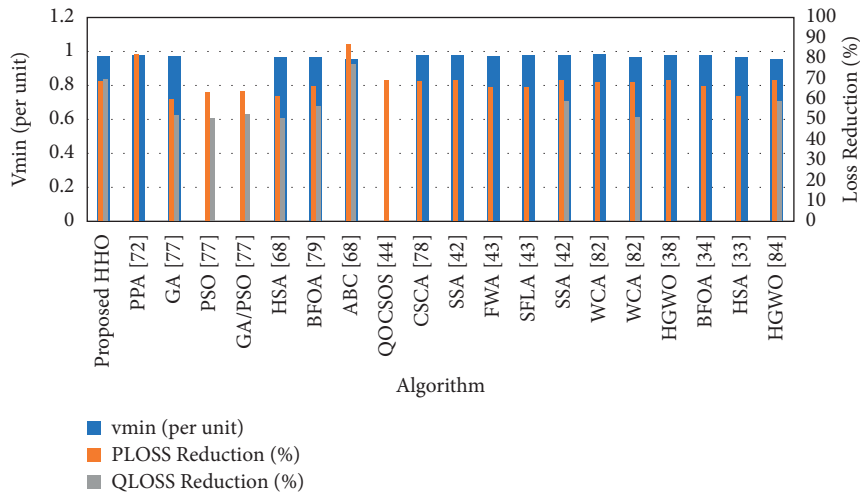
FIGURE 40: Graphical comparison of literature results with three DG (69-bus RDN).

TABLE 29: Statistical analysis of HHO.

Cases	OF	Best case	Worst case	Mean case
IEEE 33-bus RDN				
Case 1	$v_{\min}$ (per unit)	0.86524	0.86524	0.86524
Case 1	P_{LOSS}	0.252012	0.219034	0.245402
Case 2	$v_{\min}$ (per unit)	0.9027	0.88034	0.897694
Case 2	P_{LOSS}	0.580464	0.277759	0.519263
Case 3	$v_{\min}$ (per unit)	0.93054	0.93054	0.93054
Case 3	P_{LOSS}	0.697169	0.678674	0.688568
Case 4	$v_{\min}$ (per unit)	0.93054	0.93054	0.93054
Case 4	P_{LOSS}	0.695893	0.678437	0.683718
IEEE 69-bus RDN				
Case 1	$v_{\min}$ (per unit)	0.97105	0.97105	0.97105
Case 1	P_{LOSS}	0.673265	0.673048	0.673112
Case 2	$v_{\min}$ (per unit)	0.97105	0.97105	0.97105
Case 2	P_{LOSS}	0.696495	0.685316	0.691088
Case 3	$v_{\min}$ (per unit)	0.97105	0.97105	0.97105
Case 3	P_{LOSS}	0.695584	0.680438	0.690053
Case 4	$v_{\min}$ (per unit)	0.97836	0.97828	0.978318
Case 4	P_{LOSS}	0.774849	0.707672	0.73695

TABLE 30: ANOVA test.

| Source of variance	Sum of square (SS)	Degree of freedom (df)	Mean Square (MS)	F ratio	P value	F critical [83]
Between groups	0.0088	1	0.0088	0.3007	0.5873	4.1596
Within groups	0.9116	14	0.0294			
IEEE 69-bus RDN						
Between groups	0.0730	3	0.0243	0.7177	0.5471	2.8327
Within groups	1.3903	20	0.0339			
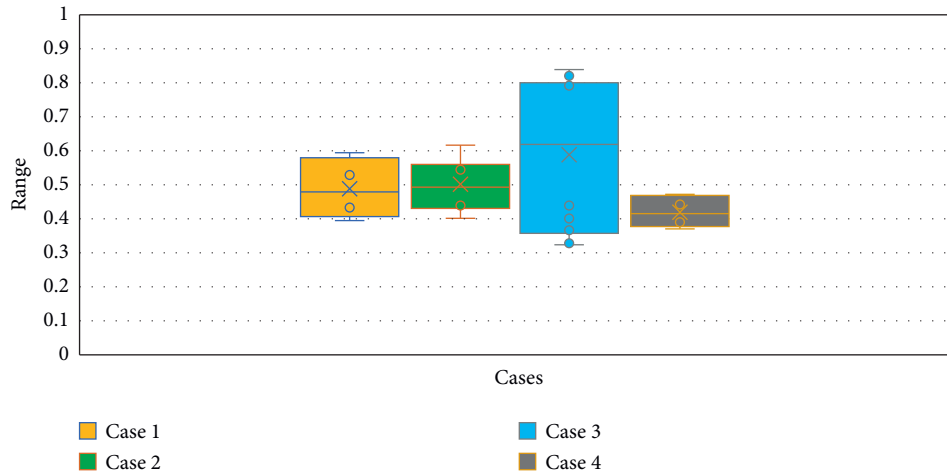
FIGURE 41: Box plot to compare objective function for four cases in IEEE 33-bus RDN.

RDN, the ANOVA test has been carried out between fourteen (14) algorithms, while for IEEE 69-bus RDN, the test has been performed between twenty (20) algorithms. The value of F for both RDNs is less than the critical level. It proves that the variation found while computing the objection function is significant and not by chance [84].

Moreover, Figures 41 and 42 illustrate the box plots for IEEE 33-bus and 69-bus RDNs, respectively. It is apparent
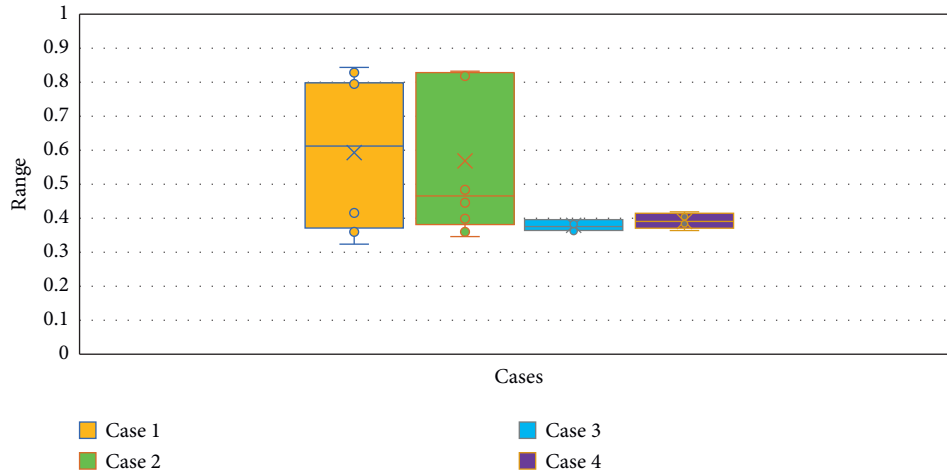
FIGURE 42: Box plot to compare objective function for four cases in IEEE 69-bus RDN.

that no outliers are present and significant data are available for statistical analysis.

5. Conclusion and Future Directions

This paper investigates reduction in total P and Q losses and minimization of bus voltage drop with the optimal DG allocation using the HHO. Four stages of DG integration were investigated in two IEEE RDNs. The objective functions were simultaneous reduction of the total P and Q losses and minimization of bus voltage drop. The summary of the conclusion is as follows:

(i) With the applied HHO, the overall result outcomes have been improved compared to other optimization algorithms for all four cases in both IEEE RDNs.

(ii) The comparison among the four cases for both IEEE RDNs was carried out. The best results were obtained when the given number of DGs could be integrated into the RDNs, as shown by Case 3 of a 33-bus RDN and Case 4 of a 69-bus RDN. Hence, the higher deployment rate of DGs in RDNs has significantly reduced the total P and Q losses and bus voltage drops with improved results with a robust trend of HHO.

Nomenclature

ACO-ABC:	Ant-colony optimization-artificial bee colony
BFOA:	Bacterial foraging optimization algorithm
CSCA:	Chaotic sine cosine
DEs:	Diesel engines
DGs:	Distributed generators
DNs:	Distribution networks
EHO:	Elephant herding optimization
EMA:	Exchange market algorithm
FC:	Fuel cell
GA:	Genetic algorithm
ICA:	Imperialist competitive algorithm
IHSA:	Improved harmony search method
MI:	Maximum iterations
MOSBA:	Multi-objective shuffled bat algorithm
MOTA:	Multi-objective Taguchi approach
MOWOA:	Multi-objective whale optimization
NSGA-II:	Non-dominated sorting genetic algorithm
PAES:	Pareto archived evolution strategy
PPA:	Plant propagation algorithm
PSO:	Particle swarm optimization
PV:	Photovoltaic
QOSIMBO-Q:	Quasi-oppositional SIMBO-Q
QOTLBO:	Quasi-oppositional TLBO
RDNs:	Radial distribution networks
SIMBO-Q:	Swine influenza model-based optimization with quarantine
SPEA-II:	Strength Pareto evolutionary algorithm II
TLBO:	Teaching-learning-based optimization
TLCHS:	Teaching-learning combined with harmony search
TM:	Taguchi method
VDI:	Voltage deviation index
VSI:	Voltage stability index
WOA:	Whale optimization algorithm
WTs:	Wind turbines.

Data Availability

Data are private and are only accessible in unique scenarios.

Conflicts of Interest

The authors declare that they have no conflicts of interest.

Acknowledgments

References

[1] M. Kashyap, A. Mittal, and S. Kansal, "Optimal placement of distributed generation using genetic algorithm approach,"

Lecture Notes in Electrical Engineering, vol. 476, pp. 587–597, 2019.

[2] A. Ali, D. Raisz, and K. Mahmoud, "Optimal oversizing of utility-owned renewable DG inverter for voltage rise prevention in MV distribution systems," *International Journal of Electrical Power & Energy Systems*, vol. 105, pp. 500–513, 2019.

[3] P. Prakash and D. K. Khatod, "Optimal sizing and siting techniques for distributed generation in distribution systems: a review," *Renewable and Sustainable Energy Reviews*, vol. 57, pp. 111–130, 2016.

[4] M. Pesaran, P. D. Huy, and V. K. Ramachandaramurthy, "A review of the optimal allocation of distributed generation: objectives, constraints, methods, and algorithms," *Renewable and Sustainable Energy Reviews*, vol. 75, pp. 293–312, 2017.

[5] M. H. Moradi, M. Abedinie, and H. Bagheri Tolabi, "Optimal multi-distributed generation location and capacity by genetic algorithms," in *Proceedings of the 2010 9th International Power and Energy Conference, IPEC 2010*, pp. 614–618, Singapore, June 2010.

[6] A. M. El-Zonkoly, "Optimal placement of multi-distributed generation units including different load models using particle swarm optimisation," *IET Generation, Transmission and Distribution*, vol. 5, no. 7, pp. 760–771, 2011.

[7] S. Kansal, V. Kumar, and B. Tyagi, "Hybrid approach for optimal placement of multiple DGs of multiple types in distribution networks," *International Journal of Electrical Power & Energy Systems*, vol. 75, pp. 226–235, 2016.

[8] D. Q. Hung and N. Mithulananthan, "Multiple distributed generator placement in primary distribution networks for loss reduction," *IEEE Transactions on Industrial Electronics*, vol. 60, no. 4, pp. 1700–1708, 2013.

[9] G. Celli, E. Ghiani, S. Mocci, and F. Pilo, "A multiobjective evolutionary algorithm for the sizing and siting of distributed generation," *IEEE Transactions on Power Systems*, vol. 20, no. 2, pp. 750–757, 2005.

[10] M. P. Lalitha, V. C. V. Reddy, N. S. Reddy, and V. U. Reddy, "DG source allocation by fuzzy and clonal selection algorithm for minimum loss in distribution system," vol. 26, no. 4, pp. 17–35, 2011.

[11] K. R. Devabalaji and K. Ravi, "Optimal size and siting of multiple DG and DSTATCOM in radial distribution system using bacterial foraging optimization algorithm," *Ain Shams Engineering Journal*, vol. 7, no. 3, pp. 959–971, 2016.

[12] S. A. ChithraDevi, L. Lakshminarasimman, and R. Balamurugan, "Stud Krill herd algorithm for multiple DG placement and sizing in a radial distribution system," *Engineering Science and Technology, an International Journal*, vol. 20, no. 2, pp. 748–759, 2017.

[13] P. D. P. Reddy, V. C. V. Reddy, and T. G. Manohar, "Whale optimization algorithm for optimal sizing of renewable resources for loss reduction in distribution systems," *Renewables: Wind, Water, and Solar*, vol. 4, no. 1, pp. 1–13, 2017.

[14] A. Selim, S. Kamel, and F. Jurado, "Efficient optimization technique for multiple DG allocation in distribution networks," *Applied Soft Computing*, vol. 86, Article ID 105938, 2020.

[15] M. H. Moradi and M. Abedini, "A combination of genetic algorithm and particle swarm optimization for optimal distributed generation location and sizing in distribution systems with fuzzy optimal theory," vol. 9, no. 7, pp. 641–660, 2012.

[16] S. Sultana and P. K. Roy, "Multi-objective quasi-oppositional teaching learning based optimization for optimal location of distributed generator in radial distribution systems," *International Journal of Electrical Power & Energy Systems*, vol. 63, pp. 534–545, 2014.

[17] S. Sharma, S. Bhattacharjee, and A. Bhattacharya, "Quasi-oppositional swine influenza model based optimization with quarantine for optimal allocation of DG in radial distribution network," *International Journal of Electrical Power & Energy Systems*, vol. 74, pp. 348–373, 2016.

[18] M. H. Moradi, A. Zeinalzadeh, Y. Mohammadi, and M. Abedini, "An efficient hybrid method for solving the optimal sitting and sizing problem of DG and shunt capacitor banks simultaneously based on imperialist competitive algorithm and genetic algorithm," *International Journal of Electrical Power & Energy Systems*, vol. 54, pp. 101–111, 2014.

[19] S. Kamel, A. Selim, W. Ahmed, and F. Jurado, "Single- and multi-objective optimization for photovoltaic distributed generators implementation in probabilistic power flow algorithm," *Electrical Engineering*, vol. 102, no. 1, pp. 331–347, 2019.

[20] S. Kamel, A. Selim, F. Jurado, J. Yu, K. Xie, and C. Yu, "Multi-objective whale optimization algorithm for optimal integration of multiple DGs into distribution systems," in *Proceedings of the 2019 IEEE PES Innovative Smart Grid Technologies Asia, ISGT 2019*, pp. 1312–1317, Chengdu, China, May 2019.

[21] C. Yammani, S. Maheswarapu, and S. K. Matam, "A multi-objective shuffled bat algorithm for optimal placement and sizing of multi distributed generations with different load models," *International Journal of Electrical Power & Energy Systems*, vol. 79, pp. 120–131, 2016.

[22] N. K. Meena, A. Swarnkar, N. Gupta, and K. R. Niazi, "Multi-objective Taguchi approach for optimal DG integration in distribution systems," *IET Generation, Transmission & Distribution*, vol. 11, no. 9, pp. 2418–2428, 2017.

[23] A. El-Fergany, "Optimal allocation of multi-type distributed generators using backtracking search optimization algorithm," *International Journal of Electrical Power & Energy Systems*, vol. 64, pp. 1197–1205, 2015.

[24] E. S. Ali, S. M. Abd Elazim, and A. Y. Abdelaziz, "Ant Lion Optimization Algorithm for optimal location and sizing of renewable distributed generations," *Renewable Energy*, vol. 101, pp. 1311–1324, 2017.

[25] M. Ghosh, S. Kumar, S. Mandal, and K. K. Mandal, "Optimal sizing and placement of DG units in radial distribution system using cuckoo search algorithm," 2021, http://www.ripublication.com.

[26] A. H. Ali, A. R. Youssef, T. George, and S. Kamel, "Optimal DG allocation in distribution systems using Ant lion optimizer," in *Proceedings of the 2018 International Conference on Innovative Trends in Computer Engineering, ITCE 2018*, vol. 2018, pp. 324–331, Aswan, Egypt, February 2018.

[27] T. P. Nguyen, T. T. Tran, and D. N. Vo, "Improved stochastic fractal search algorithm with chaos for optimal determination of location, size, and quantity of distributed generators in distribution systems," *Neural Computing & Applications*, vol. 31, no. 11, pp. 7707–7732, 2018.

[28] S. Kamel, A. Awad, H. Abdel-Mawgoud, and F. Jurado, "Optimal DG allocation for enhancing voltage stability and minimizing power loss using hybrid gray wolf optimizer," *Turkish Journal of Electrical Engineering and Computer Sciences*, vol. 27, no. 4, pp. 2947–2961, 2019.

[29] M. Daneshvar and E. Babaei, "Exchange market algorithm for multiple DG placement and sizing in a radial distribution system," *Journal of Energy Management and Technology*, vol. 2, no. 1, pp. 54–65, 2018.

[30] S. Kumar, K. K. Mandal, and N. Chakraborty, "Optimal DG placement by multi-objective opposition based chaotic differential evolution for techno-economic analysis," *Applied Soft Computing*, vol. 78, pp. 70–83, 2019.

[31] V. V. V. S. N. Murty and A. Kumar, "Optimal DG integration and network reconfiguration in microgrid system with realistic time varying load model using hybrid optimisation," *IET Smart Grid*, vol. 2, no. 2, pp. 192–202, 2019.

[32] A. Rajendran and K. Narayanan, "Optimal multiple installation of DG and capacitor for energy loss reduction and loadability enhancement in the radial distribution network using the hybrid WIPSO–GSA algorithm," vol. 41, no. 2, pp. 129–141, Article ID 1451371, 2018.

[33] R. S. Rao, K. Ravindra, K. Satish, and S. V. L. Narasimham, "Power loss minimization in distribution system using network reconfiguration in the presence of distributed generation," *IEEE Transactions on Power Systems*, vol. 28, no. 1, pp. 317–325, 2013.

[34] I. A. Mohamed and M. Kowsalya, "Optimal size and siting of multiple distributed generators in distribution system using bacterial foraging optimization," *Swarm and Evolutionary Computation*, vol. 15, pp. 58–65, 2014.

[35] M. Kefayat, A. Lashkar Ara, and S. A. Nabavi Niaki, "A hybrid of ant colony optimization and artificial bee colony algorithm for probabilistic optimal placement and sizing of distributed energy resources," *Energy Conversion and Management*, vol. 92, pp. 149–161, 2015.

[36] S. K. Sudabattula and M. Kowsalya, "Optimal allocation of solar based distributed generators in distribution system using Bat algorithm," *Perspectives in Science*, vol. 8, pp. 270–272, 2016.

[37] R. Sanjay, T. Jayabarathi, T. Raghunathan, V. Ramesh, and N. Mithulananthan, "Optimal allocation of distributed generation using hybrid grey Wolf optimizer," *IEEE Access*, vol. 5, pp. 14807–14818, 2017.

[38] I. ben Hamida, S. B. Salah, F. Msahli, and M. F. Mimouni, "Optimal network reconfiguration and renewable DG integration considering time sequence variation in load and DGs," *Renewable Energy*, vol. 121, pp. 66–80, 2018.

[39] A. A. A. El-Ela, R. A. El-Sehiemy, and A. S. Abbas, "Optimal placement and sizing of distributed generation and capacitor banks in distribution systems using water cycle algorithm," *IEEE Systems Journal*, vol. 12, no. 4, pp. 3629–3636, 2018.

[40] S. S. Kola and T. Jayabarathi, "Optimal allocation of renewable distributed generation and capacitor banks in distribution systems using salp swarm algorithm," *International Journal of Renewable Energy Research (IJRER)*, vol. 9, no. 1, 2019.

[41] A. Onlam, D. Yodphet, R. Chatthaworn, C. Surawanitkun, A. Siritaratiwat, and P. Khunkitti, "Power loss minimization and voltage stability improvement in electrical distribution system via network reconfiguration and distributed generation placement using novel adaptive shuffled frogs leaping algorithm," *Energies*, vol. 12, no. 3, p. 553, 2019.

[42] K. H. Truong, P. Nallagownden, I. Elamvazuthi, and D. N. Vo, "A Quasi-oppositional-chaotic symbiotic organisms search algorithm for optimal allocation of DG in radial distribution networks," *Applied Soft Computing*, vol. 88, Article ID 106067, 2020.

[43] A. Alam, B. Zaheer, and M. Zaid, "Optimal placement of DG in distribution system for power loss minimization and voltage profile improvement," in *Proceedings of the 2018 International Conference on Computing, Power and Communication Technologies, GUCON 2018*, pp. 837–842, Greater Noida, India, September 2018.

[44] F. Moaidi and M. Moaidi, "Optimal placement and sizing of distributed generation in microgrid for power loss reduction and voltage profile improvement," 2019, http://publications.waset.org/10009963/optimal-placement-and-sizing-of-distributed-generation-in-microgrid-for-power-loss-reduction-and-voltage-profile-improvement.

[45] V. S. Bhadoria, N. S. Pal, and V. Shrivastava, "Artificial immune system based approach for size and location optimization of distributed generation in distribution system," *International Journal of System Assurance Engineering and Management*, vol. 10, no. 3, pp. 339–349, 2019.

[46] C. H. Prasad, K. Subbaramaiah, and P. Sujatha, "Cost–benefit analysis for optimal DG placement in distribution systems by using elephant herding optimization algorithm," *Renewables: Wind, Water, and Solar*, vol. 6, no. 1, pp. 1–12, 2019.

[47] A. S. Hassan, E. S. A. Othman, F. M. Bendary, and M. A. Ebrahim, "Optimal integration of distributed generation resources in active distribution networks for techno-economic benefits," *Energy Reports*, vol. 6, pp. 3462–3471, 2020.

[48] A. P. Sirat, H. Mehdipourpicha, N. Zendehdel, and H. Mozafari, "Sizing and allocation of distributed energy resources for loss reduction using heuristic algorithms," in *Proceedings of the 2020 IEEE Power and Energy Conference at Illinois, PECI 2020*, Champaign, IL USA, February 2020.

[49] A. M. Helmi, R. Carli, M. Dotoli, and H. S. Ramadan, "Efficient and sustainable reconfiguration of distribution networks via metaheuristic optimization," *IEEE Transactions on Automation Science and Engineering*, vol. 19, no. 1, 2021.

[50] M. Zellagui, N. Belbachir, and C. Ziad El-Bayeh, "Optimal allocation of RDG in distribution system considering the seasonal uncertainties of load demand and solar-wind generation systems," in *Proceedings of the 19th International Conference on Smart Technologies (IEEE EUROCON 2021)*, pp. 471–477, Lviv, Ukraine, July 2021.

[51] T. Agheb, I. Ahmadi, and A. Zakariazadeh, "Optimum sizing and placement of wind turbines in distribution networks considering correlation of load demand and wind power," *Iranian Journal of Electrical and Electronic Engineering*, vol. 17, no. 3, p. 1916, 2021.

[52] A. A. Heidari, S. Mirjalili, H. Faris, I. Aljarah, M. Mafarja, and H. Chen, "Harris hawks optimization: algorithm and applications," *Future Generation Computer Systems*, vol. 97, pp. 849–872, 2019.

[53] A. S. Menesy, H. M. Sultan, A. Selim, M. G. Ashmawy, and S. Kamel, "Developing and applying chaotic Harris hawks optimization technique for extracting parameters of several proton exchange membrane fuel cell stacks," *IEEE Access*, vol. 8, 2020.

[54] H. Chen, S. Jiao, M. Wang, A. A. Heidari, and X. Zhao, "Parameters identification of photovoltaic cells and modules using diversification-enriched Harris hawks optimization with chaotic drifts," *Journal of Cleaner Production*, vol. 244, Article ID 118778, 2020.

[55] M. Chakravorty and D. Das, "Voltage stability analysis of radial distribution networks," *International Journal of Electrical Power & Energy Systems*, vol. 23, no. 2, pp. 129–135, 2001.

[56] K. Balu and V. Mukherjee, "Optimal siting and sizing of distributed generation in radial distribution system using a novel student psychology-based optimization algorithm," *Neural Computing & Applications*, vol. 33, pp. 1–29, 2021.

[57] A. Mohamed Imran, M. Kowsalya, and D. P. Kothari, "A novel integration technique for optimal network

reconfiguration and distributed generation placement in power distribution networks," *International Journal of Electrical Power & Energy Systems*, vol. 63, pp. 461–472, 2014.

[58] S. Kasi and R. Neela, "Harris hawks optimization algorithm based power loss minimization in micro grid incorporated with distributed generation," *IOP Conference Series: Materials Science and Engineering*, vol. 1070, no. 1, Article ID 012099, 2021.

[59] M. Rizwan, L. Hong, W. Muhammad, S. W. Azeem, and Y. Li, "Hybrid Harris Hawks optimizer for integration of renewable energy sources considering stochastic behavior of energy sources," *International Transactions on Electrical Energy Systems*, vol. 31, no. 2, Article ID e12694, 2021.

[60] S. Chakraborty, S. Verma, A. Salgotra, R. M. Elavarasan, D. Elangovan, and L. Mihet-Popa, "Solar-based DG allocation using Harris hawks optimization while considering practical aspects," *Energies*, vol. 14, no. 16, p. 5206, 2021.

[61] H. Hamour, S. Kamel, E. Mohamed, and E. A. Mohamed, "Harris Hawks optimization technique for optimal reconfiguration of radial distribution networks efficient power flow solution paradigm view project," in *Proceedings of the IEEE Aswan International Workshop on Computational Methods in Power Systems (CMPS 2018)*, Aswan, Egypt, February 2018.

[62] H. M. Alabool, D. Alarabiat, L. Abualigah, and A. A. Heidari, "Harris hawks optimization: a comprehensive review of recent variants and applications," *Neural Computing & Applications*, vol. 33, no. 15, pp. 8939–8980, 2021.

[63] P. Mehta, P. Bhatt, and V. Pandya, "Optimal selection of distributed generating units and its placement for voltage stability enhancement and energy loss minimization," *Ain Shams Engineering Journal*, vol. 9, no. 2, pp. 187–201, 2018.

[64] D. K. Rukmani, "A new approach to optimal location and sizing of DSTATCOM in radial distribution networks using bio-inspired cuckoo search algorithm," *Energies*, vol. 13, no. 18, p. 4615, 2020.

[65] E. A. Al-Ammar, "ABC algorithm based optimal sizing and placement of DGs in distribution networks considering multiple objectives," *Ain Shams Engineering Journal*, vol. 12, no. 1, pp. 697–708, 2021.

[66] S. M. Mousavi and H. A. Abyaneh, "Effect of load models on probabilistic characterization of aggregated load patterns," *IEEE Transactions on Power Systems*, vol. 26, no. 2, pp. 811–819, 2011.

[67] A. Bayat, A. Bagheri, and R. Noroozian, "Optimal siting and sizing of distributed generation accompanied by reconfiguration of distribution networks for maximum loss reduction by using a new UVDA-based heuristic method," *International Journal of Electrical Power & Energy Systems*, vol. 77, pp. 360–371, 2016.

[68] F. M. F. Flaih, X. Lin, M. K. Abd, S. M. Dawoud, Z. Li, and O. S. Adio, "A new method for distribution network reconfiguration analysis under different load demands," *Energies*, vol. 10, no. 4, p. 455, 2017.

[69] A. Waqar, "Analysis of optimal deployment of several DGs in distribution networks using plant propagation algorithm," *IEEE Access*, vol. 8, pp. 175546–175562, 2020.

[70] A. Mohamed Imran and M. Kowsalya, "A new power system reconfiguration scheme for power loss minimization and voltage profile enhancement using Fireworks Algorithm," *International Journal of Electrical Power & Energy Systems*, vol. 62, pp. 312–322, 2014.

[71] S. Naveen, K. Sathish Kumar, and K. Rajalakshmi, "Distribution system reconfiguration for loss minimization using modified bacterial foraging optimization algorithm," *International Journal of Electrical Power & Energy Systems*, vol. 69, pp. 90–97, 2015.

[72] T. T. Nguyen and A. V. Truong, "Distribution network reconfiguration for power loss minimization and voltage profile improvement using cuckoo search algorithm," *International Journal of Electrical Power & Energy Systems*, vol. 68, pp. 233–242, 2015.

[73] E. Dall'Anese and G. B. Giannakis, "Sparsity-leveraging reconfiguration of smart distribution systems," *IEEE Transactions on Power Delivery*, vol. 29, no. 3, pp. 1417–1426, 2014.

[74] H. B. Tolabi, A. L. Ara, and R. Hosseini, "A new thief and police algorithm and its application in simultaneous reconfiguration with optimal allocation of capacitor and distributed generation units," *Energy*, vol. 203, Article ID 117911, 2020.

[75] D. B. Prakash and C. Lakshminarayana, "Multiple DG placements in radial distribution system for multi objectives using Whale Optimization Algorithm," *Alexandria Engineering Journal*, vol. 57, no. 4, pp. 2797–2806, 2018.

[76] M. G. Hemeida, A. A. Ibrahim, A. A. A. Mohamed, S. Alkhalaf, and A. M. B. El-Dine, "Optimal allocation of distributed generators DG based Manta Ray Foraging Optimization algorithm (MRFO)," *Ain Shams Engineering Journal*, vol. 12, no. 1, pp. 609–619, 2021.

[77] B. Jyothsna Rani and A. Srinivasula Reddy, "Optimal allocation and sizing of multiple DG in radial distribution system using binary particle swarm optimization," *International Journal of Intelligent Engineering and Systems*, vol. 12, no. 1, 2019.

[78] C. K. Das, O. Bass, G. Kothapalli, T. S. Mahmoud, and D. Habibi, "Optimal placement of distributed energy storage systems in distribution networks using artificial bee colony algorithm," *Applied Energy*, vol. 232, pp. 212–228, 2018.

[79] S. H. Lee and J. W. Park, "Optimal placement and sizing of multiple dgs in a practical distribution system by considering power loss," *IEEE Transactions on Industry Applications*, vol. 49, no. 5, pp. 2262–2270, 2013.

[80] M. S. Rawat and S. Vadhera, "Heuristic optimization techniques for voltage stability enhancement of radial distribution network with simultaneous consideration of network reconfiguration and DG sizing and allocations," *Turkish Journal of Electrical Engineering and Computer Sciences*, vol. 27, no. 1, pp. 330–345, 2019.

[81] M. Montazeri and A. Askarzadeh, "Capacitor placement in radial distribution networks based on identification of high potential busses," *International Transactions on Electrical Energy Systems*, vol. 29, no. 3, p. e2754, 2019.

[82] P. Dinakara Prasad Reddy, V. C. Veera Reddy, and T. Gowri Manohar, "Optimal renewable resources placement in distribution networks by combined power loss index and whale optimization algorithms," *Journal of Electrical Systems and Information Technology*, vol. 5, no. 2, pp. 175–191, 2018.

[83] S. Raj and B. Bhattacharyya, "Optimal placement of TCSC and SVC for reactive power planning using Whale optimization algorithm," *Swarm and Evolutionary Computation*, vol. 40, pp. 131–143, 2018.

[84] A. Jafari, H. Ganjeh Ganjehlou, T. Khalili, B. Mohammadi-Ivatloo, A. Bidram, and P. Siano, "A two-loop hybrid method for optimal placement and scheduling of switched capacitors in distribution networks," *IEEE Access*, vol. 8, pp. 38892–38906, 2020.